DISSERTATION

Development and Application of 1,3a,6a-Triazapentalene Derivatives as a Novel Fluorescent Molecule

Ayumi Osawa

Hokkaido University

2015

Contents

Abbreviation

Ac	acetyl group
Bu	butyl
CASPT2	complete active space second-order perturbation theory
DAPI	4',6-diamidino-2-phenylindole
dba	dibenzylideneacetone
DBU	1,8-diazabicyclo[5.4.0]-7-undecene
DCM	dichloromethane
DFT	density functional theory
DMAP	4(-*N*,*N*-dimethylamino)pyridine
DMF	*N*,*N*-dimethylformamide
DMSO	dimethylsulfoxide
DNA	deoxyribonucleic acid
ECHO	exciton-controlled hybridization-sensitive oligonucleotide
EDCI	1-ethyl-3-(3-dimethylaminopropyl)-Carbodiimide
equiv	equivalent
Et	ethyl group
EWG	electron withdrawing group
GFP	green fluorescent protein
i-	iso
LG	leaving group
Me	methyl group
Mes	2,4,6-trimethylphenyl group
Ms	methanesulfonyl group
NHS	*N*-hydroxysuccinimide
NMR	nuclear magnetic resonance
PeT	photo-induced electron transfer
Ph	phenyl group
Pr	propyl group
quant	quantitative yield
RNA	ribonucleic acid
rt	room temperature
t-	tertiary
TAP	1,3a,6a-triazapentalene
TBAF	tetra-*normal*-butylammonium fluoride
TBS	*tertiary*-butyldimethylsilyl group
TD-DFT	time-dependent density functional theory
TEA	triethylamine
Tf	trifluoromethanesulfonyl group
TFA	trifluoroacetic acid or trifluoroacetyl group
TFAA	trifluoroacetic anhydride
TGA	thermogravimetry analysis
THF	tetrahydrofuran
TMS	trimethylsilyl group
Ts	(4-methylphenyl)sulfonyl group
UV	ultraviolet
Φ_F	fluorescence quantum yield
λ_{abs}	absorption maximum wavelength
λ_{em}	emission maximum wavelength
λ_{ex}	excitation maximum wavelength
σ_p	Hammett value at *para*-position

Introduction

All of life phenomena are caused by numerous reactions and interactions of biofunctional molecules such as protein, DNA, hormones and so on. Therefore, clarification of their biological role leads to understanding of life phenomena and development of cure of diseases and new drugs. For this purpose, various methods for study of their function have been developed. In particular, fluorescence imaging technologies is one of the most powerful tools for analysis of biofunctional molecules inside cells and tissues due to their high sensitive visualization. For example, fluorescent proteins such as green fluorescent protein (GFP) have played an important role to analyze amount and localization of focused proteins.[1] The biogenetic protocol for the introduction of fluorescent protein into focused protein has been well established, and this reliable method become a routine operation in laboratory.

On the other hand, fluorescent small compounds are used for fluorescence imaging of other type of biologically active molecules such as inorganic active species[2,3], nucleotides[4,5], peptides[6], and bioactive small molecules[7] (Figure 1). For example, fura-2 (**1**), which was developed by Tsien, is the most popular probe for Ca^{2+} ion and frequently used to analyze concentration of Ca^{2+} ion by variation of absorbance and emission intensity *in vivo*.[2a,b] Nagano and co-workers reported rationally designed fluorescent probes for reactive oxygen species such as singlet oxygen in the basis of a PeT mechanism.[3] In nucleotide chemistry, exciton-controlled hybridization-sensitive oligonucleotide (ECHO) probe has received attention for detection of target sequence of DNA or RNA. Oligonucleotide including D_{514} (**3**) exhibits no fluorescence without a complementary nucleotide but strong fluorescence after hybridization with a target nucleotide because fluorescent chromophore can intercalate into resulting hybridized nucleotide.[4]

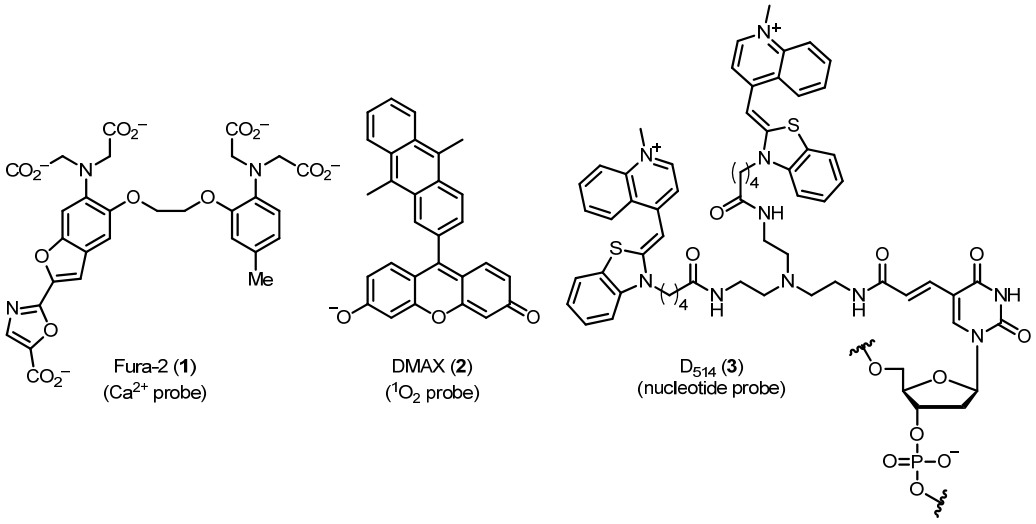

Figure 1. Structure of various probes

In contrast, development of smaller molecules including oligopeptides and low-molecular-weight drugs as fluorescent probes are still limited although several achievements were reported[7]. The main reason is that the introduction of fluorescent molecule to biologically active small compound readily induces the change of biological activities due to the structural modification. For example, although Alexa Fluor 405 (**4**), Cy3 (**5**), and Texas Red (**6**) are commonly used for fluorescence labeling,[8] they are sometimes too large to ignore their molecular size compared to bioactive small compounds. Furthermore, their ionic structure, which makes their hydrophobic core skeleton soluble to water, also affects the polarity of their fluorescent probes. Therefore, preparation of their fluorescent probes has generally depended on trial and error. For example, screening of effective fluorescent chromophores and linkers is mainly adopted for the preparation of suitable probes.

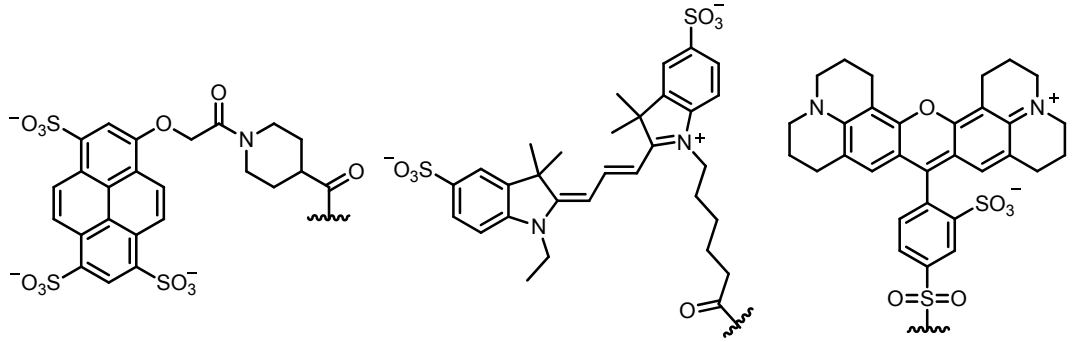

Alexa Fluor 405 (**4**)
λ_{ex} = 401 nm
λ_{em} = 421 nm

Cy3 (**5**)
λ_{ex} = 554 nm
λ_{em} = 568 nm

Texas Red (**6**)
λ_{ex} = 595 nm
λ_{em} = 615nm

Figure 2. Selected examples of reported fluorescent molecules.

Recently, fluorescent probes of mugineic acid have been developed in our group.[9] Mugineic acid is a phytosiderophore as a natural iron chelator and secreted from the roots of barley[10], and its tracking inside cell and tissues were required for functional studies. The coumarin derivative **7a** was demonstrated to be incorporated into cell through transporter (HvYS1)[11,12] that was overexpressed on cell membrane, whereas stronger fluorescent acridine derivative **7b** was not incorporated into cell (Figure 3). This result clearly showed that the properties of fluorescent chromophore affected biological activities.

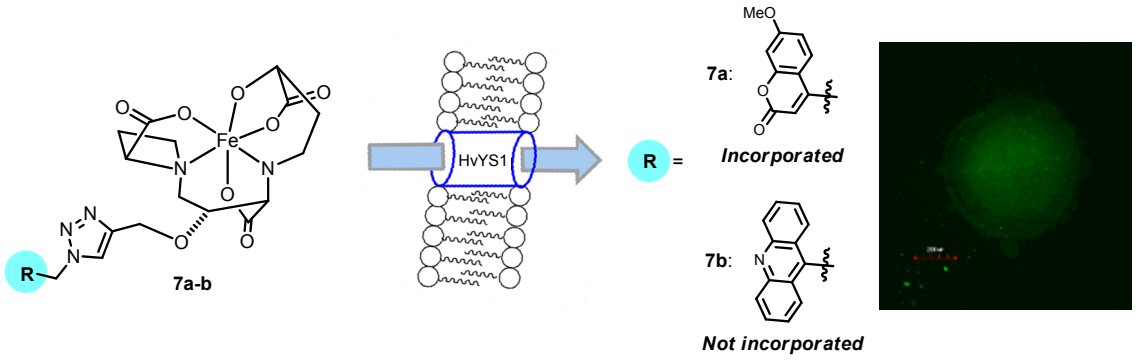

Figure 3. The incorporation of fluorescent probes of mugineic acid into *Xenopus* oocyte cells through transporter HvYS1 overexpressed on cell membrane. The coumarin derivative **7a** was incorporated into cell, whereas the acridine derivative **7b** was not incorporated. The picture was fluorescence image of incorporation of **7a** into *Xenopus* oocyte cell.

Because of above factors, the author planed to develop a new fluorescent chromophore. First of all, the author focused his attention on a heterocyclic aromatic compound 1,3a,6a-triazapentalene (TAP, **8a**). TAP possesses a specific dipole structure within a compact 10π-electron system and exhibits a totally neutral character due to delocalization of electrical charge (Figure 3).[13] Therefore, it was expected that TAP would be a quite small fluorescent chromophore although the fluorescent properties of **8a** have not yet been elucidated. Thus, in order to investigate the optical properties of TAP, it was needed to develop a common and efficient method for the synthesis of TAP.

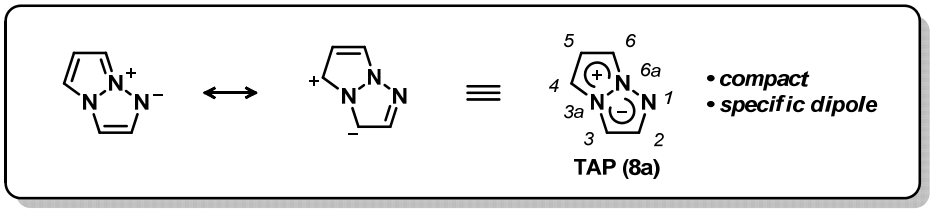

Figure 4. The structure and the numbering of 1,3a,6a-triazapentalene (TAP, **8a**).

There have been several examples of the synthesis of 1,3a,6a-triazapentalene derivatives with aryl fused and heteroaryl fused systems such as benzotriazapentalene **11**.[14] For example, McRobbie and co-workers reported intramolecular N–N bond-forming reaction of nitrene intermediate **10** generated from pyrazole derivative **9** to afford **11** (Scheme 1(a)).[14a] In addition, Park and co-workers reported that tri-substituted benzotriazapentalene **14** was obtained by cyclization reaction of benzotriazole derivatives **12** via Pummerer type intermediate **13** (Scheme 1(b)).[14i,j]

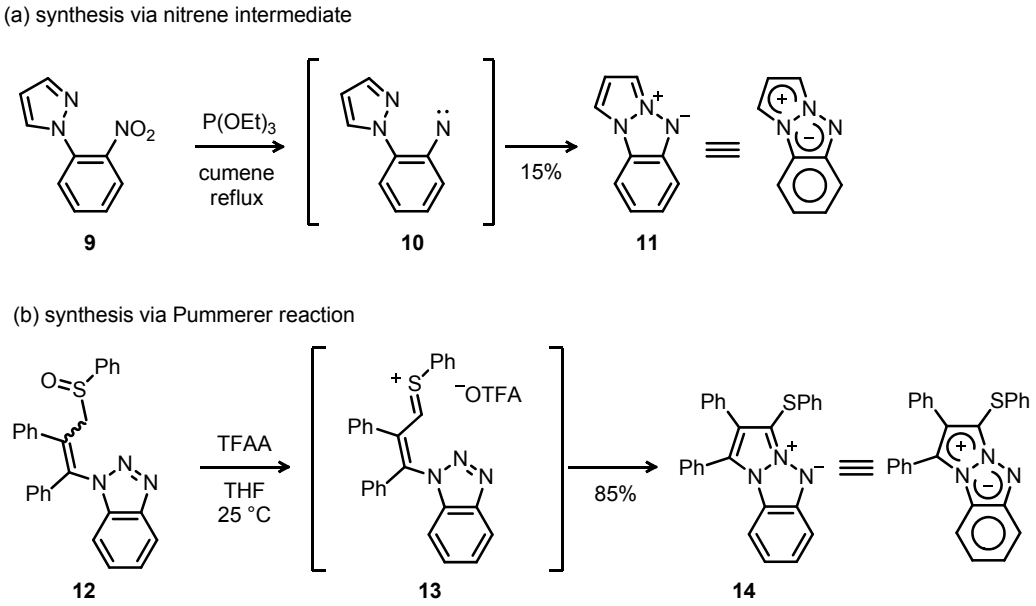

Scheme 1. Synthesis of benzotriazapentalene derivatives via nitrene-intermediate (a) and Pummerer reaction (b).

In contrast, there have been very few examples of the smaller 1,3a,6a-triazapentalene derivatives without an aryl fused system,[15] and the simple 1,3a,6a-triazapentalene (**8a**) has never been synthesized. Thus far, the only two examples of the synthesis of mono-substituted TAPs by different method were reported by Hirobe *et al*. One of them was shown in Scheme 2. The reaction of aminopyrazole (**16**), which was prepared by N-amination of pyrazole (**15**) in 52% yield, with 2-chloroacetylacetone (**17**) in benzene at reflux afforded 3-acetyl-2-methyl TAP (**8b**) in 58% yield via formation of imine intermediate **18**. Then, treatment of acetylated TAP **8b** with

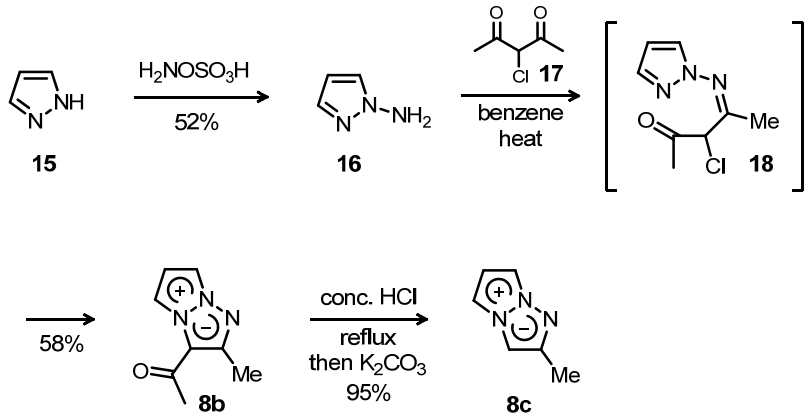

Scheme 2. Synthesis of TAP derivative **8b** and **8c** reported by Hirobe *et al.*

concentrated hydrochloric acid under reflux condition followed by neutralization with potassium carbonate gave 2-methyl TAP (**8c**) in 95% yield. Another example was synthesis of 2-phenyl TAP (**8d**) as shown in Scheme 3. The reaction of α-pyrazolyl acetophenone (**20**) with a sulfonylhydoxylamine resulted in enamine **21** as an intermediate and the subsequent intramolecular substitution forming a N-N bond afforded 2-phenyl TAP (**8d**) in 66% yield. However, fluorescence properties of synthetic **8c** and **8d** have not been mentioned.

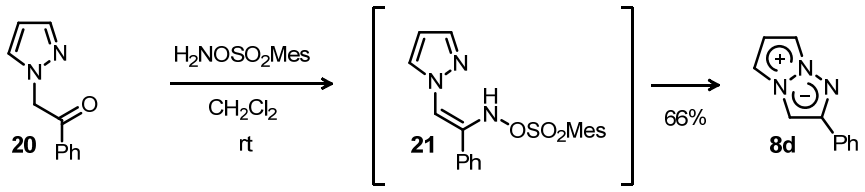

Scheme 3. Synthesis of 2-phenyl TAP (**8d**) reported by Hirobe *et al*.

In this context, the author first attempted to establish a versatile and common method for the synthesis of various TAPs without aryl fused systems and has successfully developed a new single-step synthesis of TAPs (Chapter 1). In Chapter 2, the optical properties of synthetic TAPs were investigated, and their interesting fluorescent characters were revealed. Finally, the utility of TAP as a fluorescent labeling reagent was evaluated in Chapter 3.[16]

Chapter 1

Establishment of the New Preparative Method for 1,3a,6a-Triazapentalene Derivatives

1-1. Synthetic Plan

The author has first attempted to establish a versatile and common method for the synthesis of simple mono-substituted TAPs without aryl fused systems to elucidate the properties of the TAP skeleton as a fluorescent chromophore. The author focused on the triazole structure included in TAP, and therefore, planed to apply a click reaction of alkyne with azide (Scheme 4). That is, the Cu(I)-catalyzed click reaction[17] of alkyne **23** with azide **22**, which possesses two leaving groups at each of the C2 and C3 positions, would afford a triazole **A**, which should undergo intramolecular cyclization to give a triazolium ion **B**. Under basic conditions, the intermediate **B** would be subsequently converted to **8** by a sequential reaction of E2 elimination and deprotonation.

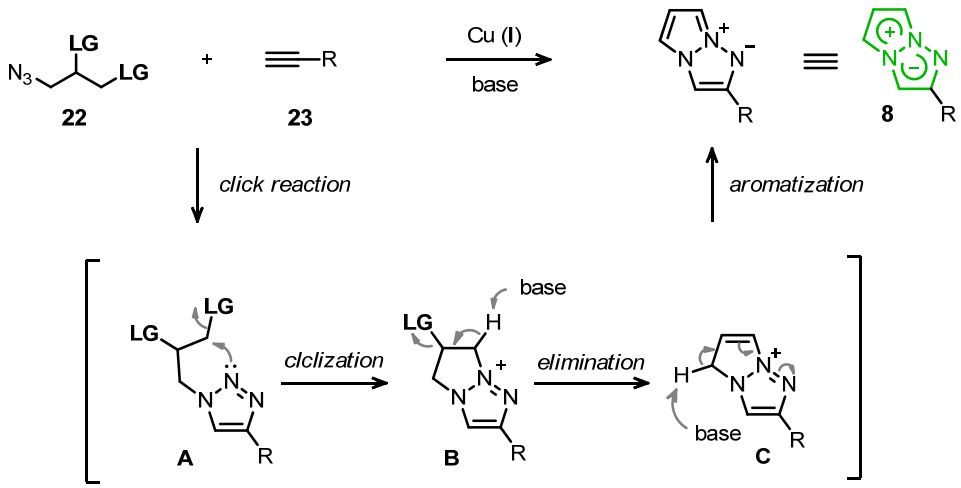

Scheme 4. A synthetic plan for TAP applying a click reaction.

1-2. Establishment of Preparative Method for TAPs

The author began the investigation of the click reaction with 3-azidopropane-1,2-diol bis(trifluoromethanesulfonate) (**22a**) as an azide fragment because of its high reactivity and ready availability. The azide **22a** was easily obtained from economical 3-chloro-1,2-propanediol (**24**)[18] by azidation followed by triflation[19] of two hydroxyl groups in 82% two-step yield and it was stable enough to be purified by silica-gel column chromatography and stored for a year in a freezer.

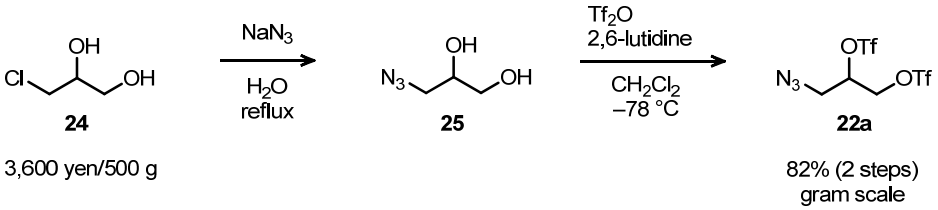

Scheme 5. Preparation of the azide fragment **22a**.

To determine whether the click reaction of azide **22a** proceeds uneventfully, the author first tried the click reaction without a base. Treatment of 1-pentadecyne (**23e**) with a 1.0 equiv of **22a** in the presence of 5 mol% of copper(I) iodide and 5 mol% of bis[2-(*N*,*N*-dimethylamino)ethyl] ether[20] as a ligand afforded a bicyclic triazolium ion **26e** in 29% NMR yield, along with a trace amount of **8e** (Table 1, entry 1). The formation of **26e** suggested that the triazole generated in the click reaction underwent intramolecular substitution to form the bicyclic framework and this encouraged us to examine the coexisting bases. The similar click reactions in the presence of a 5 equiv of 2,6-lutidine or DBU as a base did not give the desired **8e** because they reacted with **22a** faster than the click reaction (entries 2, 3). In contrast, the use of diisopropylethylamine afforded the desired **8e** in 66% yield (entry 4), and a higher yield (80%) was obtained with triethylamine (entry 5). Finally, **8e** was obtained in quantitative yield when a 1.2 equiv of **22a** was used (entry 6), although the isolated yield of **8e**

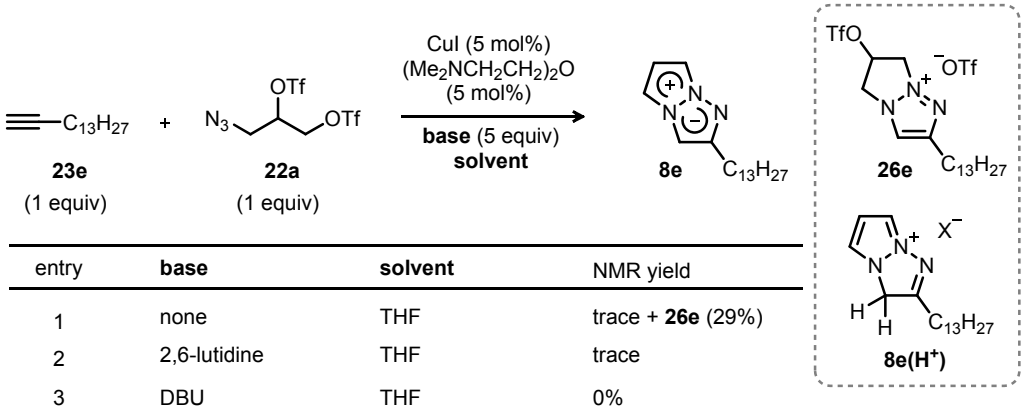

entry	**base**	**solvent**	NMR yield
1	none	THF	trace + **26e** (29%)
2	2,6-lutidine	THF	trace
3	DBU	THF	0%
4	*i*-Pr_2EtN	THF	66%
5	Et_3N	THF	80%
6[a]	Et_3N	THF	quant
7	Et_3N	ether	41%
8	Et_3N	t-BuOH	49%
9[b]	Et_3N	H_2O	56% (isolated)
10	Et_3N	DMSO	0%

[a] 1.2 equiv of **22a** was used. [b] Phenylacetylene (**23c**) was used.

Table 1. Optimization of the reaction condition for preparation of TAP.

was reduced to 71% because of partial generation of protonated blue product **8e(H$^+$)**, which strongly adsorbed on silica gel, during column chromatography. In addition, this reaction also proceeded in other solvents such as ether and *t*-BuOH. Furthermore, it is noteworthy that the reaction with phenylacetylene (**23c**) proceeded even in water, whereas the reaction in aprotic polar solvents such as DMSO did not proceed due to decomposition of **22a**.

In addition, triflate groups were necessary in this reaction and the click reaction of the azides **22b** and **22c** possessing mesyloxy and tosyloxy groups as a leaving group gave the corresponding triazoles **27bc** and **27cc** in quantitative yields, respectively, and the triazolium ion **26c** and TAP **8c** were not detected.

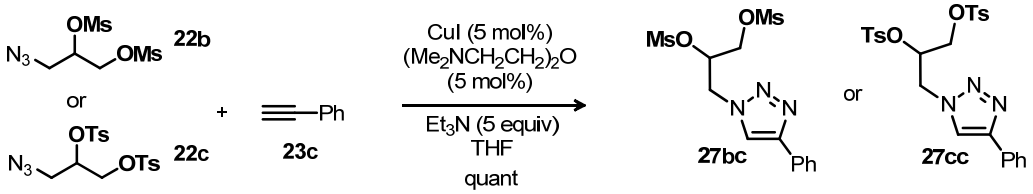

Scheme 6. The similar reaction of phenylacetylene (**23c**) with the azide fragments possessing mesylate **22b** and tosylate **22c**

Since the highly reactive azide **22a** is potentially hazardous, the manipulation of **22a** requires extreme caution. The multigram-scale preparation of **22a** was actually conducted several times without any accident, and the author found that a solution of **22a** in 1,4-dioxane was stable enough to be heated to 100 °C for 2 h. Observation of the thermal stability of **22a** by thermogravimetry analysis (TGA) indicates slow thermal degradation at > 90 °C (Figure 5).[21] Furthermore, microscopic observation of the thermolytic behavior of **22a** using a melting point apparatus revealed that **22a** was partially volatilized at 92 °C. Therefore, the azide **22a** is basically stable below 90 °C. However, it is still best to handle this molecule with great care.

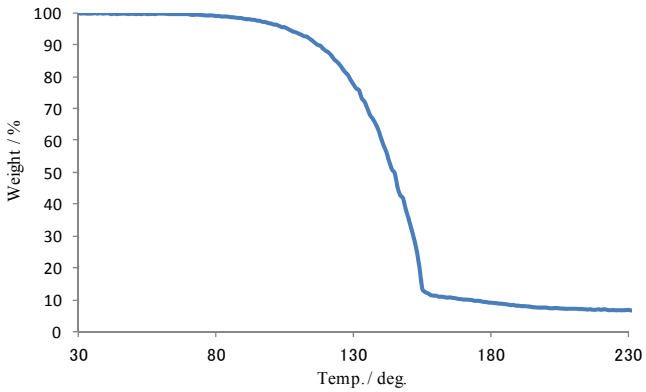

Figure 5. Thermogravimetry analysis (TGA) of the azide **22a**. It was showed that 5% loss of the weight was observed at 107 °C.

Having established the optimal condition for preparation of TAP, the reaction of various alkynes was examined. The click reaction of 1-hexyne (**23f**) with **22a** afforded the desired 2-butyl-TAP (**8f**) in 84% isolated yield. The aliphatic acetylenes possessing a functional group such as methyl propargyl ether (**23g**) and methyl propiolate (**23h**) also gave the corresponding desired TAPs, **8g**, and **8h** in 80% and 90% yields, respectively. The reaction of phenyl acetylene (**23c**) and biphenyl acetylene (**23i**) afforded TAP **8c** and **8i** in 89% and 81% yields, respectively. While the reaction of electron-rich derivative **22j** showed a slight decline in yield to give TAP **8j** in 56% yield, the phenyl acetylene derivatives having an electron withdrawing group such as a chloro group (**23k**), an ester group (**23l**), and a nitro group (**23m**) also gave the desired TAPs **8k**, **8l** and **8m** in 81%, 73% and 96% yields, respectively. The TAP derivatives possessing

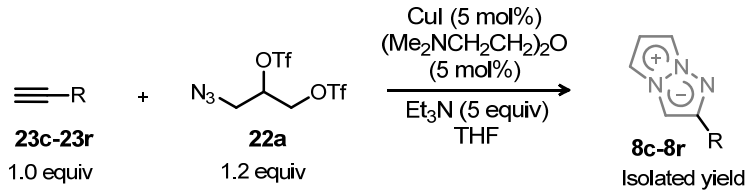

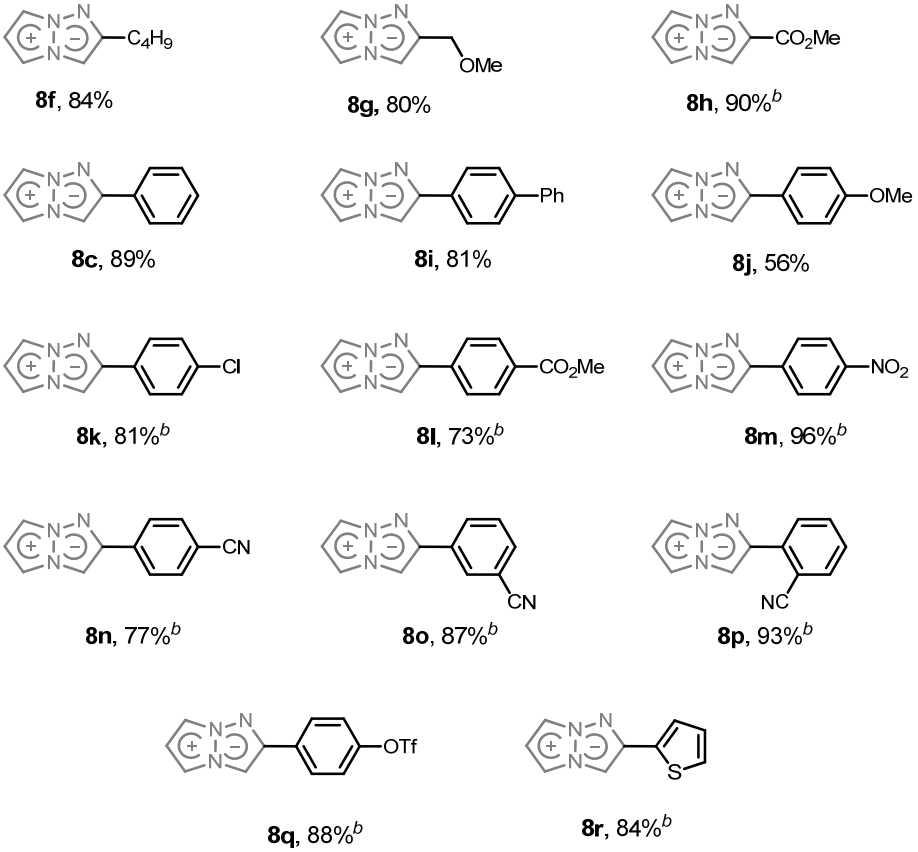

[a]isolated yield. [b]alkyne (1.2 equiv), azide (1.0 equiv), THF (0.01 M).

Table 2. The synthesis of TAPs possessing various functional groups.[a]

cyano group at *para* (**8n**), *meta* (**8o**), and *ortho* (**8p**) position on benzene ring were also obtained in good yields (77%, 87% and 93%, respectively). The reaction of triflate derivative **23q**, which has a coupling site for further reactions, also afforded **8q** in 88% yield. Furthermore, thiophene derivative as a heteroaromatic analog was also reactive to afford desired TAP (**8r**) in 84% yield. Thus, it was confirmed that the established preparative method for the TAPs **8** is applicable to various acetylenes.

The structure of **8n** was unequivocally established by an X-ray crystallographic analysis, which elucidated that **8n** has a 10π-electron resonance structure as an aromatic ring, as shown in Figure 6. The structures of the other TAPs were also confirmed by the correlation of spectral data with **8n**.[22]

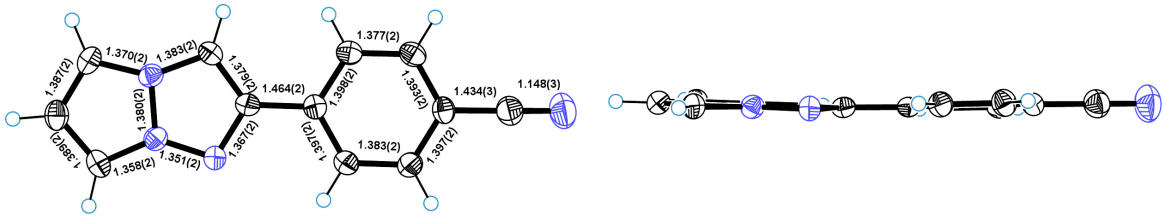

Figure 6. ORTEP drawing of the molecular structure and bond lengths of **8n**.

Next, the first synthesis of unsubstituted TAP (**8a**) was examined in order to elucidate the physical and fluorescence properties of the TAP skeleton. A similar click reaction of **22a** with (trimethylsilyl)acetylene (**23s**) afforded **8s** in 71% NMR yield. It was found that **8s** decomposed readily during silica-gel column chromatography. Therefore, the crude **8s** was directly subjected to desilylation with TBAF to give **8a** in 46% overall yield as a volatile oil (Scheme 7).

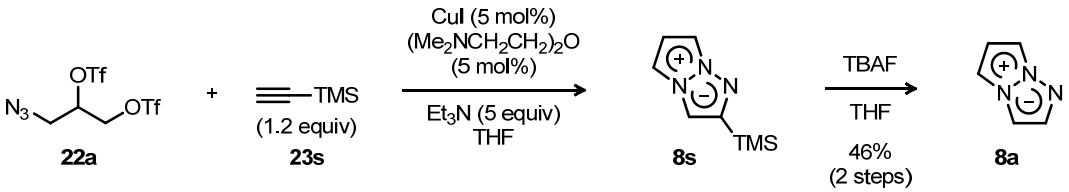

Scheme 7. The first synthesis of unsubstituted TAP **8a**.

In summary, the single-step synthesis of TAPs via click-cyclization-aromatization cascade reaction has been established and successfully obtained TAP derivatives possessing various functional groups in good yields. Furthermore, the parent analog **8a** was first synthesized by desilylation of 2-trimethylsilyl-TAP (**8s**).

Chapter 2

Investigation of the Optical Properties of 1,3a,6a- Triazapentalene Derivatives

2-1. Basic optical properties of 1,3a,6a-Triazapentalenes

Having prepared various TAP derivatives, the author next tried to investigate their optical properties. First, the measurement of absorption and fluorescence spectra of simple **8a** exhibited obvious absorption (λ_{abs} = 288 nm) and fluorescence (λ_{em} = 389 nm) bands, respectively (Figure 7). This was a first example of experimental demonstration that TAP skeleton not possessing additional fused ring was fluorescent chromophore, although fluorescence quantum yield (Φ_F) was not high (Φ_F = 0.014). On the other hand, benzotriazapentalene (**11**), prepared by the procedure of Bettinetti,[14b] exhibited almost no fluorescence (Φ_F < 0.001).

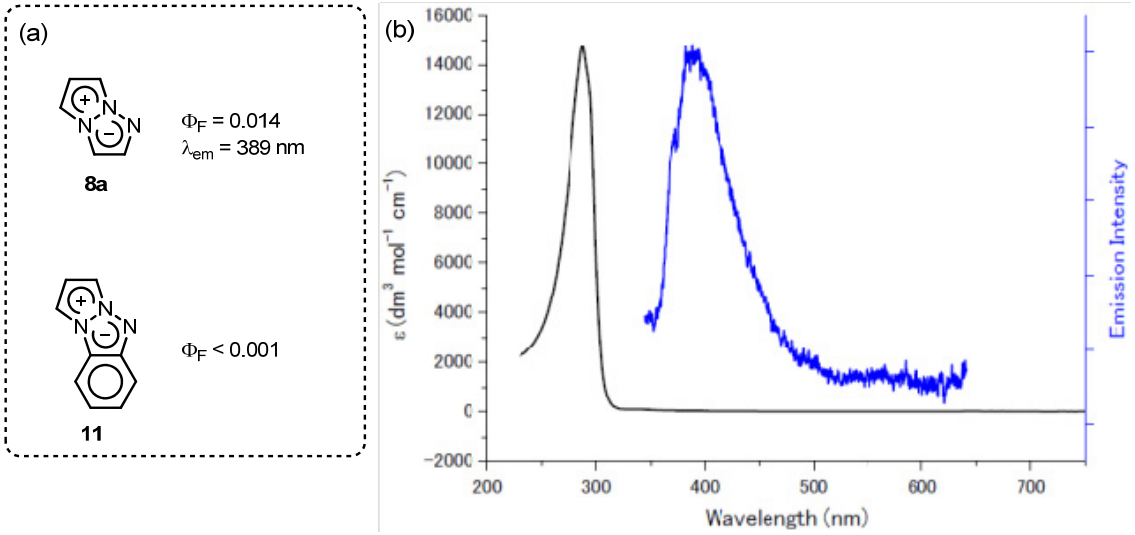

Figure 7. (a) The structures of unsubstituted simple TAP (**8a**) and benzotriazapentalene (**11**) and (b) absorption (left) and fluorescence (right) spectra of **8a**.

Having been encouraged by the above result, the author next turned to investigate optical properties of the other selected TAPs **8c-m** and the results were summarized in Table 3. In contrast to **8a**, 2-substituted derivatives had characteristic absorption bands from 300 nm to 500 nm (see experimental section). In addition, noteworthy fluorescence was also observed. For example, 2-methoxycarbonyl TAP (**8h**) exhibited much stronger fluorescence (Φ_F = 0.18) and longer fluorescence wavelength (λ_{em} = 431 nm) than those of **8a** with large Stokes shift (89 nm) despite its compact molecular size. Furthermore, it was found that fluorescence maxima of

2-phenyl analogs possessing various functional groups at 4'-position on benzene ring varied widely. For example, methoxy- phenyl (**8j**, λ_{em} = 413 nm), phenyl (**8c**, λ_{em} = 419 nm), biphenyl (**8i**, λ_{em} = 456 nm) and chlorophenyl (**8k**, λ_{em} = 432 nm) analogs emitted from violet to blue light (Figure 8). On the other hand, the derivatives possessing a strong electron-withdrawing group such as methoxycarbonyl (**8l**, λ_{em} = 456 nm), cyano (**8n**, λ_{em} = 456 nm) and nitro group (**8m**, λ_{em} = 456 nm) exhibited red-shifted fluorescence emitting from green to yellow light.

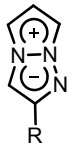	 **8a**	 **8h**	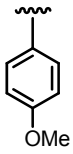 **8j**	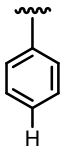 **8c**	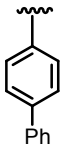 **8i**	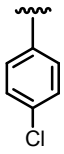 **8k**	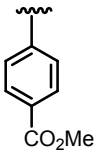 **8l**	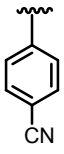 **8n**	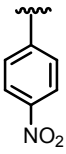 **8m**
λ_{abs} (nm)	-	342	330	326	345	324	376	381	412
λ_{em} (nm)	389	431	413	419	456	432	510	509	556
Stokes Shift (nm)	-	89	83	93	111	108	134	128	144
Φ_F[d]	0.014[b]	0.18[c]	0.053[b]	0.026[b]	0.20[c]	0.059[b]	0.44[c]	0.15[c]	0.14[c]
σ_p	-	-	-0.28	0	0.02	0.22	0.47	0.71	0.81
color	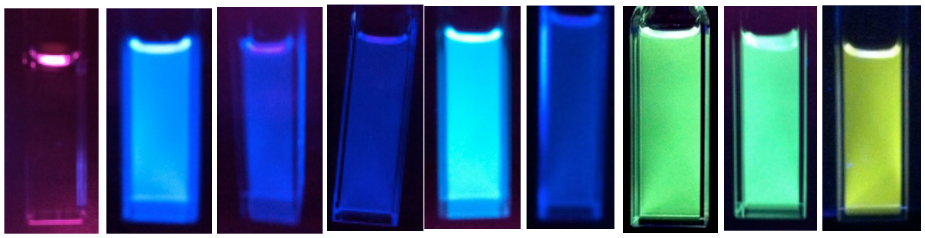								

[a]in CH_2Cl_2. [b]excited at 330 nm. [c]excited at 370 nm. [d]refered to 9,10-DPA

Table 3. The optical properties of selected TAPs.

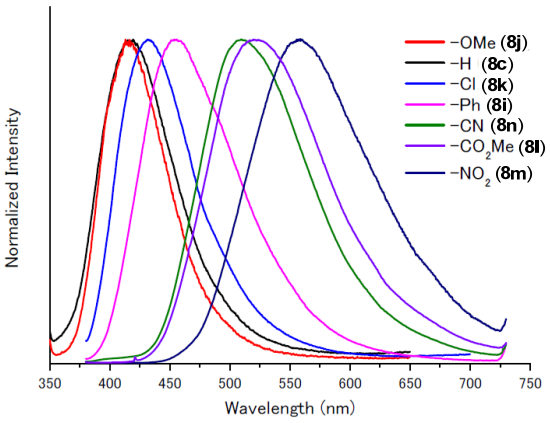

Figure 8. Fluorescence spectra of phenyl analogs.

Therefore, since the author focused on the electric factor of a substituent at 4'-position on benzene ring, the correlation of fluorescence maxima with Hammett value (σ_p)[23] was investigated (Figure 9). As a result, the interesting correlation was observed that emission maxima shifted from 413 nm (**8j**) to 556 nm (**8m**) with increasing the Hammett values of 4'-substituent. That is, the suitable choice of substituent on benzene ring enabled to design fluorescent molecules which displayed desired color.[24]

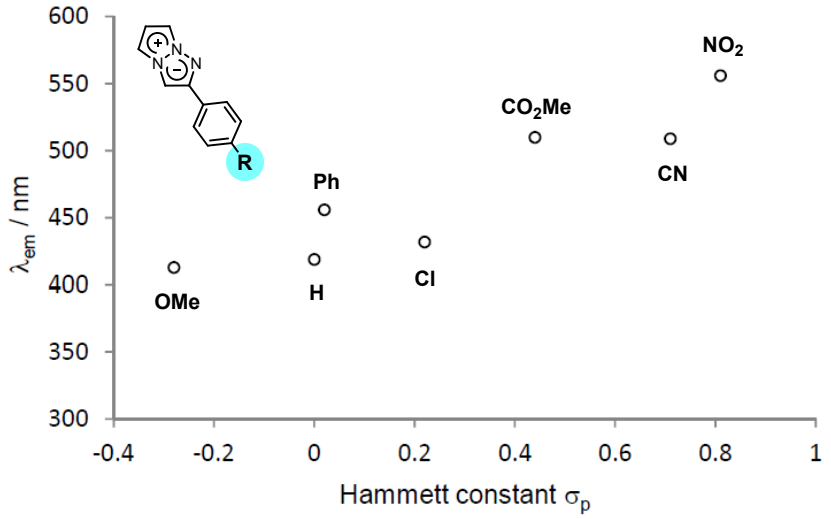

Figure 9. The correlation of fluorescence maxima (λ_{em}) with Hammett constant (σ_p).

In addition, these phenyl analogs had large Stokes shift (83-144 nm)[25]. In terms of practical fluorescence microscope observation, fluorescent molecules with large Stokes shift, which is represented by difference between emission and absorption maxima, are preferred for detection of fluorescence so that the overlap with exciting light would be suppressed.

Next, photo-stability of TAPs was examined in order to confirm the availability of TAPs for a dye. Although simple TAP derivatives **8a** and **8h** along with electron-rich analog **8j** occurred degradation by irradiation of UV light (254 nm, 6 W) within several minutes, **8h** was stable enough to observe fluorescence with longer wavelength light (380 nm) during measurement. In contrast, phenyl TAP analogs possessing cyano (**8n**) and nitro group (**8m**) as electron-withdrawing group have slightly decomposed but mainly remained even in 60 min. Therefore, it was revealed that TAPs having electron-deficient benzene ring was stable enough to use as a fluorescent probe even under UV irradiation. Further investigation and improvement of photo-stability of TAPs is currently underway in our group.

2-2. Solvent Effect: Positive Fluorosolvatochromism

Next, solvent effect of optical properties was investigated. In concrete term, absorption and fluorescence spectra of 4'-cyanophenyl derivative (**8n**) were measured in benzene, dichloromethane, acetone, acetonitrile, respectively (Figure 10). Notably, while absorption maxima did not change in each solvent, fluorescence maxima shifted to longer wavelengths with increasing solvent polarity. Thus, **8n** was revealed to show strong positive fluorescence solvatochromism.[26] In living cells, it is known that there are locally hydrophobic points such as surface of cell membrane and pocket of proteins in contrast to aqueous environment and some kinds of solvatochromic molecules change the fluorescence color depending on surrounding environment[27, 28]. Therefore, it is possible that TAP and its probe molecule also would be used for an environmentally sensitive probe.

(a)

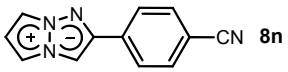

solvents	PhH	CH_2Cl_2	Me_2CO	MeCN
λ_{abs} (nm)	381	381	384	380
λ_{em} (nm)	464	509	536	548
Φ_F [a,b]	0.17	0.15	0.0066	0.021
color	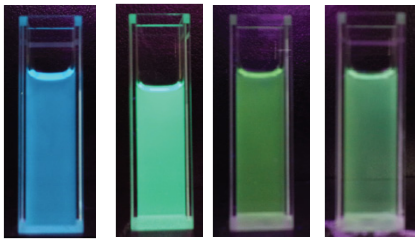			

[a]excited at 380 nm. [b]refered to 9,10-DPA.

(b)

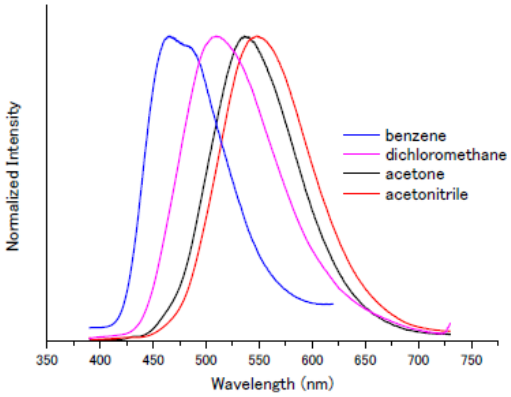

Figure 10. (a) The optical properties of **8n** in various solvents and (b) fluorescence spectra.

2-3. Fluorescence of TAPs in the Solid States

The author found that some of the present TAPs exhibited fluorescence even in the solid state as the data were shown in Figure 11 (next page). The solid 4-cyanophenyl analog **8n** showed a long-wavelength shift (λ_{em} = 526 nm) as compared with the fluorescence in dichloromethane (λ_{em} = 509 nm). Although the Φ_F value of **8n** in the solid state (Φ_F = 0.13) is slightly smaller than that in dichloromethane (Φ_F = 0.15), it is noteworthy that the solid compound still exhibits intense fluorescence despite its compact molecular size. The solid methoxycarbonyl analog **8l** also exhibited remarkable fluorescence in the wavelength region similar to that in dichloromethane, whereas the Φ_F value substantially decreased (Φ_F = 0.06).

In contrast, the solid state of nitrophenyl analog **8m** showed no fluorescence despite its intense fluorescence in dichloromethane (Φ_F = 0.16). Elucidation of the mechanistic details of these solid-state fluorescence properties and their applications to light-emitting devices are currently underway in our laboratory.

(a)

	λ_{em}^{max} (nm)	Φ_F	color
8n 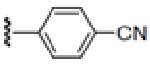	526	0.13	
8l 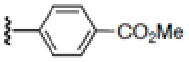	503	0.06	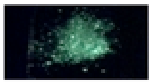
8m 	N/A	0.00	

(b)

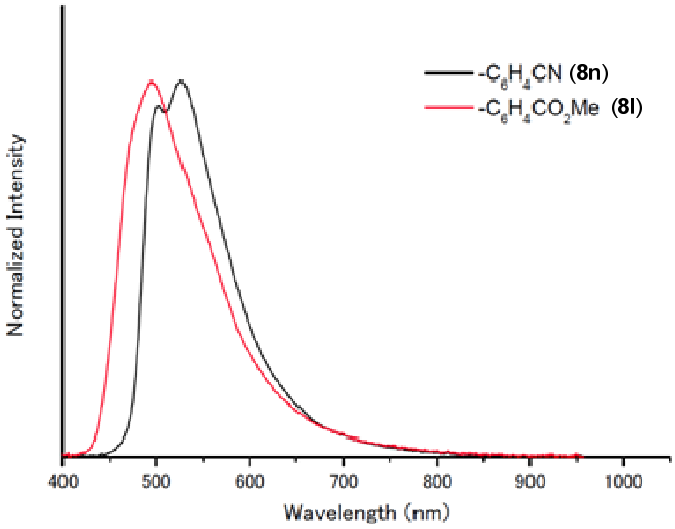

Figure 11. Fluorescence behavior of selected TAPs in the solid state. (a) fluorescence parameters of TAPs **8l-n**, (b) fluorescence spectra of **8l** and **8n** in the solid state.

2-4. pH response of TAPs

During development of preparative method for TAPs, it was observed that a solution of several derivatives in $CDCl_3$ changed color from colorless or pale yellow to green or blue. This interesting phenomena was expected to be caused by trace amount of hydrogen chloride (HCl or DCl) generated from degradation of $CDCl_3$, because the use of $CDCl_3$ treated with basic alumina suppressed change of color. In order to confirm this hypothesis, a solution of TAP **8n** in dichloromethane (0.002 M) was treated with TFA as an acid. As a result, change of color from

pale yellow to blue was observed and new broad absorption band appeared in a range of 550 nm to 750 nm (Figure 12). By NMR analysis, it was determined that an acidified product was 3-protonated compound **8n(H$^+$)**. Furthermore, treatment of the blue solution with triethylamine as a base induced color change to give a pale yellow solution. Repeated treatment with TFA and Et_3N was revealed that this process was reversible. Further investigation of pH dependence is ongoing in our group.

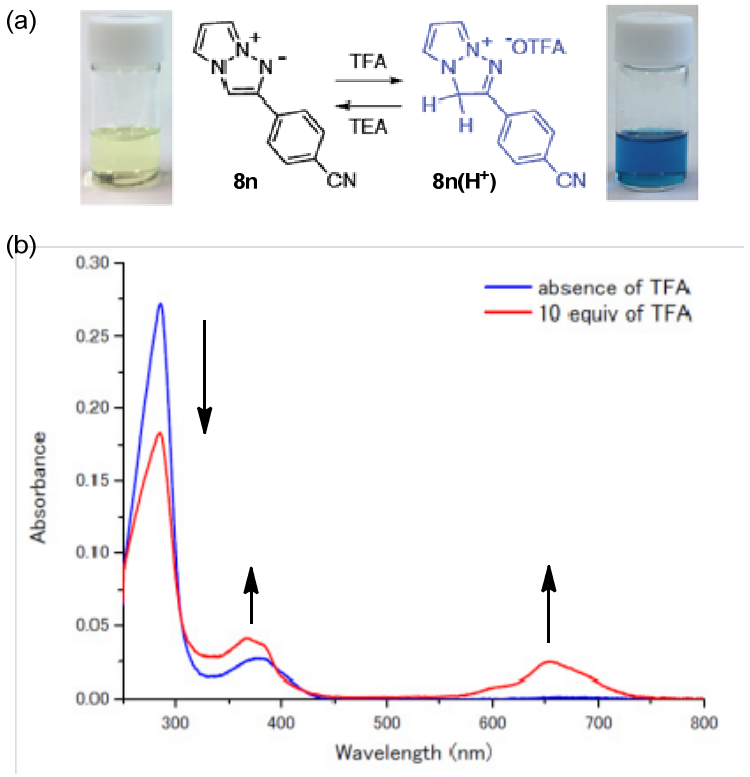

Figure 12. Acid-base behavior of **8n**. (a) the structure of TAP **8n** and 3-protonated TAP **8n(H$^+$)**, (b) absorption spectra of **8n** and **8n(H$^+$)**

2-6. Effect of Substituent at 4-position on TAP

Since it has been elucidated that substituent at 2-position on TAP skeleton played an important role of fluorescence enhancement and wavelength control, effect of substituent at other positions has next attracted our attention. Herein, the author described the properties of 2,4-di- substituted TAPs.[29]

The syntheses of 2,4-di-substituted TAPs were shown in Scheme 8. Azidoditriflates possessing methyl (**22d**) or phenyl (**22e**) group were readily obtained from the corresponding epoxyalcohol **28d** and **28e** by regio-selective ring-opening reaction with azide[30] followed by triflation of two hydroxyl groups. Prepared azide fragments were applied to our click reaction

with phenylacetylene (**23c**) and 4-cyano-phenylacetylene (**23n**) to afford desired 2,4-di-substituted TAPs in good yields.

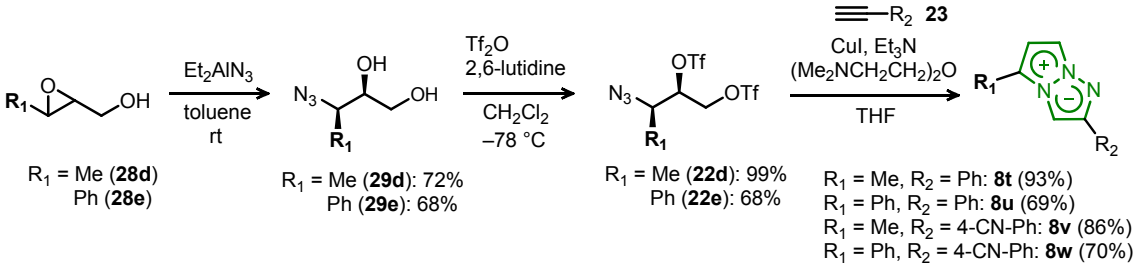

R_1 = Me (**28d**)
Ph (**28e**)

R_1 = Me (**29d**): 72%
Ph (**29e**): 68%

R_1 = Me (**22d**): 99%
Ph (**22e**): 68%

R_1 = Me, R_2 = Ph: **8t** (93%)
R_1 = Ph, R_2 = Ph: **8u** (69%)
R_1 = Me, R_2 = 4-CN-Ph: **8v** (86%)
R_1 = Ph, R_2 = 4-CN-Ph: **8w** (70%)

Scheme 8. Synthesis of 2,4-di-substituted TAPs.

The optical properties of synthesized 2,4-di-substituted TAPs and the corresponding 2-mono-substituted TAPs were listed in Table 4. In comparison with 2-phenyl TAP (**8c**), 4-methyl analog (**8t**) showed 18 nm longer fluorescence wavelength shift and decreasing to 0.015 in Φ_F, whereas 4-phenyl analog (**8u**) exhibited 38 nm longer absorption wavelength shift and 21 nm shorter fluorescence wavelength shift with decreased Φ_F value (0.014). On the other

TAP		λ_{abs} (nm)	λ_{em} (nm)	Φ_F[a]
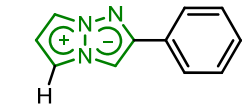	**8c**	326	419	0.026[b]
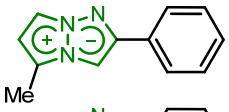	**8t**	330	437	0.015[b]
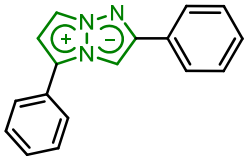	**8u**	364	398	0.014[b]
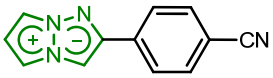	**8n**	381	509	0.15[c]
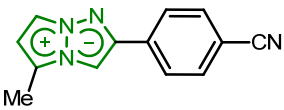	**8v**	389	543	0.18[c]
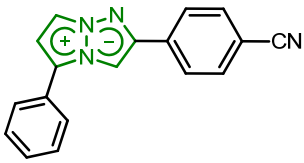	**8w**	387	542	0.46[c]

[a] In CH_2Cl_2 and 9,10-DPA was used as standard. [b] excited at 340 nm. [c] excited at 370 nm.

Table 4. The optical properties of 2,4-di-substituted TAPs.

hand, fluorescence maxima of 4-substituted- 2-cyanophenyl TAPs shifted to 543 nm (**8v**) and 542 nm (**8w**) in contrast to **8n** (λ_{em} = 509 nm), while absorption maxima displayed slightly longer shifts. Notably, fluorescence quantum yield of **8w** dramatically increased from 0.15 (**8n**) to 0.46 (**8w**), whereas that of **8v** exhibited slight increase. A general effect of an introduction of 4-substitutent have been unclear yet but further investigation is ongoing in our group.

In summary of Chapter 2, optical properties, especially fluorescence character, of TAPs were revealed. First, it was found that the parent small TAP **8a** showed fluorescence. TAPs exhibited intense fluorescence and large Stokes shift despite its compact molecular size. In particular, fluorescence wavelength of 2-phenyl TAP analogs shifted to longer wavelength with increasing Hammett value of substituent at 4'-position on benzene ring. Therefore, it would be possible to control fluorescence wavelength by the suitable choice of functional groups. In the next chapter, the author would describe an actual example of wavelength control by using this character and development of fluorescent labeling reagent based on TAP.

Chapter 3

Application of 1,3a,6a-Triazapentalene Derivatives as a Fluorescent Labeling Reagent

3-1. Strategy for Fluorescent Labeling of Bioactive Small Molecules

Since it was clarified that TAPs displayed interesting and useful fluorescence properties, the author next studied on application of TAPs for fluorescence labeling and planed three labeling methods; (i) labeling via an amino group by condensation with carboxylic acid to generate stable amide bond, (ii) labeling via a thiol group using Michael acceptor such as maleimide, and (iii) labeling of an alkyne via click reaction constructing TAP skeleton (Figure 13). In this chapter, the author focused on fluorescent labeling via an amino group (i) because amide bond linkage is most common in fluorescent labeling chemistry.[7]

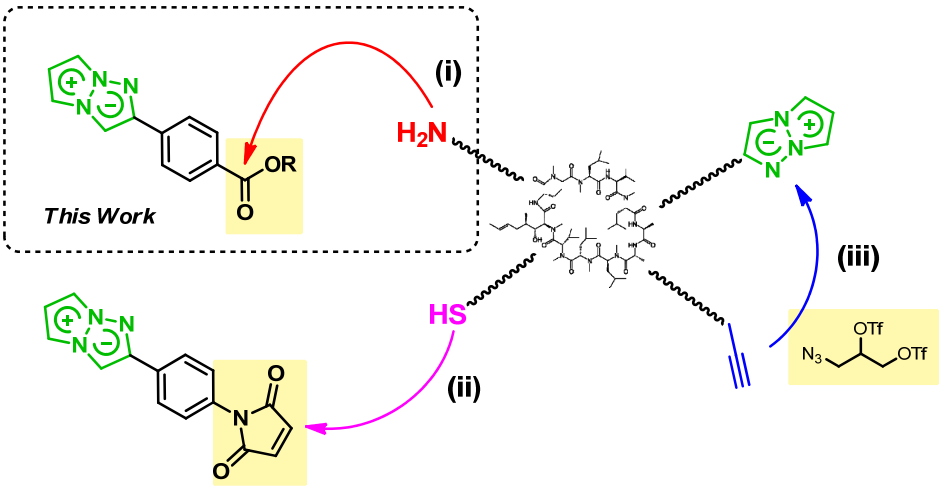

Figure 13. Fluorescence labeling method. (i) amine-labeling, (ii) thiol-labeling, (iii) alkyne-labeling.

First, fluorescence labeling of an amino acid with TAP was examined (Scheme 9). Methyl ester moiety of small TAP **8h** emitting blue light was hydrolyzed with 1 equiv of lithium hydroxide to afford lithium carboxylate (**8x**), which emitted blue light (λ_{em} = 449 nm) even in water although fluorescence quantum yield was not high (Φ_F = 0.034). Then, condensation of **8x** with glycine ethyl ester (**30**) under a usual condition[31] resulted in labeled product **8y** in 52% two-step yield. Thus, it was successful to label glycine derivative with TAP and confirm fluorescence of **8y** (λ_{em} = 418 nm, Φ_F = 0.033). However, although **8x** was the most compact TAP derivatives that can be connected by amide linkage, fluorescence observation of **8y** required excitation with UV light and fluorescence wavelength was not long enough to imaging inside cell. This result turned our attention for expansion of fluorescence wavelength to the

yellow and red color region.

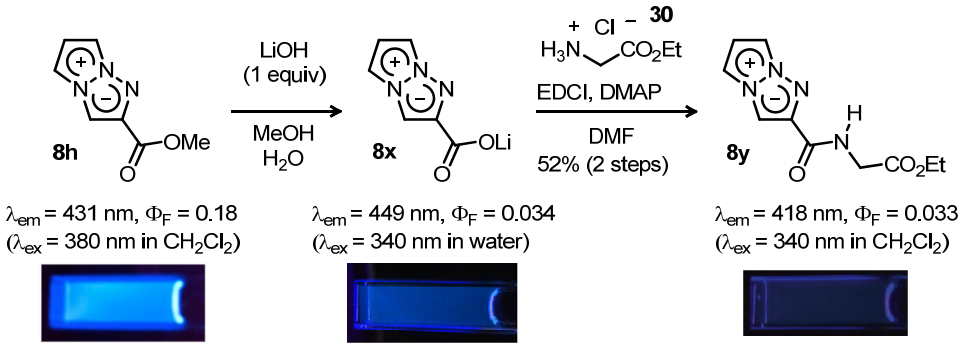

Scheme 9. Fluorescent labeling of glycine derivative.

In order to obtain TAPs with longer wavelength, it was assumed that the effect of substituent on benzene ring would be useful. As described in Chapter 2, fluorescence wavelength shifted from blue to lime-green with increasing the electron-withdrawing ability of 4'-subsitutent on benzene ring (Figure 14). However, since TAP (**8m**) possessing nitro group which is one of the strongest electron-withdrawing groups exhibited lime-green fluorescence, modification of substituent only at 4'-position was considered to be limited to extend further longer-wavelength shift. Therefore, an introduction of additional electron-withdrawing group at suitable position, for example, 2'- and/or 6'-position was seemed to be effective for further modification.

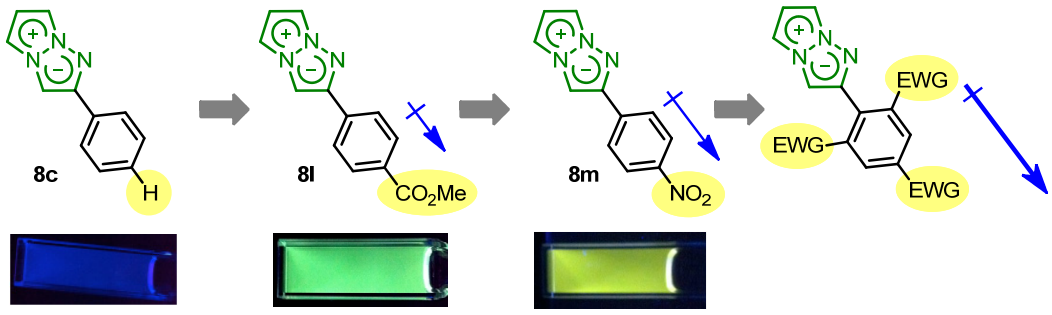

Figure 14. A trend of fluorescent color and a plan for development of TAP emitting further long-wavelength light.

3-2. Orientational effect of substituent on 2-phenyl ring.

A cyano group was chosen as additional electron-withdrawing group due to its small size and stability against UV irradiation. Thus, in order to investigate a suitable position for introduction of the cyano group to the benzene ring, the optical properties of 2-phenyl TAPs possessing *para*- (**8n**), *meta*- (**8o**), and *ortho*-cyano group (**8p**) were investigated. In contrast to

8n, *meta*-analog **8o** exhibited shorter shift of absorption (λ_{abs} = 327 nm) and fluorescence maxima (λ_{em} = 493 nm), whereas fluorescence quantum yield was increased to 0.24. On the other hand, *ortho*-cyano analog **8p** showed similar absorption (λ_{abs} = 376 nm) and fluorescence maxima (λ_{em} = 515 nm) to these of **8n** and higher fluorescence quantum yield (Φ_F = 0.24). Therefore, introduction of electron-withdrawing group to *ortho*-position was expected to be more suitable for expansion of fluorescence wavelength to the yellow and red color region.

TAP		λ_{abs} (nm)	λ_{em} (nm)	Φ_F[a]	color
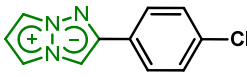	**8n**	381	509	0.15	
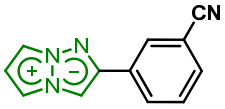	**8o**	327	493	0.24	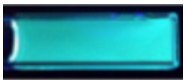
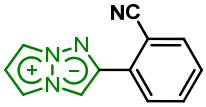	**8p**	376	515	0.24	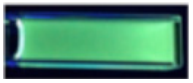

[a] excited at 370 nm in CH_2Cl_2 using 9,10-DPA as a standard.

Table 5. Oriented effect of cyano group on benzene ring.

3-3. Rational Design and Synthesis of TAPs with long wavelength

Based on the structure of TAP **8l** bearing an ester group as a linking site, TAPs possessing one or two *ortho*-cyano groups were designed. That is, **8l** and *ortho*-cyano analog **8p** emitted green light, and then the introduction of a cyano group to **8l** was expected to induce a further longer shift from 520 nm (green). Furthermore, **8aa**, which has additional cyano group, was expected to exhibit greater shift.

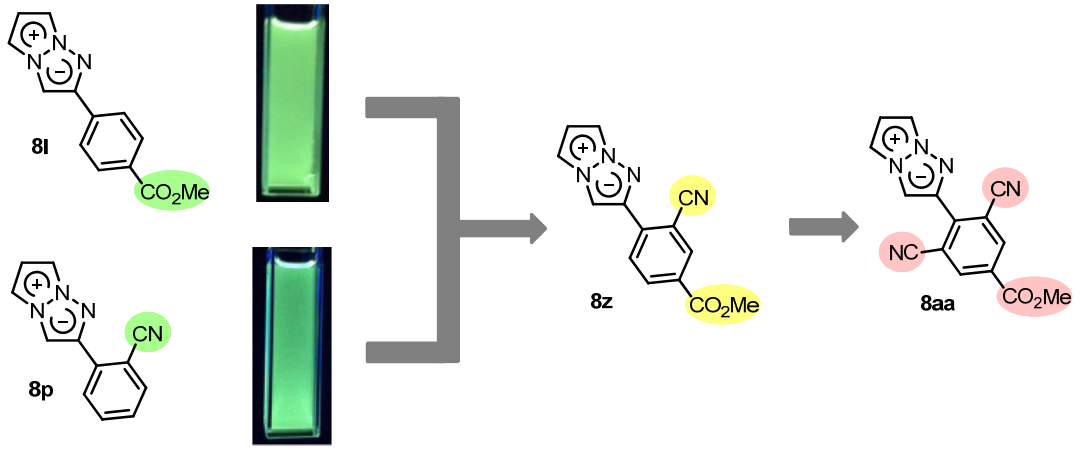

Figure 15. Rational design of TAPs with long wavelength

The author first examined to synthesize an alkyne fragment **23z**. After commercially available iodide **31** was converted into TBS-protected alkyne **32** by Sonogashira coupling[32] with TBS-acetylene, **32** was treated with $Pd(PPh_3)_4$ and tributylamine in MeOH/DMF under a CO atmosphere to give methyl ester **33**. Finally, treatment of **33** with TBAF and AcOH afforded desired alkyne **23z**. Preparation of an alkyne fragment possessing two cyano groups was next examined. Although the Sonogashira coupling of the known iodide **34**[33] under various conditions initially afforded not desired silyl alkyne **35** but mainly deiodide product, the combination of $Pd_2(dba)_3 \cdot CHCl_3$, tri(2-furyl)phosphine, and triethylamine in DMF at 50 °C was found to afford the desired coupling product **35**.[34] Then, removal of the TBS group gave the alkyne fragment **23aa**.

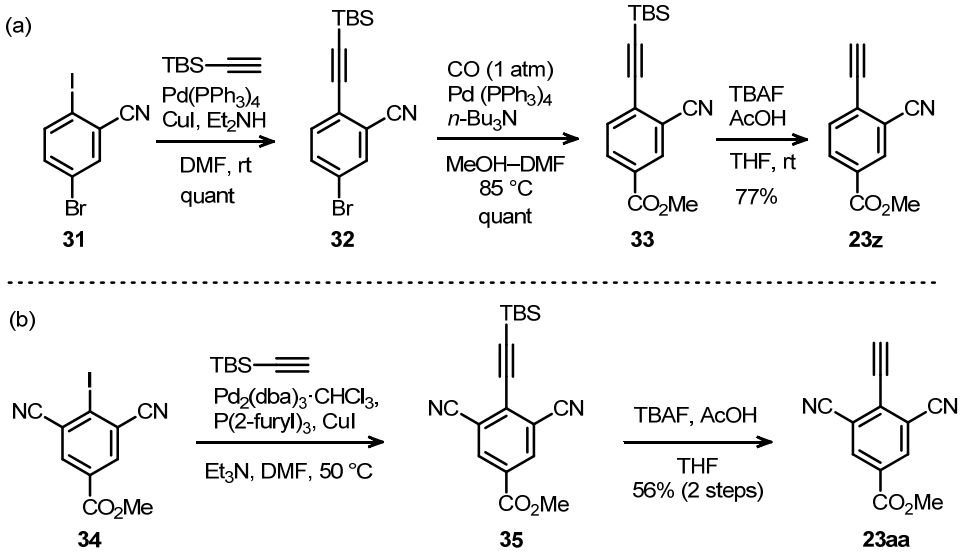

Scheme 10. The preparation of the alkyne fragments **23z** (a) and **23aa** (b)

With alkyne fragments in hand, the click reaction of **23z** and **23aa** with azide fragment **22a** was investigated. As a result, these reactions smoothly proceeded to give the desired TAPs **8z** and **8aa** in 71% and 72% yields, respectively.

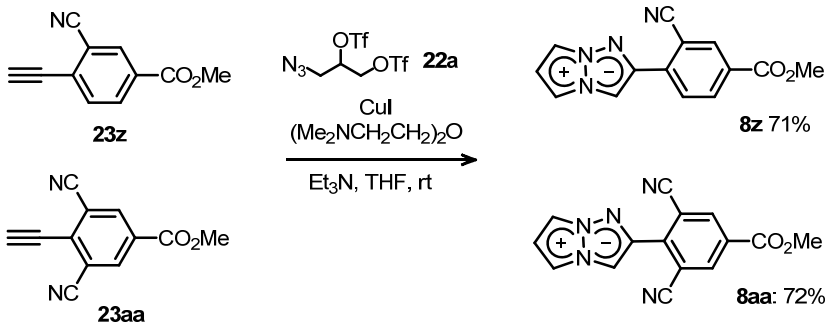

Scheme 11. The synthesis of TAPs **8z** and **8aa**

The optical properties of synthesized TAPs **8z** and **8aa** were investigated. As was expected, the mono-cyano analog **8z** exhibited longer-wavelength shift of fluorescence from 510 nm of **8l** to 572 nm, and it emitted yellow fluorescence resulting from 44 nm longer shifts of absorption maxima (λ_{abs}: from 376 to 420 nm). Although fluorescence quantum yield was decreased to 0.34, this value was high enough to use as a fluorescent probe. Furthermore, TAP **8aa**, which possessed two cyano groups, showed further longer wavelength shift of absorption (λ_{abs} = 466 nm) and fluorescence (λ_{em} = 632 nm) to emit a red light although fluorescence quantum yield decreased to 0.096. It was noteworthy that Stokes shifts of **8z** (152 nm) and **8aa** (166 nm) also became larger than that of **8l** (134 nm). There have been a few examples of fluorescent molecules that exhibited such a large Stokes shift in the region over 550 nm of wavelength. In addition, **8l** and **8z** in the solid state also emitted green (λ_{em} =496 nm) and yellow (λ_{em} =549 nm) lights, whereas fluorescence quantum yields showed low values (Φ_F = 0.06 in each case). On the other hand, di-cyano analog **8aa** exhibited almost no fluorescence.

TAP		state	λ_{abs} (nm)	λ_{em} (nm)	Φ_F[a]	color
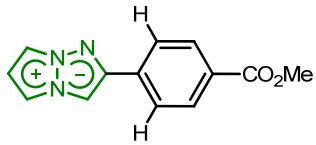	**8l**	solution[a]	376	510	0.44	
		solid	N/A	496	0.06	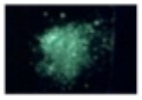
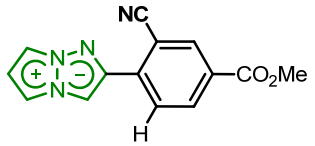	**8z**	solution[a]	420	572	0.34	
		solid	N/A	549	0.06	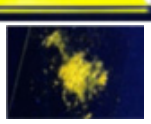
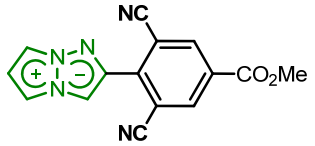	**8aa**	solution[a]	466	632	0.096	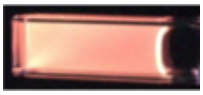

[a] in CH_2Cl_2

Table 6. The optical properties of a basic ester derivative **8l**, mono-cyano analog **8z**, and di-cyano analog **8aa**.

As described above, it was successful to develop TAPs which exhibited longer-wavelength fluorescence. However, extinction coefficient (ε) of these compounds within visible light region was not high although fluorescence quantum yield was acceptable value. For example, ε values of **8z** presented 6.3×10^2 dm^3 mol^{-1} cm^{-1} (420 nm) and 9.5×10^3 dm^3 mol^{-1} cm^{-1}

(285 nm), respectively (absorption spectra were shown in experimental section). Therefore, next subject was improvement of ε value to obtain more bright fluorescence derivative. As one of the solution toward this problem, the author has found that 4-phenyl analogs enhanced extinction coefficient (Table 7). In the absorption spectra of 4-phenyl analogs **8ab** and **8ac**, which were prepared by click reaction with the corresponding azide **22e**, new strong absorption bands appeared within a range from around 300 nm to 380 nm. Their ε values were 2.3×10^4 (λ_{abs} = 345 nm, **8ab**) and 3.8×10^4 (λ_{abs} = 336 nm, **8ac**) $dm^3\ mol^{-1}\ cm^{-1}$. Furthermore, extinction coefficient existing in longer-wavelength region was increased to ca. 7.5×10^3 (λ_{abs} = ca. 375 nm, **8ab**) and 4.6×10^3 (λ_{abs} = 432 nm, **8ac**), respectively, although fluorescence quantum yields were decreased to 0.35 and 0.07. Therefore, further modification of substituent at 4-position on TAP skeleton might be effective to develop more bright TAPs.

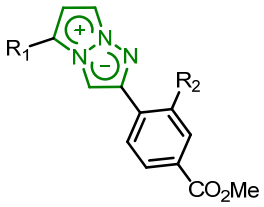

R_1	R_2	8	yield/%	ε /$dm^3\ mol^{-1}\ cm^{-1}$ (λ_{abs}/nm)	Φ_F (λ_{em}/nm)
H	H	**8l**	–	1.2×10^3 (376)	0.44 (510)
Ph	H	**8ab**	82	ca. 7.5×10^3 (ca. 375) 2.3×10^4 (345)	0.35 (548)
H	CN	**8z**	–	6.3×10^2 (420)	0.34 (572)
Ph	CN	**8ac**	88	4.6×10^3 (432) 3.8×10^4 (336)	0.07 (613)

Table 7. The optical properties of **8l**, **8ab**, **8z**, and **8ac**.

In addition, fluorosolvatochromism of yellow fluorescent TAP **8z** was investigated. Aprotic solvents such as benzene, dichloromethane, and acetone showed positive solvatochromism emitting green, yellow, and orange light, respectively. Interestingly, fluorescence spectra in protic solvents such as methanol and water shifted to shorter region and

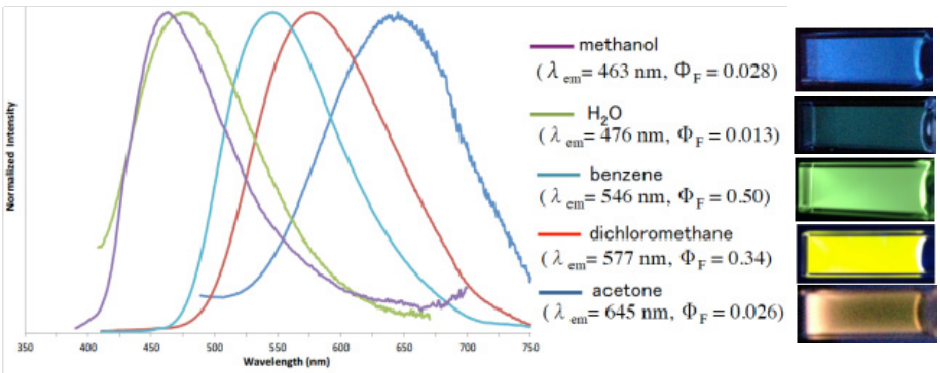

Figure 16. Fluorescence spectra and color of **8z** in various solvents

fluorescence quantum yields were decreased. Therefore, it was expected that fluorescent color would change depending on environmental change inside cell. For example, when a fluorescent probe labeled by TAP would move from hydrophilic environment to hydrophobic environment, fluorescent color might change from blue to yellow enhancing fluorescence intensity.

3-4. Cell Staining Study toward Application for a Fluorescent Probe

Next, in order to demonstrate the utility of TAPs for fluorescent probes, fluorescence observation of TAPs inside cell was attempted. Thus, HeLa cell was treated with a solution of yellow fluorescent TAP **8z** (10 μM in 0.02% DMSO) without washing the cell medium, and monitored in the 572–642 nm wavelength region. As shown in figure 17(b), **8z** was incorporated into cell within several minutes to observe fluorescence staining of its cytoplasm successfully, whereas treatment of HeLa cell with DMSO as a control was not stained (Figure 17(a)). In addition, the cytotoxicity of this incorporation of **8z** was not detected during fluorescence observation. Interestingly, the incorporated **8z** displayed clear yellow emission regardless of blue color in water as it was described in the previous section. Furthermore, the more bright points in cytoplasm were appeared. These phenomena might be caused by hydrophobic effect involving polarity inside cell and localization of **8z** into specific organelle. Further detailed investigation is currently underway in collaborative research.

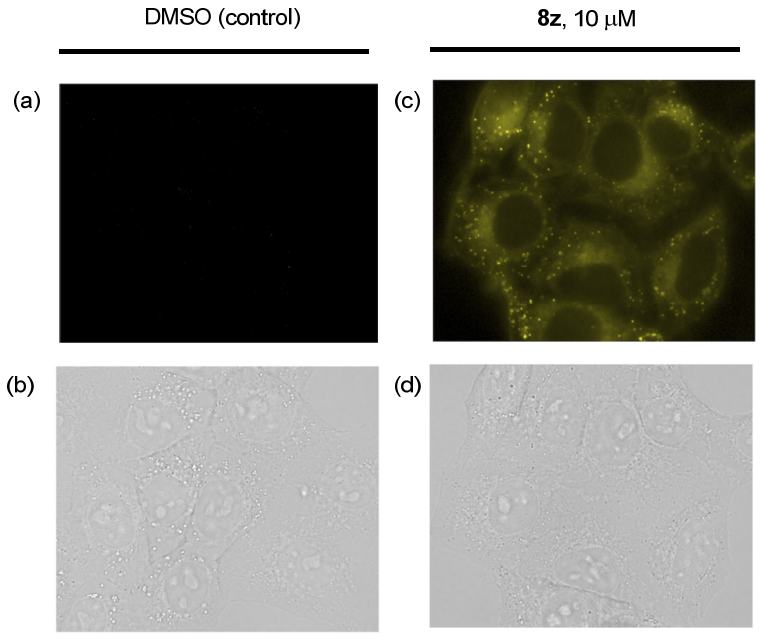

Figure 17. Observation of **8z** in HeLa cells. Living cells were cultured in 0.02% DMSO as a control (a and b) or with 10 μM **8z** in 0.02% DMSO (c and d). Uptake of **8z** was monitored by using a fluorescence microscope (BZ-9000; Keyence) in a bright-field image (b and d) or in a fluorescence image with a BZ set (FF01- 452/45 nm exciter, FF01-607/70 nm emitter, FF511 nn-Di01 dichroic mirror) (a and c).

3-5. Synthesis of a NHS Ester Derivative of TAP as a Fluorescent Labeling Reagent.

Having prepared yellow and red fluorescent TAPs, the author next tried to synthesize a NHS ester as a fluorescent labeling reagent. Yellow fluorescent TAP **8z**, which was adopted as a basic structure due to its high Φ_F value, was treated with lithium hydroxide at 50 °C followed by acidification to afford carboxylic acid **8ae** (Scheme 12). The next condensation reaction of **8ad** with *N*-hydroxysuccinimide (**36**) under usual conditions using DCC, EDCI, and other condensation agents was smoothly proceed to give desired NHS ester **8ae**. However, excess amount of *N*-hydroxysuccinimide and urea derivatives generated as by-product were not able to separate from **8ae** mainly because separation process induced degradation of **8ae**. On the other hand, the use of polymer-supported DCC-type carbodiimide reagent, which was easily removed by filtration after completion of the reaction, was effective to obtain pure form of **8ae** (gram scale) in 60% two-step yield after recrystallization.

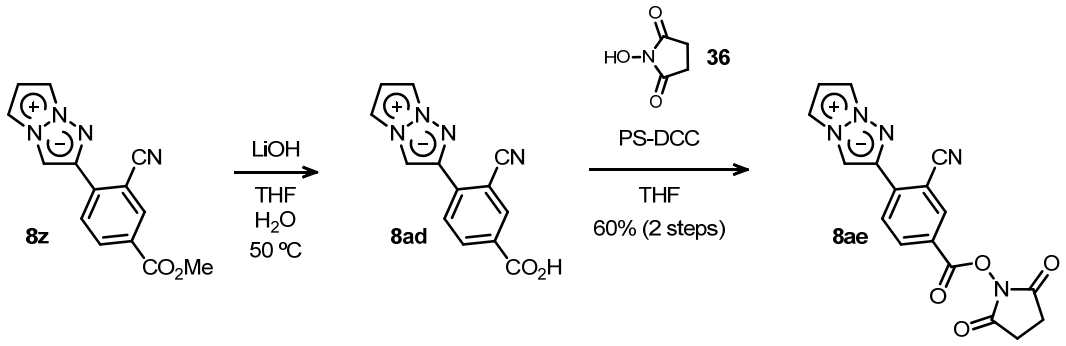

Scheme 12. Synthesis of the NHS ester **8ae**

Having prepared the NHS ester **8ae**, fluorescence labeling of amino acids with **8ae** was examined (Table 8). Treatment of glycine ethyl ester with **8ae** in the presence of triethylamine in DMF afforded the labeled product **37a** in 95% yield. The similar reaction of tripeptide smoothly proceeded to give the desired product **37b** in 82% yield. Furthermore, mugineic acid derivative as a more complicated amino acid also readily reacted with **8ae**, and fluorescent labeled mugineic acid **37c** was obtained in 84% yield. Thus, it was found that TAP NHS ester derivative **8ae** is useful as fluorescent labeling reagent for amines, and **8ae** is soon-to-be commercial available from Tokyo Chemical Industry Co., Ltd (TCI).

In addition, it was confirmed that labeled compounds exhibited yellow fluorescence similar to ester derivative **8z**. In particular, optical properties of the labeled glycine **37a** and tri-peptide **37b** were investigated (Table 9). Absorption maxima of **37a** and **37b** showed 397 nm and 389 nm, respectively, and fluorescence maxima exhibited very similar value (λ_{em} = 567 nm) in dichloromethane, each other. Additionally, fluorescence quantum yield of **37a** showed high value (Φ_F = 0.37), whereas that of **37b** was slightly decreased in contrast to **37a**, but high

enough to use as a fluorescent probe. Furthermore, the emissions of **37a** and **37b** were observed in water and showed similar trend to ester analog **8z**, which is described in section 3-3. Therefore, TAP labeled molecules would be useful fluorescent probes especially for recognition of environmental changes *in vivo* experiment.

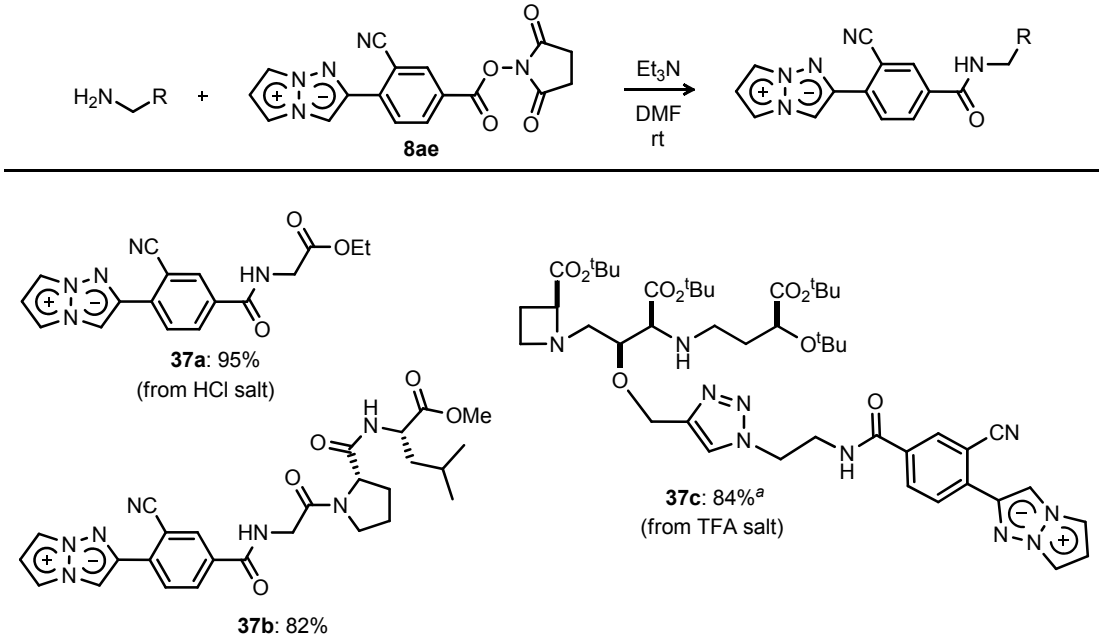

[a] using THF as a solvent. Reaction details were shown in experimental section.

Table 8. Fluorescent labeling of amino acids by TAP NHS ester **8ae**.

labeled compound	λ_{abs} /nm	λ_{em} /nm	Φ_F	color in CH_2Cl_2
37a	397 (393)	567 (457)	0.37 (0.019)	
37b	389 (353)	567 (459)	0.24 (0.077)	

Each parameter was measured in CH_2Cl_2. A value in parenthesis was measured in water.

Table 9. The optical measurement of the labeled compounds **37a** and **37b**.

3-6. The Theoretical Explanation of Spectral Changed of TAPs by Quantum Chemical Calculations.

In order to investigate the origin of spectral change along with 2-substituent, quantum chemical calculation was attempted. First, geometry optimization of simple TAP **8a** was performed by DFT calculation using B3LYP/6-31 + G(d,p) in ground state ($(S_0)_{min}$) and by TD-DFT calculation using CAM- B3LYP/6-31 + G(d,p) in lowest excited state ($(S_1)_{min}$)[35]. As a result, it was found that the bond lengths of C4-N3a and N1-N6a were elongated as a result of photo-excitation (Figure 18).

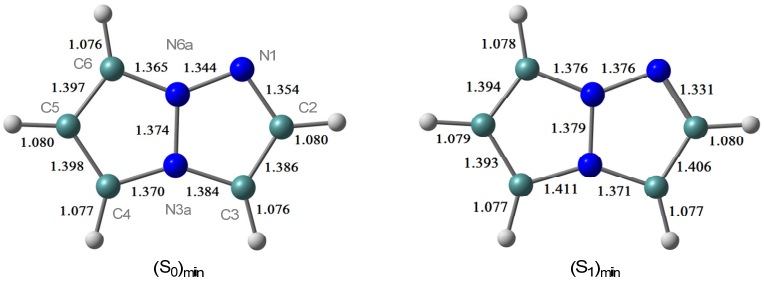

Figure 18. The equilibrium structure of TAP **8a** in the S_0 and S_1 in the gas phase. The values indicated the bond lengths (Å).

Next, vertical excitation energies were calculated by CASPT2 calculation in the reference SA-CASSCF (10, 8)[36, 37]. The resulting molecular orbitals were shown in Figure 19. It was found that the lowest singlet excitation was HOMO-LUMO π-π* transition and the calculated excitation wavelength was 291 nm, which agreed with the experimental one (288 nm). On the other hand, the calculated fluorescence wavelength of **8a** by CASPT2 was 82 nm shorter than the experimental one (λ_{em}(cal.) / λ_{em}(exp.) = 307 nm / 389 nm).

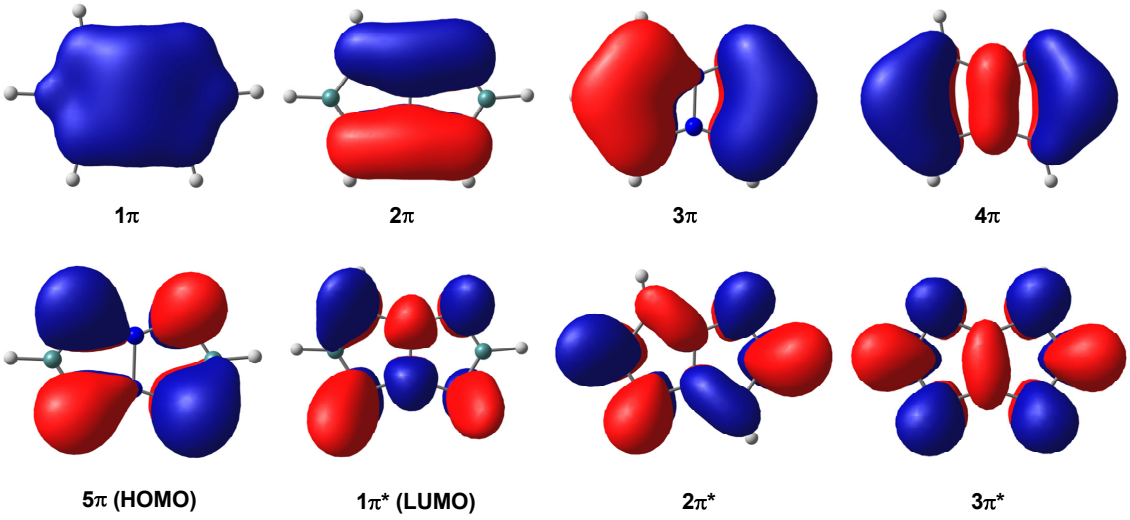

Figure 19. The molecular orbital of **8a** calculated by CASPT2 calculation in the reference SA-CASSCF (10, 8).

Similarly, the equilibrium structures of TAP **8n** in the ground (S_0) and excited (S_1) states were estimated and summarized in Figure 20. The bond lengths of C2-C3 and C2-C1' were elongated in the S_1 state.

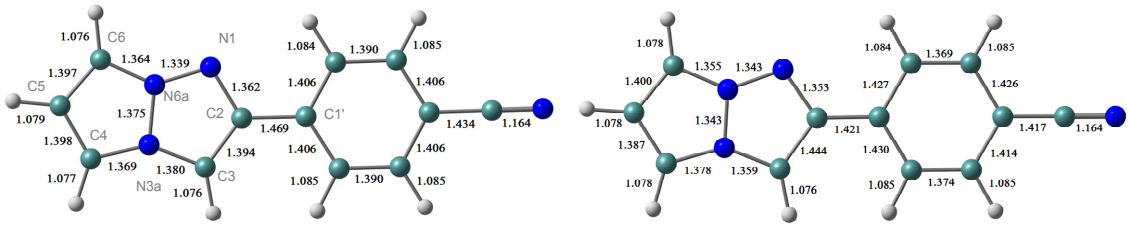

$(S_0)_{min}$ $(S_1)_{min}$

Figure 20. The equilibrium structure of TAP **8n** in the S_0 and S_1 in the gas phase. The values indicated the bond lengths (Å).

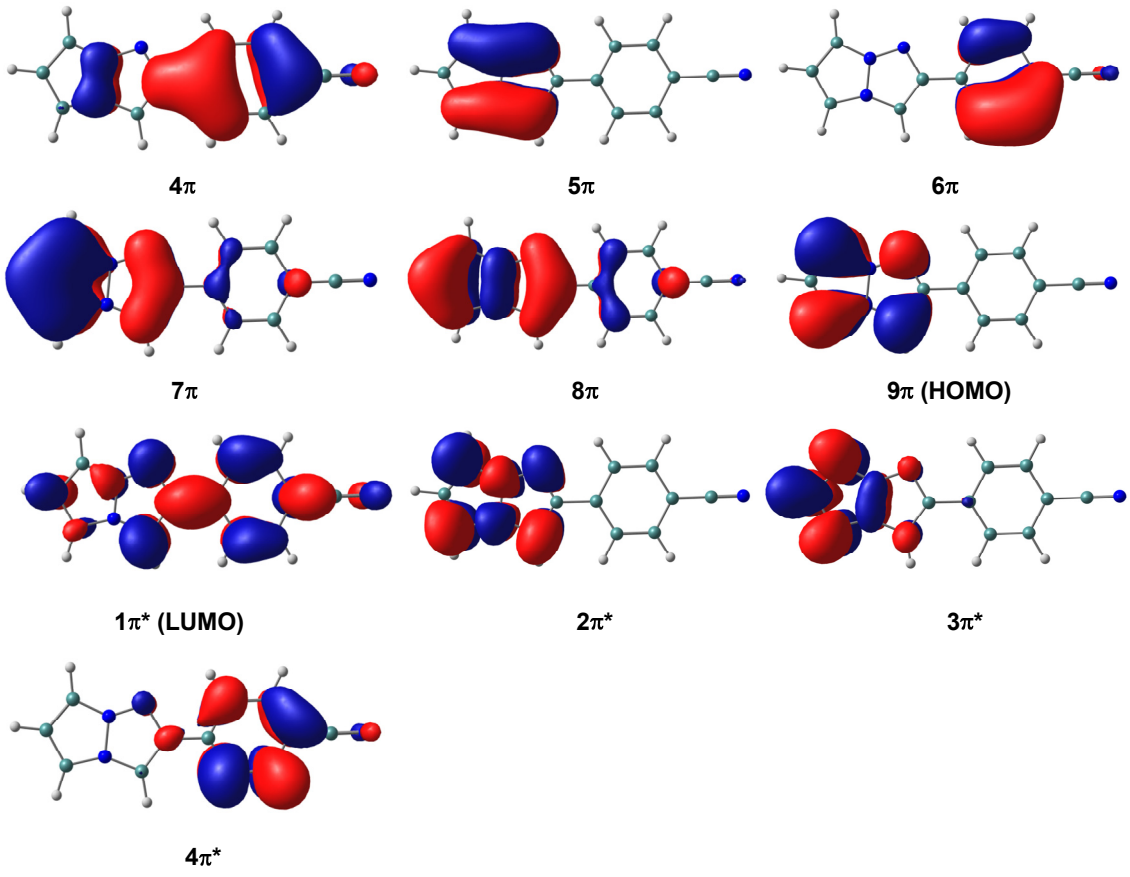

Figure 21. The molecular orbital of **8n** calculated by CASPT2 calculation in the reference SA-CASSCF (12, 10).

The vertical excitation energies were calculated by CASPT2 calculation in the reference SA-CASSCF (12, 10)[36, 37]. The resulting molecular orbital was shown in Figure 21. The lowest singlet excitation was assigned to HOMO-LUMO π-π* transition, which was characterized by an intramolecular charge transfer (ICT) from TAP skeleton to the phenyl ring. This result revealed that absorption and fluorescence change of 2-subsituted TAPs from simple TAP **8a** caused by change from simple π-π* transition to ICT transition. Furthermore, red shift of fluorescence wavelength was observed since the electron-withdrawing ability of 2-substituent was stronger, CT character was larger. As well as the result of **8a**, the calculated excitation wavelength was 380 nm, which agreed with the experimental one (381 nm), whereas the calculated fluorescence wavelength by CASPT2 was 79 nm shorter than the experimental one (λ_{em}(cal.) / λ_{em}(exp.) = 430 nm / 509 nm).

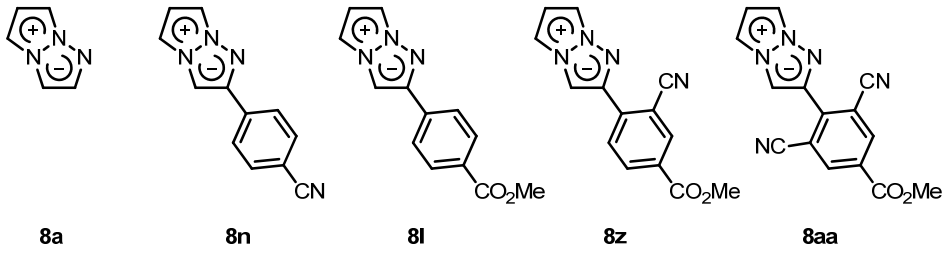

Figure 22. The selected TAPs for theoretical calculation analysis.

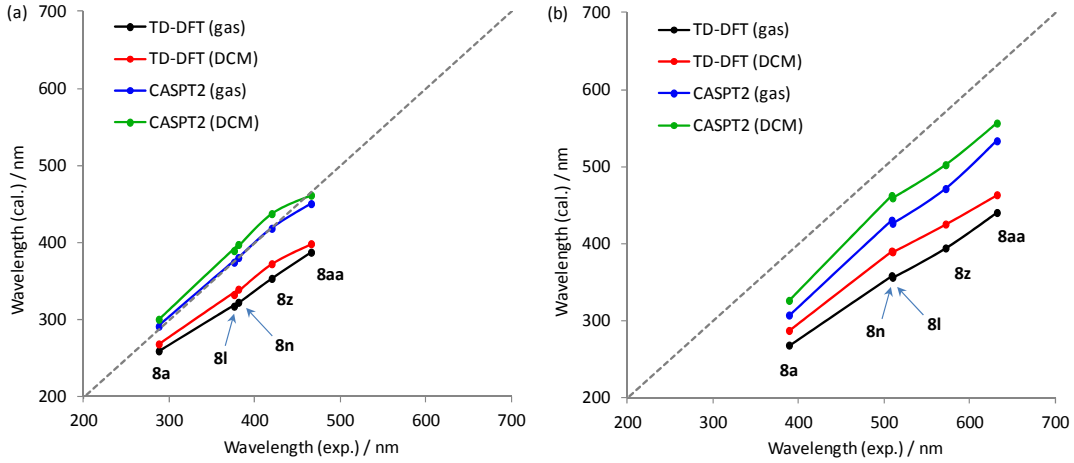

Figure 23. The comparison of (a) the absorption and (b) the fluorescence wavelengths between the calculated and experimental values. The central broken line indicated a perfect cal. /exp. match.

Because calculated wavelengths of **8n** exhibited the similar behavior to **8a**, the difference between calculated and experimental wavelengths of selected TAPs (Figure 22) was investigated using TD-DFT and CASPT2 calculation in the gas phase and dichloromethane,

respectively[38, 39]. For the absorption wavelengths, respective calculation result showed linear graph and the calculated value by CASPT2 mostly agreed with the experimental one (Figure 23(a)). On the other hand, although the calculated fluorescence wavelengths were shorter than the experimental ones, the graphs showed a good correlation between the calculated and experimental values (Figure 23(b)). The overestimation of the fluorescence energies may be attributed to the insufficient treatment of the solvent environments because excitation involved a significant CT character. These results were expected to help to predict wavelengths of TAPs.

In summary, a novel fluorescent labeling reagent based on TAP was developed. Several amino acids were successfully labeled by this reagent and the labeled products also exhibited intense fluorescence. In addition, yellow fluorescent TAP **8z** was incorporated into HeLa cells and stained its cytoplasm. Therefore, TAP is expected to be useful fluorescent probes in the field of life science.

Experimental Section

General Method and Procedure.

All the reactions were carried out under an argon atmosphere. Tetrahydrofuran (THF) was freshly prepared by distillation from benzophenone ketyl before use. Triethylamine was distilled from CaH_2 under argon atmosphere and stored over NaOH. Other anhydrous solvents and reagents were commercial grade and used as supplied.

NMR spectra were recorded on a JEOL JNM-ECA-500 (500 MHz) and a JEOL JNM-AL400 (400 MHz). Chemical shifts were reported in parts per million (ppm). For ^{1}H NMR spectra ($CDCl_3$ and D_2O), tetramethylsilane and the residual solvent peak were used as the internal reference (0.00, 7.26 and 4.65 ppm), whereas the central solvent peak and methanol were used as the reference (77.0 and 49.5 ppm) for ^{13}C NMR spectra. Mass spectra were recorded on a JEOL JMS-T-100GCV (FD) a Thermo Scientific Exactive (ESI) or a Waters Micromass LCT Premier (ESI). Infrared (IR) spectra were recorded on a JASCO FT/IR-4100 and a JASCO FT/IR-4200 spectrometer using CaF_2 and NaCl plate. Analytical thin layer chromatography (TLC) was performed with E. Merck pre-coated TLC plates, silica gel 60F-254, layer thickness 0.25 mm. Flash chromatography was performed on Kanto Chemical 60 N (0.04–0.05 mm) mesh silica gel.

Absorption spectra were recorded on a Hitachi U-3300 and a JASCO V-600 spectrometer and corrected fluorescence spectra were recorded on a Hitachi F-4500 and a JASCO FP-8200 spectrofluorometer. Sample solutions were degassed thoroughly by purging with an Ar gas stream for 30 min prior to the experiments and then sealed in their cells. Fluorescence quantum yields were estimated by using 9,10-diphenylanthracene (9,10-DPA) in cyclohexane ($\Phi_F = 0.91$) or rhodamine B in ethanol ($\Phi_F = 0.94$) as a standard.

Thermogravimetry analyses (TGA) were performed on a SHIMADZU TGA-50 at scanning rate of 3.0 K min^{-1} under nitrogen.

Experimental Details for Synthesis of 1,3a,6a-Triazapentalene derivatives

Preparation of Azide Reagent 22a

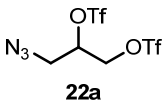

22a

3-azidopropane-1,2 -diyl bis(trifluoromethanesulfonate) (22a)

To a solution of 3-chloro-1,2-propandiol (1.92 g, 17.3 mmol) in water (17 mL) was added sodium azide (1.39 g, 20.8 mmol) at room temperature. After the mixture was heated to reflux for 5.5 h, sodium chloride was added until saturation at 0 °C. The resulting mixture was extracted with ethyl acetate (x 5). The combined organic layers were dried over anhydrous $MgSO_4$, filtered, and concentrated under reduced pressure. The residue was dissolved in anhydrous CH_2Cl_2 (87 mL). To this solution were added 2,6-lutidine (10.1 mL, 86.5 mmol) and Tf_2O (5.82 mL, 34.6 mmol) in this order at -78 °C. The mixture was stirred for 5 min, quenched with saturated aqueous NH_4Cl, and extracted with hexane (x 3). The combined organic layers were washed with brine, dried over $MgSO_4$, filtered, and concentrated in vacuum. The residue was purified by silca gel column chromatography (hexane/AcOEt = 95/5, 90/10 to 70/30) to give **22a** (5.38 g, 14.1 mmol, 82%) as a pale yellow oil. ^{1}H NMR (500 MHz, $CDCl_3$) δ 5.10 (quint, *J* = 5.2 Hz, 1H), 4.71 (d, *J* = 5.2 Hz, 2H), 3.83 (dd, *J* = 13.7, 5.2 Hz, 1H), 3.77 (dd, *J* = 13.5, 5.4 Hz, 1H); ^{13}C NMR (125 MHz, $CDCl_3$) δ 118.5 (q, *J* = 319 Hz), 118.3 (q, *J* = 319 Hz), 81.4, 72.1, 50.1; IR (neat) 2114, 1457, 1418, 1220, 1139 cm^{-1}. TGA: (heat from 30 °C to 500 °C at 3.0 °C / min) The weight loss of **22a** (8.646 mg) reached to 5% at 107 °C.

Synthesis of 2-substituted TAPs

Preparation of ligand·copper solution

To a solution of bis[2-(*N*,*N*-dimethylaminoethyl)]ether (19.0 μL, 0.10 mmol) in THF (10 mL) was added copper(I) iodide (19 mg, 0.10 mmol) at room temperature. The mixture was stirred until homogeneous.

Typical procedure of the click reaction

Method A:

To the flask containing azide **22a** (217 mg, 0.568 mmol)were transferred 2.8 mL (0.028 mmol of ligand·copper complex) of above copper·ligand solution , Et_3N (400 μL, 2.84 mmol), and alkyne **23** (0.682 mmol) at room temperature, successively. The mixture was stirred for 1 h and concentrated under reduced pressure. The residue was purified by silica gel column chromatography to give **8**.

Method B:

To a solution of **22a** (74.7 mg, 0.196 mmol) and alkyne **23** (0.235 mmol) in THF (20 mL) were added Et_3N (138 μL, 0.980 mmol), and 980 μL of the ligand·copper solution (0.01 M, 9.80 μmol), successively at room temperature. The mixture was stirred for 1h and concentrated under reduced pressure. The residue was purified by silica gel column chromatography to give **8**.

The method B is recommended for syntheses of 2-aryl derivatives, especially possessing electronwithdrawing group, in order to avoid generation of 1-allyl triazole derivatives as byproducts or precipitation of the products.

The synthetic TAPs mentioned in Chapter 1 except for **8m** are yellow-colored materials just after purification by silica gel column chromatography. However, the yellow color readily changed to green by a trace amount of acids such as a derivation from $CDCl_3$.

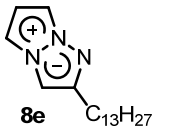

2-*n*-tridecyl-1,3a,6a-triazapentalene (8e)

Yellow oil; ^{1}H NMR (500 MHz, $CDCl_3$) δ 7.32 (d, J = 2.3 Hz, 1H), 7.00 (d, J = 2.3 Hz, 1H), 6.89 (s, 1H), 6.53 (t, J = 2.9 Hz, 1H), 2.63 (t, J = 7.7 Hz, 2H), 1.69 (quint, J = 7.4 Hz, 2H), 1.41-1.26 (m, 20H), 0.88 (t, J = 7.2 Hz, 3H); ^{13}C NMR (125 MHz, $CDCl_3$) δ 149.4, 107.8, 101.7, 99.9, 94.4, 31.9, 29.7, 29.6 x3, 29.5, 29.4, 29.4, 29.3, 29.3, 26.7, 22.7, 14.1; IR (neat) 3155, 2924, 2853, 1465, 1436, 1376, 1284, 1246, 1163, 1138 cm^{-1}; HRMS (EI) m/z [M^+] calcd for $[C_{18}H_{31}N_3]^+$ 289.2518, found 289.2524.

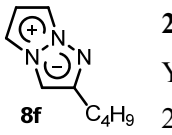

2-butyl-1,3a,6a-triazapentalene (8f)

Yellow oil; ^{1}H NMR (500 MHz, $CDCl_3$) δ 7.32 (d, J = 2.3 Hz, 1H), 7.00 (d, J = 2.9 Hz, 1H), 6.90 (s, 1H), 6.53 (t, J = 2.9 Hz, 1H), 2.64 (t, J = 7.7 Hz, 2H), 1.68 (quint, J = 7.4 Hz, 2H), 1.42 (sex, J = 7.4 Hz, 2H), 0.94 (t, J = 7.4 Hz, 3H); ^{13}C NMR (125 MHz, $CDCl_3$) δ 149.3, 107.9, 101.7, 99.9, 94.4, 31.4, 26.4, 22.4, 13.8; IR (neat) 3153, 2955, 2930, 2860, 1457, 1436, 1376, 1242, 1138 cm^{-1}; HRMS (EI) m/z [M^+] calcd for $[C_9H_{13}N_3]^+$ 163.1109, found 163.1104.

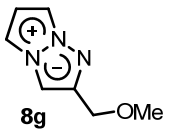

2-(methoxymethyl)-1,3a,6a-triazapentalene (8g)

Yellow oil; ^{1}H NMR (500 MHz, $CDCl_3$) δ 7.37 (d, J = 2.9 Hz, 1H), 7.13 (s, 1H), 7.08 (d, J = 2.9 Hz, 1H), 6.59 (t, J = 2.9 Hz, 1H), 4.50 (s, 2H), 3.45 (s, 3H); ^{13}C NMR (125 MHz, $CDCl_3$) δ 145.4, 108.5, 102.1, 100.6, 95.6, 66.7, 58.4; IR (neat) 3148, 2977, 2926, 2897, 2817 cm^{-1}; HRMS (EI) m/z [M^+] calcd for $[C_7H_9N_3O]^+$ 151.0749, found 151.0749.

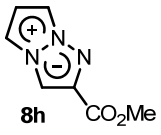

2-(methoxycarbonyl)-1,3a,6a-triazapentalene (8h)

Yellow solid; mp 94-100 °C (recrystalized from ether); ^{1}H NMR (500 MHz, $CDCl_3$) δ 7.68 (d, *J* = 1.1 Hz, 1H), 7.46 (d, *J* = 2.9 Hz, 1H), 7.22 (d, *J* = 2.9 Hz, 1H), 6.75 (t, *J* = 2.9 Hz, 1H), 3.96 (s, 3H); ^{13}C NMR (125 MHz, $CDCl_3$) δ 162.0, 139.0, 110.8, 102.7, 101.8, 100.3, 52.2; IR (neat) 3154, 3120, 3033, 3008, 2958, 2928, 1746, 1733, 1218 cm^{-1}; HRMS (EI) m/z [M^+] calcd for $[C_7H_7N_3O_2]^+$ 165.0538, found 165.0540. UV/Vis (CH_2Cl_2): λ_{max} (log ε) = 342 (3.43), 281 (4.20) nm. FL (CH_2Cl_2): λ_{em} = 431 nm; Φ_F = 0.18 (reference to 9,10-DPA; excited at 370 nm).

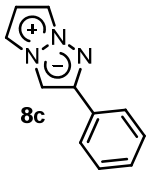

2-phenyl-1,3a,6a-triazapentalene (8c)

Yellow solid; mp 75-77 °C (recrystalized from CH_2Cl_2); ^{1}H NMR (500 MHz, $CDCl_3$) δ 7.77 (d, *J* = 6.9 Hz, 2H), 7.43-7.40 (m, 3H), 7.38 (d, *J* = 1.1 Hz, 1H), 7.35 (tt, *J* = 7.2, 1.6 Hz, 1H), 7.10 (d, *J* = 2.3 Hz, 1H), 6.60 (t, *J* = 2.9z, 1H); ^{13}C NMR (125 MHz, $CDCl_3$) δ 147.7, 131.4, 128.7, 128.3, 125.8, 108.7, 102.2, 100.7, 93.2; IR (neat) 3153, 3072, 3036, 2698, 2653 cm^{-1}; HRMS (EI) m/z [M^+] calcd for $[C_{11}H_9N_3]^+$ 138.0796, found 138.0779. UV/Vis (CH_2Cl_2): λ_{max} (log ε) = ~326 (3.48), 288 (3.97), 282 (3.97), 251 (4.17) nm. FL (CH_2Cl_2): λ_{max} = 419 nm; Φ_F = 0.026 (reference to 9,10-DPA; excited at 340 nm).

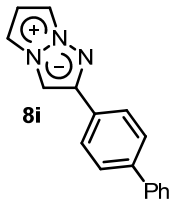

2-(biphenyl-4-yl)-1,3a,6a-triazapentalene (8i)

Yellow solid; ^{1}H NMR (500 MHz, $CDCl_3$) δ 7.85 (d, *J* = 8.6 Hz, 2H), 7.66 (d, *J* = 8.6 Hz, 2H), 7.64 (d, *J* = 7.4 Hz, 2H), 7.48-7.42 (m, 4H), 7.36 (t, *J* = 7.4 Hz, 1H), 7.13 (d, *J* = 2.8 Hz, 1H), 6.62 (t, *J* = 2.8 Hz, 1H); ^{13}C NMR (125.8 MHz, $CDCl_3$) δ 147.4, 141.0, 140.6, 130.4, 128.8, 127.4, 127.4, 127.0, 126.2, 108.8, 102.2, 100.8, 93.3; IR (neat) 3566, 3147, 3133, 3062, 3033, 2955, 2926, 2853 cm^{-1}; HRMS (EI) m/z [M^+] calcd for $[C_{17}H_{13}N_3]^+$ 259.1109, found 259.1107. UV/Vis (CH_2Cl_2): λ_{max} (log ε) = 345 (3.70), 289 (4.53) nm. FL (CH_2Cl_2): λ_{max} = 456 nm; Φ_F = 0.20 (reference to 9,10-DPA; excited at 370 nm).

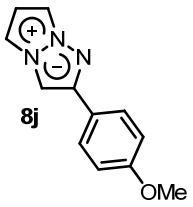

2-(4-methoxyphenyl)-1,3a,6a-triazapentalene (8j)

Yellow solid; ^{1}H NMR (500 MHz, $CDCl_3$) δ 7.70 (d, *J* = 8.6 Hz, 2H), 7.41 (d, *J* = 2.3 Hz, 1H), 7.31 (s, 1H), 7.09 (d, *J* = 2.9 Hz, 1H), 6.95 (d, *J* = 9.2 Hz, 2H), 6.58 (t, *J* = 2.6 Hz, 1H), 3.85 (s, 3H); ^{13}C NMR (125 MHz, $CDCl_3$) δ 159.8, 147.6, 127.1, 124.1, 114.1, 108.5, 102.1, 100.6, 92.6, 55.3; IR (neat) 3154, 2992, 2960, 2937, 2837, 2109, 1251, 1028 cm^{-1}; HRMS (EI) m/z [M^+] calcd for $[C_{12}H_{11}N_3O]^+$ 213.0902, found 213.0889. UV/Vis (CH_2Cl_2): λ_{max} (log ε) = ~330 (3.71), 285 (4.22), 260 (4.30) nm. FL (CH_2Cl_2): λ_{em} = 413 nm; Φ_F = 0.053 (reference to 9,10-DPA; excited

at 340 nm).

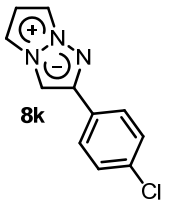

2-(4-chlorophenyl)-1,3a,6a-triazapentalene (8k)

Blue solid; mp 133–135 °C; ^{1}H NMR (500 MHz, $CDCl_3$) δ 7.70 (d, *J* = 8.6 Hz, 2H), 7.42 (d, *J* = 2.3 Hz, 1H), 7.38 (d, *J* = 8.6 Hz, 2H), 7.36 (s, 1H), 7.11 (d, *J* = 2.8 Hz, 1H), 6.61 (t, *J* = 2.8 Hz, 1H); ^{13}C NMR (125 MHz, $CDCl_3$) δ 146.5, 134.0, 130.0, 129.8, 127.0, 108.9, 102.3, 101.0, 93.2; IR (neat) 3153, 2922, 2852, 1413, 1242, 1142, 1104, 1038, 947, 838 cm^{-1}; HRMS (ESI) m/z $[M+H]^+$ calcd for $[C_{11}H_8N_3O_2+H]^+$ 218.0480, found 218.0481. UV/Vis (CH_2Cl_2): λ_{max} (log ε) = ~324 (3.58), ~276 (4.12), 258 (4.22) nm. FL (CH_2Cl_2): λ_{max} = 432 nm; Φ_F = 0.059 (reference to 9,10-DPA; excited at 370 nm).

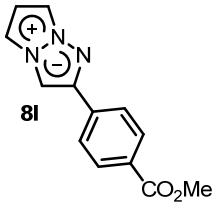

2-(4-(methoxycarbonyl)phenyl)-1,3a,6a-triazapentalene (8l)

Green solid; mp 148–153 °C; ^{1}H NMR (500 MHz, $CDCl_3$) δ 8.09 (d, *J* = 8.6 Hz, 2H), 7.84 (d, *J* = 8.6 Hz, 2H), 7.47 (s, 1H), 7.45 (d, *J* = 2.8 Hz, 1H), 7.15 (d, *J* = 2.8 Hz, 1H), 6.64 (t, *J* = 2.9 Hz, 1H), 3.94 (s, 1H); ^{13}C NMR (125 MHz, $CDCl_3$) δ 166.8, 146.4, 135.8, 130.0. 129.6, 125.5, 109.2, 102.4, 101.1, 94.0, 52.1; IR (neat) 3152, 3134, 3120, 1710, 1433, 1417, 1280, 1104 cm^{-1}; HRMS (ESI) m/z $[M+Na]^+$ calcd for $[C_{13}H_{11}N_3O_2+Na]^+$ 264.0744, found 264.0745. UV/Vis (CH_2Cl_2): λ_{max} (log ε) = 376 (3.09), 287 (4.14) nm. FL (CH_2Cl_2): λ_{max} = 521 nm; Φ_F = 0.44 (reference to 9,10-DPA; excited at 370 nm).

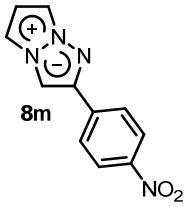

2-(4-nitrophenyl)-1,3a,6a-triazapentalene (8m)

Red crystal; dec. 179 °C (recrystalized from ether) ^{1}H NMR (500 MHz, $CDCl_3$) δ 8.28 (d, *J* = 9.2 Hz, 2H), 7.93 (d, *J* = 8.6 Hz, 2H), 7.52 (s, 1H), 7.47 (d, *J* = 2.3 Hz, 1H), 7.19 (d, *J* = 2.9 Hz, 1H), 6.68 (t, *J* = 2.9 Hz, 1H); ^{13}C NMR (125 MHz, $CDCl_3$) δ 147.4, 145.3, 138.0, 126.3, 124.2, 109.6, 102.8, 101.5, 94.4; IR (neat) 3150, 3118, 1508, 1340, 1324 cm^{-1}; HRMS (EI) m/z $[M^+]$ calcd for $[C_{11}H_8N_4O_2]^+$ 228.0647, found 228.0636. UV/Vis (CH_2Cl_2): λ_{max} (log ε) = 412 (3.32), 300 (4.25) nm. FL (CH_2Cl_2): λ_{max} = 556 nm; Φ_F = 0.14 (reference to 9,10-DPA; excited at 370 nm).

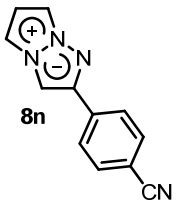

2-(4-cyanophenyl)-1,3a,6a-triazapentalene (8n)

Yellow solid; dec. 150 °C (recrystalized from CH_2Cl_2); ^{1}H NMR (500 MHz, $CDCl_3$) δ 7.87 (d, *J* = 8.0 Hz, 2H), 7.70 (d, *J* = 8.0 Hz, 2H), 7.47 (s, 1H), 7.46 (d, *J* = 2.9 Hz, 1H), 7.17(d, *J* = 2.8 Hz, 1H), 6.66 (t, *J* = 2.8 Hz, 1H); ^{13}C NMR (125 MHz, $CDCl_3$) δ 145.7, 136.0, 132.5, 126.2, 118.8, 111.5, 109.5, 102.6,

101.4, 94.1; IR (neat) 3157, 3124, 3114, 2224 cm^{-1}; HRMS (EI) m/z [M^+] calcd for $[C_{12}H_8N_4]^+$ 208.0749, found 208.0739. UV/Vis (CH_2Cl_2): λ_{max} (log ε) = 381 (3.48), 286 (4.44) nm. FL (CH_2Cl_2): λ_{max} = 509 nm; Φ_F = 0.15 (reference to 9,10-DPA; excited at 370 nm).

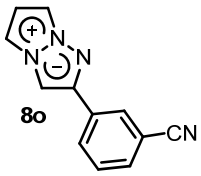

2-(3-cyanophenyl)-1,3a,6a-triazapentalene (8o)

Green solid; mp 118–123 °C (recrystalized from ether); ^{1}H NMR (500 MHz, $CDCl_3$) δ 8.04 (t, *J* = 1.8 Hz, 1H), 7.98 (ddd, *J* = 8.0, 1.7, 1.1 Hz, 1H), 7.59 (ddd, *J* = 8.0, 1.7, 1.2 Hz, 1H), 7.51 (t, *J* = 8.0 Hz, 1H), 7.44 (d, *J* = 2.3 Hz, 1H), 7.42 (s, 1H), 7.16 (d, *J* = 2.9 Hz, 1H), 6.65 (t, *J* = 2.9 Hz, 1H); ^{13}C NMR (125 MHz, $CDCl_3$) δ 145.3, 132.8, 131.4, 129.8, 129.4, 129.2, 118.6, 112.8, 109.2, 102.6, 101.4, 93.5; IR (neat) 3150, 2227, 1435, 1378, 1144, 969, 844 cm^{-1}; HRMS (ESI) m/z [M+H]$^+$ calcd for $[C_{12}H_8N_4]^+$ 209.0822, found 209.0824. UV/Vis (CH_2Cl_2): λ_{max} (log ε) = 327 (3.45), 282 (4.15), 274 (4.16), 260 (4.20) nm. FL (CH_2Cl_2): λ_{max} = 493 nm; Φ_F = 0.24 (reference to 9,10-DPA; excited at 370 nm).

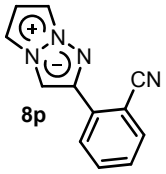

2-(2-cyanophenyl)-1,3a,6a-triazapentalene (8p)

Light green solid; mp 85–87 °C (recrystalized from ether); ^{1}H NMR (500 MHz, $CDCl_3$) δ 8.09 (dd, *J* = 8.0, 1.1 Hz, 1H), 7.93 (d, *J* = 1.2 Hz, 1H), 7.74 (dd, *J* = 8.0, 1.1 Hz, 1H), 7.66 (td, *J* = 8.0, 1.2 Hz, 1H), 7.46 (d, *J* = 2.9 Hz, 1H), 7.43 (td, *J* = 8.0, 1.2 Hz, 1H), 7.19 (d, *J* = 2.8 Hz, 1H), 6.68 (t, *J* = 2.9 Hz, 1H); ^{13}C NMR (125 MHz, $CDCl_3$) δ 143.4, 134.4, 133.9, 133.0, 128.4, 128.1, 119.1, 109.5, 109.0, 102.3, 101.4, 96.0; IR (neat) 3152, 2223, 1474, 1424, 949 cm^{-1}; HRMS (ESI) m/z [M+Na]$^+$ calcd for $[C_{12}H_8N_3O_2+Na]^+$ 231.0641, found 231.0642. UV/Vis (CH_2Cl_2): λ_{max} (log ε) = 376 (3.11), 287 (4.19), ~270 (4.10), 260 (4.12) nm. FL (CH_2Cl_2): λ_{max} = 515 nm; Φ_F = 0.24 (reference to 9,10-DPA; excited at 370 nm).

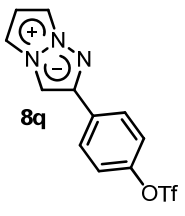

2-(4-(trifluoromethylsulfonyloxy)phenyl)-1,3a,6a-triazapentalene (8q)

Yellow solid; mp 106-114 °C (recrystalized from ether); ^{1}H NMR (500 MHz, $CDCl_3$) δ 7.84 (dt, *J* = 9.2, 2.4 Hz, 2H), 7.44 (d, *J* = 2.3 Hz, 1H), 7.40 (s, 1H), 7.33 (dt, *J* = 9.4, 2.3 Hz, 1H), 7.15 (d, *J* = 2.9 Hz, 2H), 6.64 (t, *J* = 2.8 Hz, 1H); ^{13}C NMR (125 MHz, $CDCl_3$) δ 149.2, 145.9, 132.1, 127.6, 121.7, 118.8 (q, *J* = 320 Hz), 109.2, 102.6, 101.3, 93.6; IR (neat) 3151, 3052, 2924, 2853, 1420, 1252, 1213, 1139 cm^{-1}; HRMS (EI) m/z [M^+] calcd for $[C_{12}H_8F_3N_3O_3S]^+$ 331.0238, found 331.0227

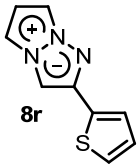

2-(thiophen-2-yl)-1,3a,6a-triazapentalene (8r)

Red solid; mp 71–73 °C (recrystalized from ether); ^{1}H NMR (500 MHz, $CDCl_3$) δ 7.40 (d, *J* = 2.8 Hz, 1H), 7.36 (d, *J* = 3.4 Hz, 1H), 7.31 (brs, 1H), 7.30 (d, *J* = 5.2 Hz, 1H), 7.10–7.04 (m, 2H), 6.58 (t, *J* = 2.8 Hz, 1H); ^{13}C NMR (125 MHz, $CDCl_3$) δ 142.6, 133.8, 127.4, 125.0, 124.1, 108.7, 102.4, 101.0, 92.9; IR (neat) 3147, 3101, 3069, 1437, 1414, 1381, 1238, 1222, 1034 cm^{-1}; HRMS (ESI) m/z $[M+H]^+$ calcd for $[C_9H_7N_3S+H]^+$ 190.0433, found 190.0435. UV/Vis (CH_2Cl_2): λ_{max} (log ε) = 341 (3.16), 285 (3.97) nm. FL (CH_2Cl_2): λ_{em} = 439 nm; Φ_F = 0.049 (reference to 9,10-DPA; excited at 350 nm).

Synthesis of Unsubstituted TAP 8a

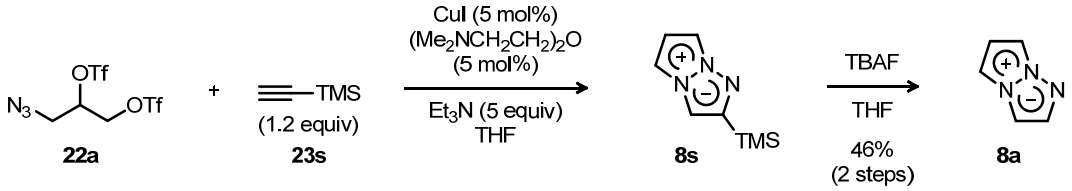

2-(trimethylsilyl)-1,3a,6a-triazapentalene (8s)

To a solution of azide **22a** (165.0 mg, 0.433 mmol) in THF (2.2 mL) were added (trimethylsilyl)acetylene (73.4 μL, 0.519 mmol), TEA (304 μL, 2.16 mmol) and the ligand-Cu(I) complex solution (2.2 mL, 0.02 mmol), prepared according to the typical procedure, at room temperature. The mixture was stirred for 3 h and concentrated *in vacuo*. The residue was diluted with pentane, washed with water and brine, dried over anhydrous $MgSO_4$, filtered, and concentrated *in vacuo* to give 2-trimethylsilyl derivative **8s** (71% NMR yield using pyrazine as an internal standard) as a yellow oil. ^{1}H NMR (500 MHz, $CDCl_3$) δ 7.44 (dd, *J* = 2.8, 1.2 Hz, 1H), 7.08 (d, *J* = 1.2 Hz, 1H), 7.07 (d, *J* = 2.8 Hz, 1H), 6.62 (t, *J* = 2.9 Hz, 1H), 0.33 (s, 9H); ^{13}C NMR (125 MHz, $CDCl_3$) δ 147.7, 109.4, 101.6, 101.6, 99.6, -1.4.

1,3a,6a-triazapentalene (8a)

To a solution of TBAF in THF (1.0 M, 0.65 mL, 0.650 mmol) was added the crude **8s** at 0 °C. The mixture was stirred at room temperature for 3 h and directly subjected to silica gel column chromatography (pentane/ether = 5/1) to give unsubstituted triazapentalene **8a** (22 mg, 46% in 2 steps) as a pale yellow volatile oil. ^{1}H NMR (500 MHz, $CDCl_3$) δ 7.47 (s, 1H), 7.43 (d, *J* = 2.8 Hz, 1H), 7.12 (s, 1H), 7.12 (s, 1H), 6.63 (td, *J* = 2.8, 1.2 Hz, 1H); ^{13}C NMR (125 MHz, $CDCl_3$) δ 134.5, 108.9, 102.2, 100.4, 96.6; IR (neat) 3149, 2951, 2924, 2856, 2203, 2104, 1152 cm^{-1}; HRMS (FI) m/z $[M^+]$ calcd for $[C_5H_5N_3]^+$ 107.0483, found 107.0491. UV/Vis (CH_2Cl_2): λ_{max} (log ε) = 288 (4.17) nm. FL (CH_2Cl_2): λ_{em} = 389 nm; Φ_F = 0.014 (reference to 9,10-DPA;

excited at 330 nm).

Preparation of 3-Protonated TAP

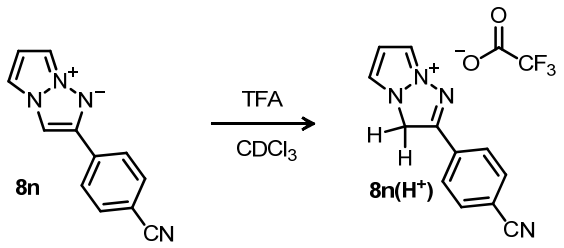

2-(4-cyanophenyl)-3*H*-pyrazolo[1,2-*a*][1,2,3]triazol-8-ium 2,2,2-trifluoroacetate (8n(H^+))

To a solution of **8n** (1.1 mg, 5.3 μmol) in $CDCl_3$ (0.6 mL) was added TFA (3.2 μL, 42 μmol) and the mixture was directly analyzed with NMR. ^{1}H NMR (500 MHz, $CDCl_3$) δ 8.64 (d, J = 2.8 Hz, 1H), 8.30 (d, J = 2.9 Hz, 1H), 8.11 (d, J = 8.6 Hz, 2H), 7.90 (d, J = 8.6 Hz, 2H), 7.04 (t, J = 2.8 Hz, 1H), 6.18 (brs, 1H); ^{13}C NMR (125 MHz, $CDCl_3$) δ 169.5, 133.4, 132.0, 129.0, 129.0, 125.2, 118.2, 117.0, 112.4, 56.9.

Synthesis of the Azide Reagents 22d and 22e

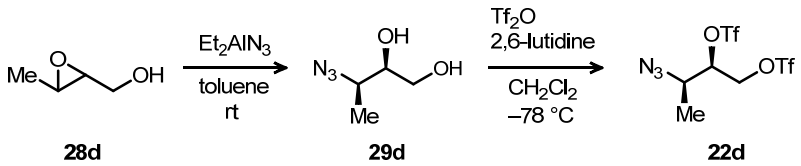

***rac*-(2*S*,3*S*)-3-azidobutane-1,2-diol (29d)**

To a solution of NaN_3 (263 mg, 3.92 mmol) in toluene (2.6 mL) was added Et_2AlCl (4.1 mL, 1.05 M solution in hexane, 4.31 mmol) at 0 °C. After the resulting mixture was stirred at room temperature for 4h, the epoxide **28d** (173 mg, 1.96 mmol) in toluene (1.3 mL) was added via cannula at –78 °C. The reaction mixture was stirred at –78 °C for 1 h and at room temperature for 16 h, then water (2 mL), potassium fluoride (5 g), THF (20 mL) were added carefully at 0 °C. After the suspension mixture was stirred at room temperature for 5 h, $MgSO_4$ was added. The mixture was stirred at room temperature for 1 h, then filtered through Celite and concentrated under reduced pressure. The residue was purified by silica gel column chromatography to give **29d** (184 mg, 1.40 mmol, 72%) as a colorless oil; ^{1}H NMR (500 MHz, $CDCl_3$) δ 3.79–3.53 (m, 4H), 2.56 (brs, 1H, OH), 2.05 (brs, 1H, OH), 1.33 (d, J = 6.3 Hz, 3H); ^{13}C NMR (125 MHz,$CDCl_3$) δ 74.3, 63.1, 58.7, 14.8; IR (neat) 3376, 2976, 2936, 2886, 2117, 1259, 1041 cm^{-1}.

***rac*-(*2S,3S*)-3-azidobutane-1,2-diyl bis(trifluoromethanesulfonate) (22d)**

To a solution of diol **29d** (75.0 mg, 0.572 mmol) in CH_2Cl_2 (2.9 mL) were added 2,6-lutidine (330 μL, 2.86 mmol) and Tf_2O (252 μL, 1.50 mmol) in this order at –78 °C. The mixture was stirred for 15 min, quenched with saturated aqueous NH_4Cl, and extracted with hexane (x 3). The combined organic layers were washed with water and brine, dried over $MgSO_4$, filtered and concentrated in vacuum. The residue was purified by silca gel column chromatography to give **22d** (223 mg, 0.572 mmol, 99%) as a pale yellow oil. Yellow oil; ^{1}H NMR (500 MHz, $CDCl_3$) δ 4.85 (td, *J* = 5.7, 2.8 Hz, 1H), 4.75 (dd, *J* = 12.0, 5.2 Hz, 1H), 4.74 (dd, *J* = 8.0, 2.8 Hz, 1H), 4.05 (quin, *J* = 6.3 Hz, 1H), 1.48 (d, *J* = 6.3 Hz, 3H); ^{13}C NMR (125 MHz, $CDCl_3$) δ 118.5 (q, *J* = 317 Hz), 118.3 (q, *J* = 318 Hz), 85.0, 71.6, 56.3, 15.7; IR (neat) 2987, 2950, 2925, 2851, 2131, 2131, 1246, 1209 cm^{-1}.

***rac*-(*2S,3S*)-3-azido-3-phenylpropane-1,2-diyl bis (trifluoromethanesulfonate) (22e)**

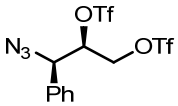

22e

This compound was prepared by the same manner as **22d** from known diol (ref (30)). 68% (ca. 9:1 diastereomeric mixture); White solid; mp 54–55 °C (recrystalized from ether); ^{1}H NMR (500 MHz, $CDCl_3$) δ 7.52–7.45 (m, 3Ha+3Hb), 7.41–7.36 (2Ha+2Hb), 5.08 (td, *J* = 6.3, 2.3 Hz, 1Ha), 5.04 (d, *J* = 6.3 Hz, 1Ha), 4.95 (d, *J* = 8.0 Hz, 1Hb), 4.79 (dd, *J* = 12.0, 5.8 Hz, 1Ha), 4.64 (dd, *J* = 12.0, 2.3 Hz, 1Ha), 4.61 (dd, *J* = 12.0, 2.3 Hz, 1Hb), 4.21 (dd, *J* = 12.0, 4.0 Hz, 1Hb); ^{13}C NMR (125 MHz, $CDCl_3$) δ 132.2 (a), 130.4 (b), 130.1 (a), 130.0 (b), 129.5 (a), 127.5 (b), 127.4 (a), 118.5 (q, *J* = 318 Hz), 118.1 (q, *J* = 317 Hz), 84.9 (a), 84.6 (b), 72.0 (b), 71.6, 64.5 (b), 64.5 (a); IR (neat) 3090, 3070, 3037, 3016, 2975, 2960, 2934, 2122, 1428, 1416, 1249, 1215, 1142 cm^{-1}.

Synthesis of 2,4-di-substituted TAPs

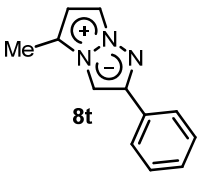

8t

4-methyl-2-phenyl-1,3a,6a-triazapentalene (8t)

Yellow amorphous material; ^{1}H NMR (500 MHz, $CDCl_3$) δ 7.79 (d, *J* = 6.8 Hz, 2H), 7.43-7.48 (m, 3H), 7.34 (t, *J* = 7.4 Hz, 1H), 7.16 (br s, 1H), 6.35 (d, *J* = 1.7 Hz, 1H), 2.42 (s, 3H); ^{13}C NMR (125 MHz, $CDCl_3$) δ 147.7, 131.7, 128.6, 128.2, 125.8, 109.8, 107.3, 102.2, 90.3, 11.2; IR (neat) 3152, 3062, 3032, 2954, 2924, 2853, 1360, 1391, 1360, 1234, 1165, 1071, 1034 cm^{-1}; HRMS (EI) m/z [M$^+$] calcd for $[C_{12}H_{11}N_3]^+$ 197.0953, found 197.0956. UV/Vis (CH_2Cl_2): λ_{max} (log ε) = 252 (4.04), ~295 (3.77), ~330 (3.51), 436 (2.74) nm. FL (CH_2Cl_2): λ_{em} = 437 nm; Φ_F = 0.015 (reference to 9,10-DPA; excited at 340 nm).

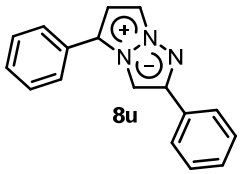

8u

2,4-diphenyl-1,3a,6a-triazapentalene (8u)

White solid; ^{1}H NMR (500 MHz, $CDCl_3$) δ 7.84 (dd, *J* = 8.6, 1.2 Hz, 2H), 7.81 (s, 1H), 7.61 (dd, *J* = 8.6, 1.2 Hz, 2H), 7.57 (d, *J* = 2.8 Hz, 1H), 7.48 (t, *J* = 8.0 Hz, 2H), 7.45 (t, *J* = 7.4 Hz, 2H), 7.37 (t, *J* = 7.4 Hz, 1H), 7.27 (t, *J* = 7.4 Hz, 1H), 6.87 (d, *J* = 2.9 Hz, 1H); ^{13}C NMR (125 MHz, $CDCl_3$) δ148.3, 131.3, 130.0, 129.2, 128.8, 128.6, 126.1, 126.0, 123.4, 115.2, 106.4, 104.3, 93.9; IR (neat) 3154, 3062, 3032, 3006, 2958, 2918, 1850, 1601, 1524, 1466, 1456, 1445, 1388, 1167, 951 cm^{-1}; HRMS (EI) m/z [M^+] calcd for $[C_{17}H_{13}N_3]^+$ 259.1109, found 259.1115. UV/Vis (CH_2Cl_2): λ_{max} (log ε) = 250 (4.33), 364 (4.21) nm. FL (CH_2Cl_2): λ_{em} = 398 nm; Φ_F = 0.014 (reference to 9,10-DPA; excited at 340 nm).

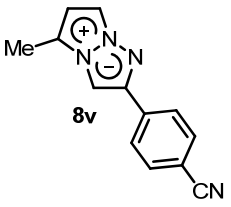

8v

2-(4-cyanophenyl)-4-methyl-1,3a,6a-triazapentalene (8v)

Green amorphous material; ^{1}H NMR (500 MHz, $CDCl_3$) δ 7.88 (d, *J* = 8.6 Hz, 2H), 7.69 (d, *J* = 8.0 Hz, 2H), 7.42 (d, *J* = 2.9 Hz, 1H), 7.23 (brs, 1H), 7.40 (d, *J* = 2.8 Hz, 1H), 2.44 (s, 3H); ^{13}C NMR (125 MHz, $CDCl_3$) δ 145.6, 136.2, 132.5, 126.0, 118.9, 111.3, 110.6, 108.0, 102.6, 91.3, 11.2; IR (neat) 3158, 3147, 3134, 3123, 2917, 2223, 1609, 1417, 1251, 1172, 1038 cm^{-1}; HRMS (ESI) m/z $[M+H]^+$ calcd for $[C_{13}H_{10}N_4+H]^+$ 223.0978, found 223.0979. UV/Vis (CH_2Cl_2): λ_{max} (log ε) = 389 (3.00), 286 (4.02) nm. FL (CH_2Cl_2): λ_{em} = 543 nm; Φ_F = 0.18 (reference to 9,10-DPA; excited at 370 nm).

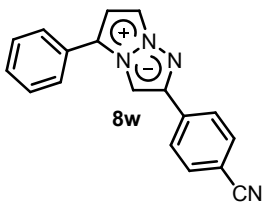

8w

2-(4-cyanophenyl)-4-phenyl-1,3a,6a-triazapentalene (8w)

Yellow solid; mp 175–177 °C; ^{1}H NMR (500 MHz, $CDCl_3$) δ 7.92 (d, *J* = 8.6 Hz, 2H), 7.85 (brs, 1H), 7.71 (d, *J* = 8.0 Hz, 2H), 7.60 (d, *J* = 7.4 Hz, 2H), 7.58 (d, *J* = 3.4 Hz, 1H), 7.50 (t, *J* = 7.4 Hz, 2H), 7.30 (t, *J* = 7.4 Hz, 1H), 6.90 (d, *J* = 2.8 Hz, 1H); ^{13}C NMR (125 MHz, $CDCl_3$) δ 146.1, 135.8, 132.6, 129.5, 129.3, 126.6, 126.2, 123.6, 118.8, 115.9, 111.8, 107.0, 104.6, 94.6; IR (neat) 3152, 3060, 2959, 2924, 2855, 2226, 1669, 1611, 1526, 1454, 1389, 1278, 1240, 1171, 845 cm^{-1}; HRMS (ESI) m/z $[M+H]^+$ calcd for $[C_{18}H_{12}N_4+H]^+$ 285.1135, found 285.1138. UV/Vis (CH_2Cl_2): λ_{max} (log ε) = ~387 (3.84), 345 (4.44), 281 (4.48) nm. FL (CH_2Cl_2): λ_{em} = 542 nm; Φ_F = 0.46 (reference to 9,10-DPA; excited at 370 nm).

Condensation of TAP with Glycine Derivative 30

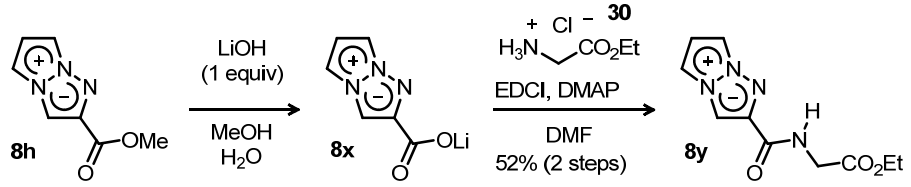

Labeled glycine (8y)

To a solution of **8h** (57.1 mg, 0.35 mmol) in MeOH (1.3 mL) and H_2O (0.4 mL) was added $LiOH \cdot H_2O$ (14.5 mg, 0.35 mmol) at 0 °C. The mixture was stirred at room temperature for 16 h, concentrated under reduced pressure to give lithium salt **8x** as a red amorphous material. The residue was dissolved in DMF (1.7 mL) and cooled to 0 °C. To the mixture were added EDCI (148 mg, 0.77 mmol), DMAP (14 mg, 0.11 mmol) and glycine ethyl ester hydrochloride (97 mg, 0.69 mmol). The mixture was stirred at room temperature for 18 h, quenched with 5% aqueous citric acid (~ pH 5), and extracted with EtOAc (x2). The combined organic layers were washed with brine, dried over anhydrous $MgSO_4$, filtered, and concentrated under reduced pressure. The residue was purified by silica gel flash column chromatography (hexane/ EtOAc = 3/2) to give **8y** (42.1 mg, 0.178 mmol, 52%) as a yellow crystal. mp 96-98 °C (recrystalized from EtOAc/hexane); ^{1}H NMR (500 MHz, $CDCl_3$) δ 7.66 (d, J = 1.2 Hz, 1H), 7.40 (d, J = 2.8 Hz, 1H), 7.29 (m, 1H), 7.20 (d, J = 2.8 Hz, 1H), 6.72 (t, J = 2.8 Hz, 1H), 4.26 (q, J = 6.9 Hz, 2H), 4.22 (d, J = 5.8 Hz, 2H), 1.31 (t, J = 6.9 Hz, 3H); ^{13}C NMR (125 MHz, $CDCl_3$) δ 169.5, 161.1, 141.7, 110.2, 102.2, 101.8, 98.5, 61.4, 41.0, 14.1; IR (neat) 3352, 3152, 2982, 2938, 1744, 1667, 1577, 1524 cm^{-1}; HRMS (EI) m/z [M^+] calcd for $[C_{10}H_{12}N_4O_3]^+$ 236.09094, found 236.09095. UV/Vis (CH_2Cl_2): λ_{max} (log ε) = 281 (4.16), 330 (3.47) nm. FL (CH_2Cl_2): λ_{em} = 418 nm; Φ_F = 0.033 (reference to 9,10-DPA; excited at 340 nm).

Lithium carboxylate (8x)

Red amorphous material; ^{1}H NMR (500 MHz, D_2O) δ 7.40 (d, J = 1.1 Hz, 1H), 7.32 (d, J = 1.1 Hz, 1H), 7.17 (d, J = 2.9 Hz, 1H), 6.57 (t, J = 2.9 Hz, 1H); ^{13}C NMR (125 MHz, D_2O) δ 170.0, 145.2, 111.6, 104.8, 104.4, 101.5; IR (neat) 3156, 1603, 1496, 1406, 1320 cm^{-1}; HRMS (ESI) m/z [M^-] calcd for $[C_6H_4N_3O_2]^-$ 150.0309, found 150.0303. UV/Vis (H_2O): λ_{max} (log ε) = 272 (4.01), 317 (3.47) nm. FL (H_2O): λ_{em} = 449 nm; Φ_F = 0.034 (reference to 9,10-DPA; excited at 340 nm). The lithium carboxylate **8x** was able to pass through the ion exchange resin (Dowex 50 W x 4) to give carboxylic acid form.

Preparation of Alkyne Fragment 23z and 23aa

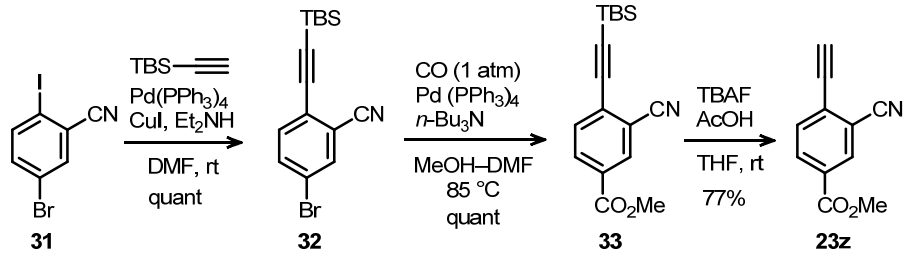

5-bromo-2-((*tert*-butyldimethylsilyl)ethynyl)benzonitrile (32)

To a solution of iodide **31** (24.9 g, 81.0 mmol), TBS-acetylene (15.1 mL, 81.0 mmol) and Et_2NH (25.1 mL, 243 mmol) in anhydrous DMF (405 mL) were added CuI (771 mg, 4.05 mmol), $Pd(PPh_3)_4$ (936 mg, 0.81 mmol) under Ar atmosphere at room temperature. After stirred for 16 h, the mixture was quenched with 1 M HCl at 0 °C and extracted with hexane (twice). The combined organic layers were washed with water and brine, dried over $MgSO_4$, filtrated and concentrated under reduced pressure. The residue was purified by silica-gel column chromatography to give the coupling product **32** (26.5 g, quant) as a yellow solid: mp 69–72 °C; ^{1}H NMR (500 MHz, $CDCl_3$) δ 7.75 (d, J = 2.0 Hz, 1H), 7.65 (dd, J = 8.5, 2.0 Hz, 1H), 7.42 (d, J = 8.0 Hz, 1H), 1.01 (s, 9H), 0.22 (s, 6H); ^{13}C NMR (125 MHz, $CDCl_3$) δ 135.4, 135.0, 133.6, 125.8, 122.0, 117.1, 115.9, 102.2, 100.0, 25.9, 16.5, –5.0; IR (neat) 3099, 3070, 2927, 2888, 2859, 2230, 2165, 1469, 1249, 825 cm^{-1}; HRMS (ESI) m/z $[M+Na]^+$ calcd for $[C_{15}H_{18}NBrSi+Na]^+$ 342.0284, found 342.0284.

Methyl 4-((*tert*-butyldimethylsilyl)ethynyl)-3-cyanobenzoate (33)

To a solution of **32** (13.9 g, 43.5 mmol) and *n*-Bu_3N (31 mL, 130 mmol) in MeOH (36 mL) and DMF (181 mL) was added $Pd(PPh_3)_4$ (2.5 g, 2.18 mmol) under Ar atmosphere at room temperature. After the flask was substituted with CO gas, the reaction mixture was heated to 85 °C for 14 h. After cooled to room temperature, the mixture was quenched with 1M HCl, diluted with hexane and filtrated through Celite. The filtrate was separated and the aqueous layer was extracted with hexane (x1). The combined organic layers were washed with water and brine, dried over $MgSO_4$, filtered and concentrated under reduced pressure. The residue was purified by silica-gel column chromatography to give ester **33** (13.0 g, quant) as a yellow oil: ^{1}H NMR (500 MHz, $CDCl_3$) δ 8.29 (d, J = 1.5 Hz, 1H), 8.16 (dd, J = 8.5, 1.5 Hz, 1H), 7.64 (d, J = 9.0 Hz, 1H), 3.95 (s, 3H), 1.03 (s, 9H), 0.24 (s, 6H); ^{13}C NMR (125 MHz, $CDCl_3$) δ 164.6, 133.6, 132.9, 132.7, 130.9, 130.0, 116.5, 116.0, 104.6, 100.4, 52.7, 26.0, 16.6, –4.9; IR (neat) 3072, 3006, 2952, 2928, 2894, 2858, 2234, 2162, 1727, 1601, 1299, 1257, 828 cm^{-1}; HRMS (ESI) m/z $[M+Na]^+$ calcd for $[C_{17}H_{21}O_2NSi+Na]^+$ 322.1234, found 322.1233.

Methyl 3-cyano-4-ethynylbenzoate (23z)

To a solution of **33** (12.9 g, 43.1 mmol) and acetic acid (3.0 mL, 51.7 mmol) in THF (216 mL) was added TBAF (47.4 mL, 1 M solution in THF, 47.4 mmol) at room temperature. After stirred for 5 min, the mixture was diluted with water, extracted with ether (x2). The combined organic layers were washed with brine, dried over $MgSO_4$, filtered and concentrated under reduced pressure. The residue was recrystalized from EtOAc to give **23z** (6.2 g, 77%) as orange crystals: mp 111–113 °C; ^{1}H NMR (500 MHz, $CDCl_3$) δ 8.30 (d, J = 1.5 Hz, 1H), 8.19 (dd, J = 8.0, 2.0 Hz, 1H), 7.68 (d, J = 8.0 Hz, 1H), 3.95 (s, 3H), 3.65 (s, 1H); ^{13}C NMR (125 MHz, $CDCl_3$) δ 164.5, 133.6, 133.1, 133.1, 130.7, 129.7, 116.3, 116.2, 86.8, 79.0, 52.8; IR (neat) 3249, 2236, 2110, 1714, 1298, 1287, 1258 cm^{-1}; HRMS (ESI) m/z $[M+H]^+$ calcd for $[C_{11}H_8NO_2]^+$ 186.0550, found 186.0552.

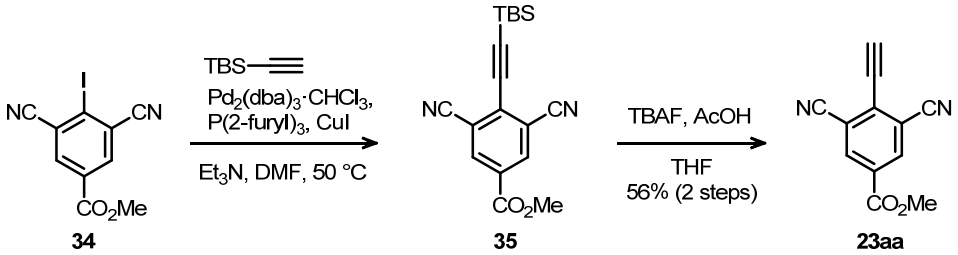

Methyl 3,5-dicyano-4-ethynylbenzoate (23aa)

To a solution of iodide **34** (511 mg, 1.64 mmol), TBS-acetylene (460 μL, 2.46 mmol) and Et_3N (691 μL, 4.92 mmol) in anhydrous DMF (16.4 mL) were added CuI (62.5 mg, 0.328 mmol), P(2-furyl)$_3$ (76.2 mg, 0.328 mmol), $Pd_2(dba)_3{\cdot}CHCl_3$ (170 mg, 0.164 mmol) under Ar atmosphere at room temperature. After stirred for 2 h at 50 °C, the mixture was quenched with 1 M HCl at room temperature, extracted with ether (twice). The combined organic layers were washed with water (x2) and brine, dried over $MgSO_4$, bleached with activated charcoal, filtrated through Celite and concentrated under reduced pressure. The crude product was dissolved in THF (16.4 mL) and then acetic acid (940 μL, 16.4 mmol) and TBAF (1.8 mL, 1 M solution in THF, 1.80 mmol) were added to the solution. After stirred for 30 min at room temperature, the reaction mixture was quenched with 1 M HCl, extracted with ether (x3). The combined organic layers were washed with brine, dried over $MgSO_4$, filtered and concentrated under reduced pressure. The residue was recrystalized from EtOAc to give **23aa** (192 mg, 56% for 2 steps) as orange crystals: dec. 157 °C; ^{1}H NMR (500 MHz, $CDCl_3$) δ 8.50 (s, 2H), 4.10 (s, 1H), 4.01 (s, 3H); ^{13}C NMR (125 MHz, $CDCl_3$) δ 136.7, 132.6, 131.5, 117.9, 114.8, 93.7, 76.1, 53.4; IR (neat) 3261, 3070, 2231, 2109, 1729, 1319, 1228 cm^{-1}; HRMS (FD) m/z $[M]^+$ calcd for $[C_{12}H_6N_2O_2]^+$ 210.0429, found 210.0434.

Synthesis of Yellow and Red Fluorescent TAPs

2-(2-cyano-4-(methoxycarbonyl)phenyl) -1,3a,6a-triazapentalene (8z)

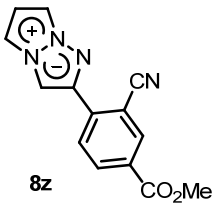

Light brown powder; ^{1}H NMR (500 MHz, $CDCl_3$) δ 8.40 (d, *J* = 1.5 Hz, 1H), 8.28 (dd, *J* = 8.5, 1.5 Hz, 1H), 8.22 (d, *J* = 8.5 Hz, 1H), 8.06 (d, *J* = 1.0 Hz, 1H), 7.48 (d, *J* = 2.5 Hz, 1H), 7.23 (d, *J* = 3.0 Hz, 1H), 6.71 (dd, *J* = 3.0, 2.5 Hz, 1H), 3.97 (s, 3H); ^{13}C NMR (125 MHz, $CDCl_3$) δ 164.9, 142.4, 138.2, 135.2, 133.7, 129.8, 128.5, 118.3, 110.0, 109.0, 102.5, 101.8, 96.7, 52.6; IR (neat) 3170, 3155, 2226, 1716, 1296 cm^{-1}; HRMS (ESI) m/z $[M+Na]^+$ calcd for $[C_{14}H_{10}N_4O_2+Na]^+$ 289.0696, found 289.0698. UV/Vis (CH_2Cl_2): λ_{max} (log ε) = 420 (2.80), 285 (3.98) nm. FL (CH_2Cl_2): λ_{max} = 572 nm; Φ_F = 0.34 (reference to rhodamine B; excited at 400 nm).

2-(2,6-dicyano-4-(methoxycarbonyl)phenyl) -1,3a,6a-triazapentalene (8aa)

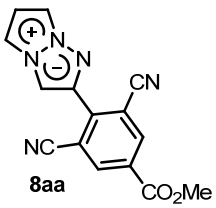

Dark brown solid; dec. 195 °C; ^{1}H NMR (500 MHz, $CDCl_3$) δ 8.61 (s, 2H), 7.80 (s, 2H), 7.59 (d, *J* = 2.0 Hz, 1H), 7.30 (d, *J* = 2.5 Hz, 1H), 6.77 (t, *J* = 2.5 Hz, 1H), 4.03 (s, 3H); ^{13}C NMR (125 MHz, $CDCl_3$) δ 163.1, 140.5, 139.4, 138.5, 130.9, 116.3, 113.9, 110.3, 103.4, 102.2, 97.4, 53.3; IR (neat) 3179, 3158, 3141, 3064, 2231, 1732, 1717, 1558, 1541, 1521, 1507, 1315, 1232 cm^{-1}; HRMS (ESI) m/z $[M+Na]^+$ calcd for $[C_{15}H_9N_5O_2+Na]^+$ 314.0648, found 314.0648. UV/Vis (CH_2Cl_2): λ_{max} (log ε) = 466 (3.20), 286 (4.42) nm. FL (CH_2Cl_2): λ_{max} = 632 nm; Φ_F = 0.096 (reference to rhodamine B; excited at 430 nm).

Synthesis of 2,4-di-substituted TAPs 8ab and 8ac.

2-(4-(methoxycarbonyl)phenyl) -4-phenyl-1,3a,6a-triazapentalene (8ab)

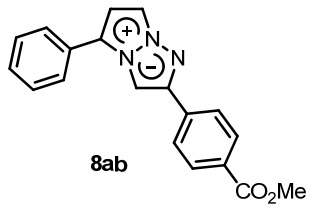

Green solid; mp. 124–127 °C; ^{1}H NMR (400 MHz, $CDCl_3$) δ 8.11 (d, *J* = 10.8 Hz, 2H), 7.90 (d, *J* = 10.8 Hz, 2H), 7.86 (s, 1H), 7.60 (d, *J* = 10.0 Hz, 2H), 7.58 (d, *J* = 3.6 Hz, 1H), 7.49 (t, *J* = 10.0 Hz, 2H), 7.32–7.24 (m, 1H), 6.88 (d, *J* = 4.0 Hz, 1H), 3.94 (s, 3H); ^{13}C NMR (125 MHz, $CDCl_3$) δ 166.7, 147.0, 135.6, 130.0, 129.8, 129.7, 129.2, 126.3, 125.6, 123.4, 115.5, 106.7, 104.4, 94.5, 52.1; IR (neat) 3155, 1950, 1715, 1277 cm^{-1}; HRMS (ESI) m/z $[M+Na]^+$ calcd for $[C_{19}H_{15}N_3O_2Na]^+$ 340.1062, found 340.1064. UV/Vis (CH_2Cl_2): λ_{max} (log ε) = 345 (4.35), 279 (4.44) nm. FL (CH_2Cl_2): λ_{max} = 548 nm; Φ_F = 0.36 (reference to rhodamine B; excited at 400 nm).

2-(2-cyano-4-(methoxycarbonyl)phenyl) -4-phenyl1,3a,6a-triazapentalene (8ac)

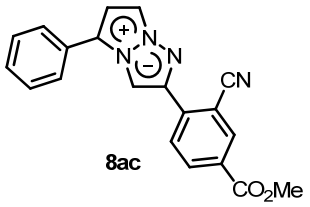

Orange solid; dec. 216 °C; ^{1}H NMR (400 MHz, $CDCl_3$) δ 8.44 (s, 1H), 8.39 (s, 1H), 8.31 (d, *J* = 8.0 Hz, 1H), 8.24 (d, *J* = 8.0 Hz, 1H), 7.66–7.59 (m, 3H), 7.50 (t, *J* = 7.6 Hz, 2H), 7.30 (t, *J* = 7.6 Hz, 1H), 6.95 (d, *J* = 2.8 Hz, 1H), 3.98 (s, 3H); ^{13}C NMR (125 MHz, $CDCl_3$) δ 164.9, 143.1, 138.0, 135.3, 133.8, 130.2, 129.4, 129.4, 128.7, 126.8, 123.7, 118.3, 116.3, 109.3, 107.6, 104.5, 96.9, 52.7; IR (neat) 3155, 2960, 2228, 1733, 1300 cm^{-1}; HRMS (ESI) m/z $[M+H]^+$ calcd for $[C_{20}H_{15}N_4O_2]^+$ 343.1195, found 343.1198. UV/Vis (CH_2Cl_2): λ_{max} (log ε) = 432 (3.66), 336 (4.58), 282 (4.48) nm. FL (CH_2Cl_2): λ_{max} = 613 nm; Φ_F = 0.070 (reference to rhodamine B; excited at 400 nm).

Synthesis of TAP NHS Ester 8ae

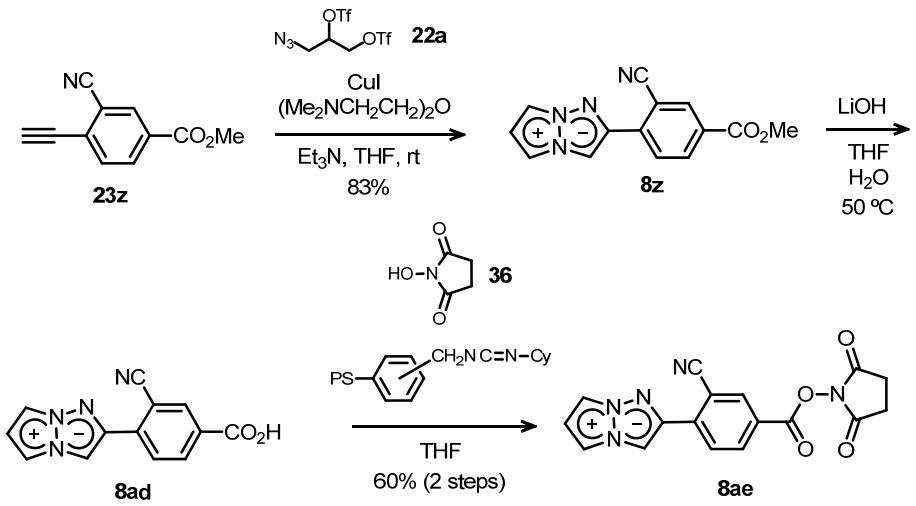

Typical procedure for large-scale synthesis of 8z.

To a solution of azide **22a** (5.10 g, 13.4 mmol) and alkyne **23z** (2.25 g, 12.2 mmol) in THF (610 mL) were added the homogeneous solution of CuI (116 mg, 0.610 mmol), bis [2-(*N*,*N*-dimethylaminoethyl)]ether (115 μL, 0.610 mmol) and Et_3N (8.6 mL, 61.0 mmol) in THF (61 mL) at room temperature. After the resulting mixture was stirred for 24 h, the solvent was removed to less than one third under reduced pressure and then aq 5% NH_3 was poured to precipitate a powder. The powder was separated by filtration and dried *in vacuo* to afford **8ad** (2.7 g, 83%) as a light brown powder.

2-(2-cyano-4-(((2,5-dioxopyrrolidin-1-yl)oxy)carbonyl)phenyl)-1,3a,6a-triaza- pentalene (8ae)

To a solution of **8z** (2.70 g, 10.1 mmol) in H_2O (50 mL) and THF (101 mL) was added $LiOH·H_2O$ (510 mg, 12.1 mmol) at room temperature. After stirred at 50 °C for 30 min, the

mixture was washed with ether (x1), acidified by 1M HCl to participate yellow solid. The solid was dissolved in THF/EtOAc mixture and the organic layer was separated. After the aqueous layer was extracted with THF/EtOAc (x2), the combined organic layers were dried over $MgSO_4$, filtered and concentrated *in vacuo*. The residue was dehydrated by toluene azeotropy and dissolved in THF (54 mL). To the mixture were added *N*-hydroxysuccinimide (1.23 g, 10.7 mmol) and *N*-cyclohexylcarbodiimidomethyl polystylene resin (8.7 g, 13.0 mmol, TCI No. C2141, 1.5 mmol/g loading) at room temperature. After the reaction mixture was stirred for 1 h, solid materials were removed by filtration and the residue was washed with THF. The filtrate was concentrated *in vacuo* to form red powder. This powder was dispersed to hexane, filtered, washed with ether and CH_2Cl_2 to give **8ae** (2.1 g, 56% for 2 steps) as a red powder: dec. 200 °C; ^{1}H NMR (500 MHz, CD_2Cl_2) δ 8.50 (d, *J* = 1.5 Hz, 1H), 8.35 (dd, *J* = 8.0, 1.5 Hz, 1H), 8.31 (d, *J* = 8.5 Hz, 1H), 8.11 (s, 1H), 7.51 (d, *J* = 2.5 Hz, 1H), 7.29 (d, *J* = 3.0 Hz, 1H), 6.75 (dd, *J* = 3.0, 2.5 Hz, 1H), 2.91 (brs, 4H); ^{13}C NMR (100 MHz, DMSO-d_6) δ 170.1, 160.2, 141.4, 139.5, 136.0, 134.2, 129.2, 124.1, 117.4, 110.5, 109.1, 103.3, 102.9, 97.4, 25.5; IR (neat) 3181, 3141, 2225, 1773, 1737, 1200 cm^{-1}; HRMS (ESI) m/z $[M+Na]^+$ calcd for $[C_{17}H_{12}N_5O_4+Na]^+$ 350.0884, found 350.0886. UV/Vis (CH_2Cl_2): λ_{max} (log ε) = 446 (3.38), 287 (4.47) nm. FL (CH_2Cl_2): λ_{max} = 624 nm (fluorescence quantum yield was not estimated because of gradual degradation of **8ae** under the measurement condition.)

Synthesis of Tripeptide II as a Substrate for Labeling Reaction

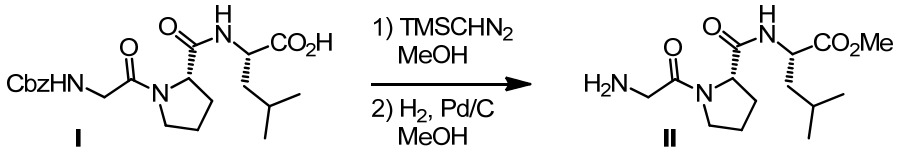

Scheme S4. Synthesis of tripeptide **II**

To a solution of **I** (104.9 mg, 0.250 mmol) in MeOH (2.5 mL) was added $TMSCHN_2$ (1.3 mL, 2.60 mmol, 2.0 M ether solution) at room temperature. After stirred for 1 h, the mixture was concentrated *in vacuo*. The residue was dissolved in MeOH (2.5 mL) and to the resulting solution was added 10% Pd/C (12 mg). After stirred for 24 h under H_2 atmosphere, the suspension was diluted with $CHCl_3$, filtered through Celite and concentrated *in vacuo*. The residue was purified by silica-gel column chromatography to give **II** (86.7 mg, quant) as a colorless amorphous solid: ^{1}H NMR (400 MHz, $CDCl_3$) δ 7.96 (d, *J* = 7.2 Hz, 1H), 4.65 (dd, *J* = 7.6, 2.4 Hz, 1H), 4.42 (ddd, *J* = 10.0, 7.6, 5.2 Hz, 1H), 4.13 (d, *J* = 16.0 Hz, 1H), 3.98 (d, *J* = 15.6 Hz, 1H), 3.71 (s, 3H), 3.73–3.60 (m, 1H), 3.51 (dd, *J* = 16.8, 8.8 Hz, 1H), 2.23–1.85 (m,

5H), 1.72–1.50 (m, 2H), 0.93 (d, J = 6.4 Hz, 3H), 0.88 (d, J = 6.4 Hz, 3H); ^{13}C NMR (400 MHz, $CDCl_3$) δ 174.0, 172.1, 167.1, 60.8, 52.4, 51.4, 46.8, 41.8, 39.4, 29.8, 25.0, 24.3, 22.8, 21.4; IR (neat) 3148 (br), 3054, 2958, 2874, 1740, 1654, 1540, 1228, 1209, 669 (br) cm^{-1}; HRMS (ESI) m/z $[M+Na]^+$ calcd for $[C_{14}H_{25}N_3O_4+Na]^+$ 322.1743, found 322.1743.

Condensation of amines with 8ae

Labeled glycine ethyl ester 37a

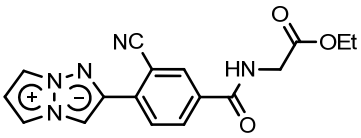

37a

To a solution of glycine ethyl ester hydrochloride (5.5 mg, 0.0394 mmol), Et_3N (27.7 μL, 0.197 mmol) in DMF (80 μL) was added NHS ester **8ae** (15.2 mg, 0.0451 mmol) at room temperature. After stirred for 15 min, the mixture was filtered through silica-gel pad ($CHCl_3$/EtOAc = 1:1). The filtrate was concentrated under reduced pressure and contaminated DMF was removed by azeotrope with toluene to afford pure **12** (12.6 mg, 95%) as a yellow amorphous powder: ^{1}H NMR (400 MHz, $CDCl_3$) δ 8.22 (d, J = 6.8 Hz, 1H), 8.20 (s, 1H), 8.05 (dd, 1H), 8.04 (d, J = 1.2 Hz), 7.48 (d, J = 2.8 Hz, 1H), 7.22 (d, J = 3.2 Hz, 1H), 6.78 (brt, 1H), 6.71 (t, J = 2.8 Hz, 1H), 4.29 (q, J = 7.2 Hz, 2H), 4.26 (d, J = 4.8 Hz, 2H), 1.33 (t, J = 7.2 Hz, 3H); ^{13}C NMR (100 MHz, $CDCl_3$) δ 169.8, 164.9, 142.4, 137.3, 133.3, 133.0, 131.2, 128.7, 118.3, 109.9, 109.2, 102.5, 101.8, 96.6, 61.9, 42.0, 14.1; IR (neat) 3394, 3343, 3158, 2982, 2932, 2228, 1747, 1651, 1608, 1540, 1511, 1208 cm^{-1}; HRMS (ESI) m/z $[M+Na]^+$ calcd for $[C_{17}H_{15}N_5O_3+Na]^+$ 360.1073, found 360.1072. UV/Vis (CH_2Cl_2): λ_{max} (log ε) = 387 (3.40), 284 (4.30) nm. FL (CH_2Cl_2): λ_{max} = 563 nm; Φ_F = 0.37 (reference to rhodamine B; excited at 400 nm).

Labeled tripeptide 37b

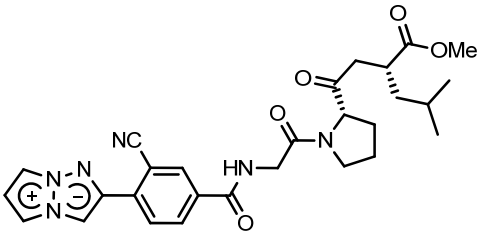

37b

To a solution of tripeptide **II** (11.0 mg, 0.0367 mmol), Et_3N (25.8 μL, 0.184 mmol) in DMF (73 μL) was added NHS ester **8ae** (12.8 mg, 0.0367 mmol) at room temperature. After stirred for 10 min, the mixture was directly purified by silica-gel column chromatography to give **11** (16.1 mg, 82%) as a yellow amorphous solid: ^{1}H NMR (400 MHz, $CDCl_3$) δ 8.24 (s, 1H), 8.18 (d, J = 8.4 Hz, 1H), 8.06 (d, J = 8.0 Hz, 1H), 8.02 (s, 1H), 7.48 (d, J = 2.8 Hz, 1H), 7.45 (brs, 1H), 7.22 (d, J = 2.8 Hz, 1H), 6.86 (d, J = 8.0 Hz, 1H), 6.70 (t, J = 2.8 Hz, 1H), 4.64–4.50 (m, 2H), 4.30 (dd, J = 17.6, 4.4 Hz, 1H), 4.22 (dd, J = 18.0, 4.0 Hz, 1H), 3.74 (s, 3H), 3.73–3.63 (m, 1H), 3.54 (dd, J = 15.6, 8.0 Hz, 1H), 2.40–2.28 (m, 1H), 2.26–1.95 (m, 3H), 1.82–1.50 (m, 3H), 0.92 (d, J = 5.6 Hz, 3H),

0.92 (d, J = 5.2 Hz, 3H); ^{13}C NMR (100 MHz, $CDCl_3$) δ 173.2, 170.5, 167.9, 164.7, 142.5, 137.2, 133.3, 133.1, 131.2, 128.6, 118.4, 109.9, 109.2, 102.5, 101.8, 96.6, 60.3, 52.3, 51.1, 46.5, 42.6, 41.3, 28.0, 25.0, 24.8, 22.7, 22.0; IR (neat) 3307, 3154, 3069, 2956, 2228, 1742, 1646, 1541, 1314, 1203 cm^{-1}; HRMS (ESI) m/z $[M+Na]^+$ calcd for $[C_{27}H_{31}N_7O_5+Na]^+$ 556.2284, found 556.2283. UV/Vis (CH_2Cl_2): λ_{max} (log ε) = 379 (3.34), 283 (4.26) nm. FL (CH_2Cl_2): λ_{max} = 561 nm; Φ_F = 0.24 (reference to rhodamine B; excited at 400 nm).

Computational Details for Theoretical Calculation

The equilibrium geometry in the electronic ground state (S_0) was determined by the density functional theory (DFT) calculations using the B3LYP functionals, while the geometry optimization in the lowest ππ* excited state S_1 (ππ*) was performed by the time-dependent DFT (TD-DFT) calculations employing the coulomb attenuated B3LYP (CAM-B3LYP) functionals. The C_s symmetry constraint was imposed for **8a**, **8l**, **8n** and **8z** while no constraint was applied for **8aa** because the twisted structure was more stable due to the steric hindrance. The choice to employ the CAM-B3LYP functionals was due to the significant charge-transfer character involved in excitation to the S_1 state. The 6-31 + G(d,p) basis set was used in the DFT calculations and the equilibrium geometries were determined both in the gas phase and in dichloromethane. The solvent effects were taken into account by the polarizable continuum solvation model (PCM),[38] where the radii are taken from the universal force field.[39] After the geometry optimization, the vertical excitation and fluorescence energies were calculated at the S_0 and S_1 equilibrium structures (denoted as $(S_0)_{min}$ and $(S_1)_{min}$), respectively, by the TD-DFT(CAM-B3LYP) method. In PCM calculations, the linear-response method with a non-equilibrium solvation was employed to obtain the vertical excitation energies at $(S_0)_{min}$, while the equilibrium solvation was adapted for the calculation of the excitation energies during the S_1 geometry optimization. The excitation energy was also refined at the DFT-optimized geometries by the CASPT2 method in order to obtain more reliable excitation energies.[36] A level shift with a value of 0.3 is applied for the CASPT2 calculations.[37] The notation of CASPT2 (*m*,*n*) was occasionally used, in which case the active space for a reference state-averaged complete active space self-consistent field (SA-CASSCF) wavefunction was composed of *m* electrons and *n* orbitals (SA-CASSCF (*m*,*n*)). The augmented correlation-consistent polarized double-zeta basis set (denoted as aug-cc-pVDZ) was employed in the CASPT2 calculations. For obtaining the oscillator strengths, the vertical excitation energies calculated by CASPT2 and the transition dipole moments calculated by SA-CASSCF were used.

For **8a**, the active space for the reference SA-CASSCF wavefunction was comprised of six π orbitals (four π orbitals were doubly-occupied and two were unoccupied in the

closed-shell configuration), and it was therefore denoted as SA-CASSCF (8,6). **8a** possessed ten π orbitals and the lowest and highest π orbitals were excluded from the active space. This was justified by the larger active space calculation, which includes all π orbitals, where only a difference of ~0.01 eV was observed in the S_1 vertical excitation energies. The active space for the other chromophores was composed of twelve electrons distributed in ten π orbitals (SACASSCF (12,10)), and the active orbitals of **8n** at $(S_0)_{min}$ were shown in Figure 20. As seen in the figure, the active space of the SA-CASSCF (12,10) wavefunction includeed orbitals that corresponded to the active orbitals of SA-CASSCF (8,6) in **8a**. For all chromophores, the S_0 and S_1 states were averaged with equal weights in the SA-CASSCF calculations, except where otherwise noted. The DFT and TD-DFT calculations were performed using the Gaussian09 program package[40] while the CASPT2 calculations were carried out using the MOLPRO2010.1 program package.[41]

	TD-DFT (gas)	TD-DFT (DCM)	CASPT2 (gas)	CASPT2 (DCM)[a]	Exp.
8a	259	268	291	300	288
8n	322	339	380	397	381
8l	317	332	374	389	376
8z	353	372	418	437	420
8aa	387	398	450	461	466

[a] the value was an estimate in DCM

Table E1. The excitation energies (wavelength in nm) for the S1 state calculated by TD-DFT and CASPT2 at $(S_0)_{min}$.

	TD-DFT (gas)	TD-DFT (DCM)	CASPT2 (gas)	CASPT2 (DCM)[a]	Exp.
8a	268	287	307	326	389
8n	358	390	430	462	509
8l	356	389	426	459	510
8z	394	425	471	502	572
8aa	440	463	533	556	632

[a] the value was an estimate in DCM

Table E2. The fluorescence energies (wavelength in nm) for the S1 state calculated by TD-DFT and CASPT2 at $(S_1)_{min}$.

Absorption and Fluorescence Spectra of Selected 1,3a,6a-Triazapentalene Derivatives

8a

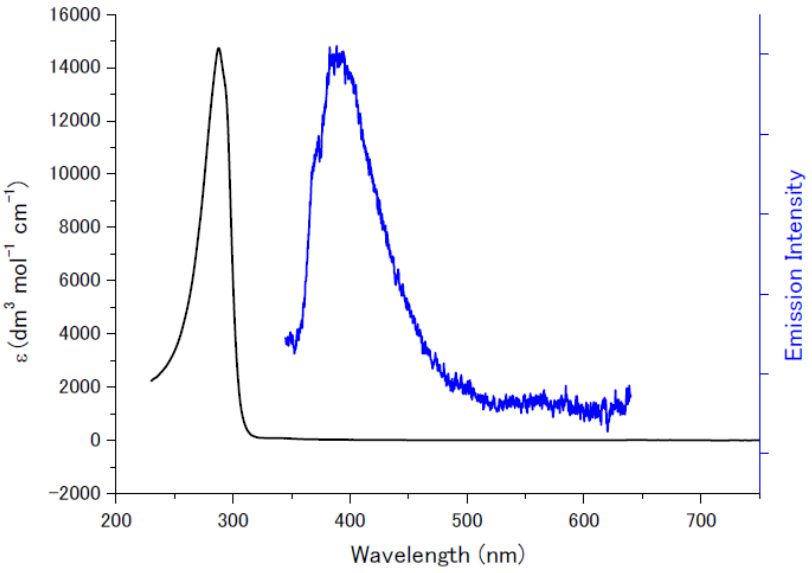

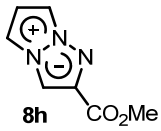
8h
CO2Me

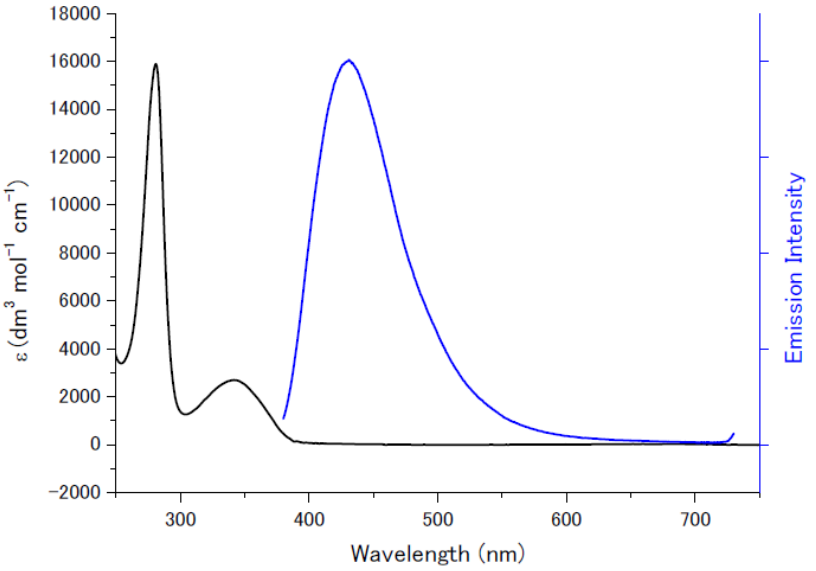
ε (dm3 mol−1 cm−1)
Emission Intensity
Wavelength (nm)

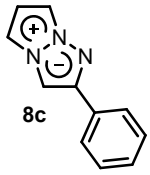
8c

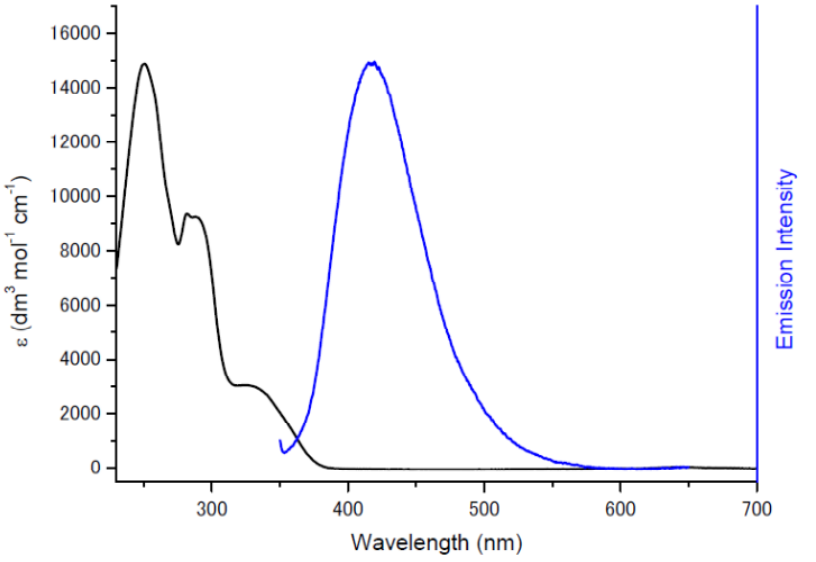
ε (dm3 mol−1 cm−1)
Emission Intensity
Wavelength (nm)

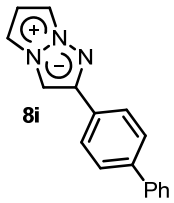
8i
Ph

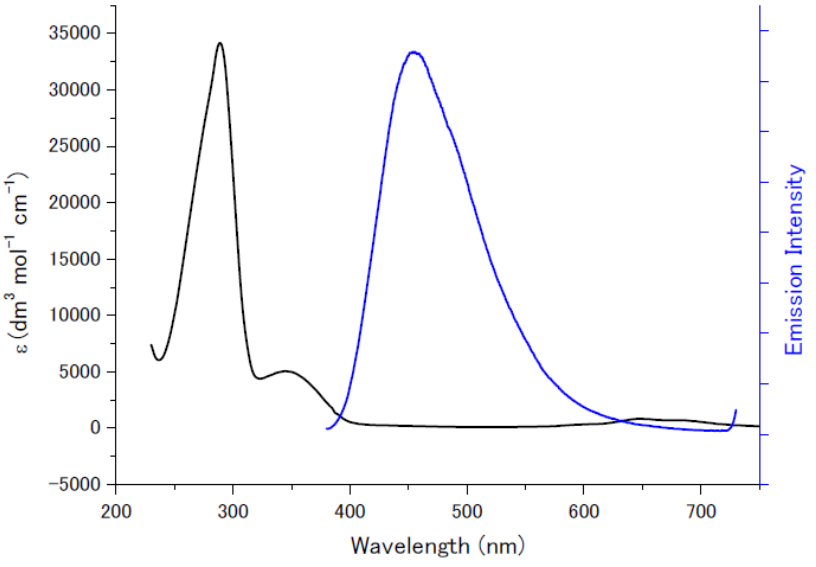
ε (dm3 mol−1 cm−1)
Emission Intensity
Wavelength (nm)

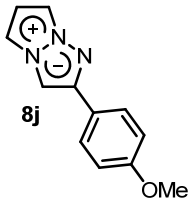
8j
OMe

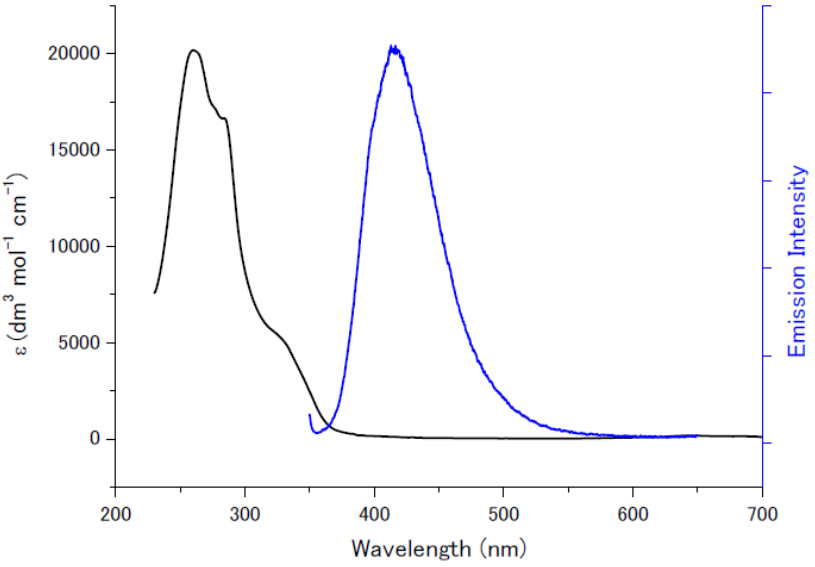
20000
15000
10000
5000
0
200
300
400
500
600
700
Wavelength (nm)
ε (dm3 mol-1 cm-1)
Emission Intensity

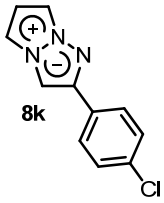
8k
Cl

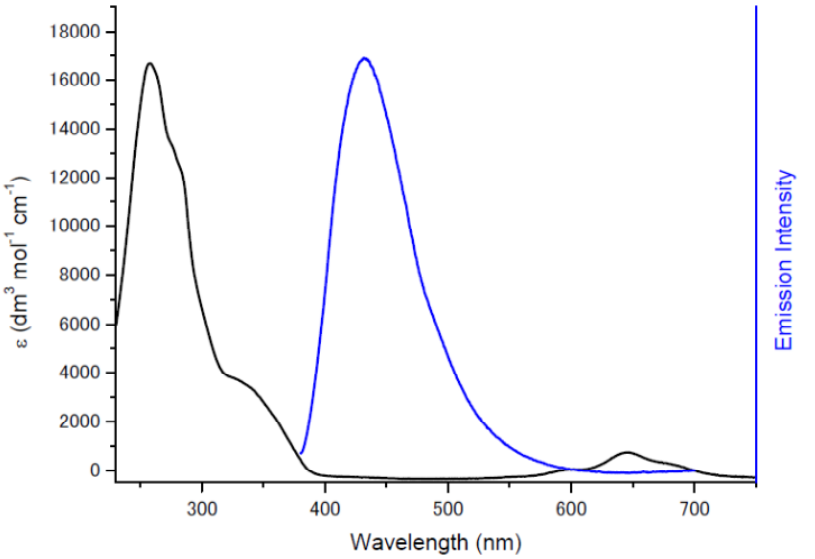
18000
16000
14000
12000
10000
8000
6000
4000
2000
0
300
400
500
600
700
Wavelength (nm)
ε (dm3 mol-1 cm-1)
Emission Intensity

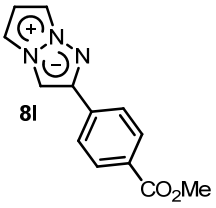
8l
CO2Me

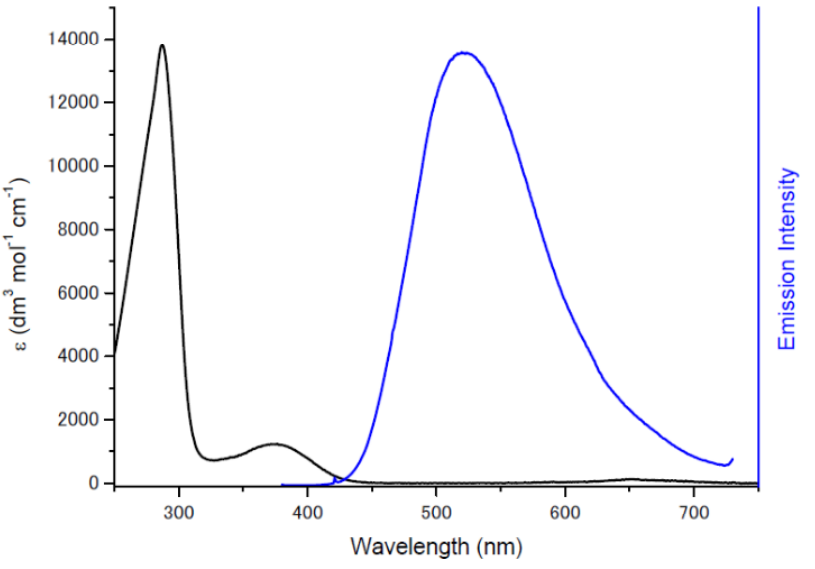
14000
12000
10000
8000
6000
4000
2000
0
300
400
500
600
700
Wavelength (nm)
ε (dm3 mol-1 cm-1)
Emission Intensity

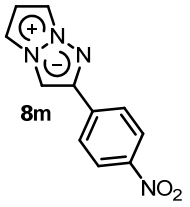
8m
NO2

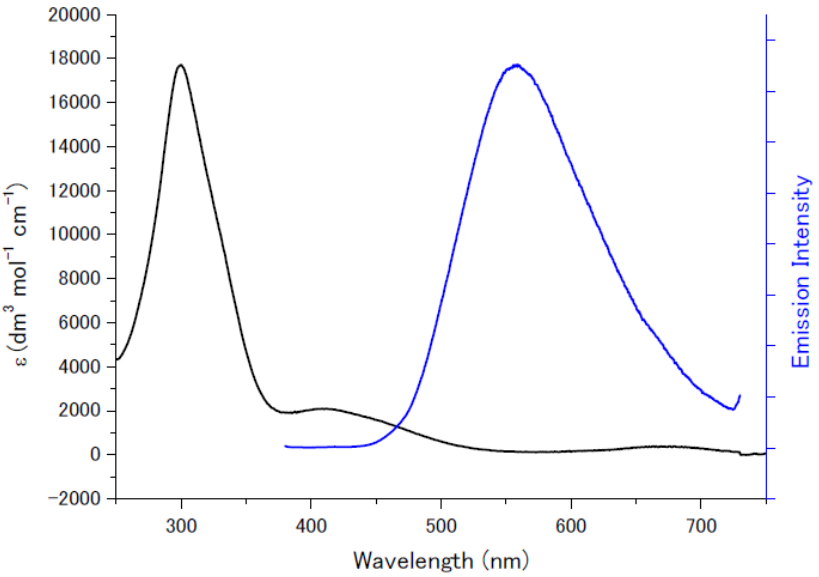
ε (dm3 mol-1 cm-1)
Emission Intensity
Wavelength (nm)

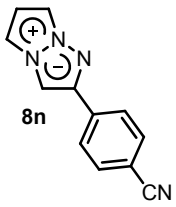
8n
CN

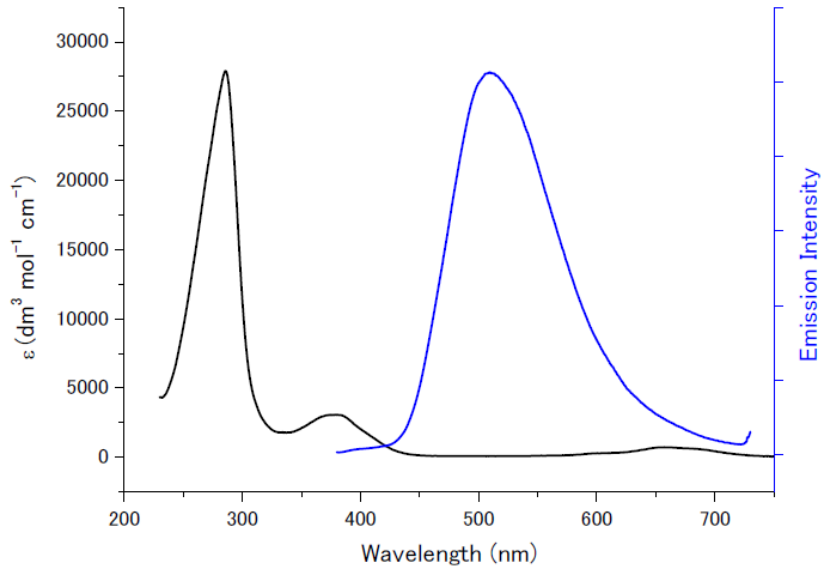
ε (dm3 mol-1 cm-1)
Emission Intensity
Wavelength (nm)

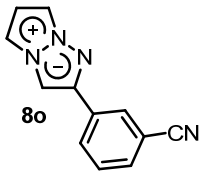
8o
CN

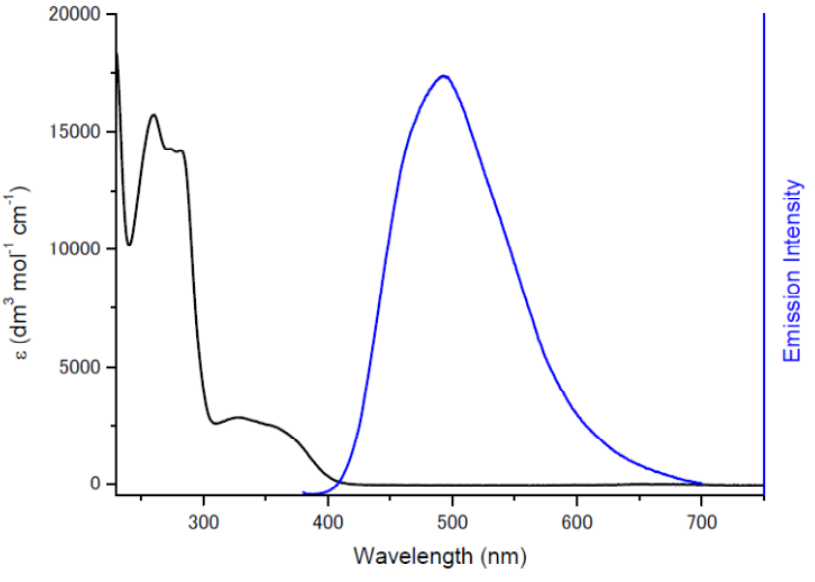
ε (dm3 mol-1 cm-1)
Emission Intensity
Wavelength (nm)

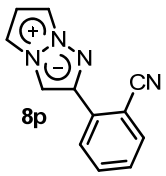
CN

8p

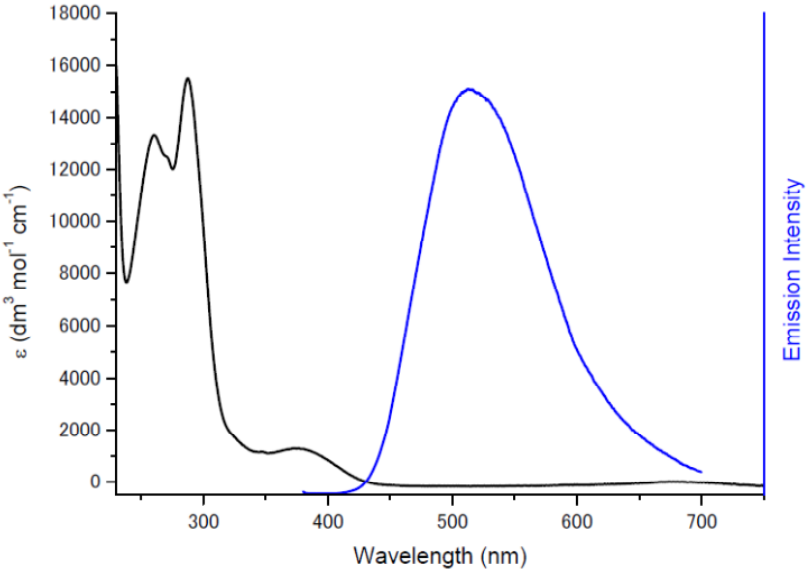
ε (dm3 mol-1 cm-1)
Emission Intensity
Wavelength (nm)

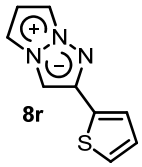
S

8r

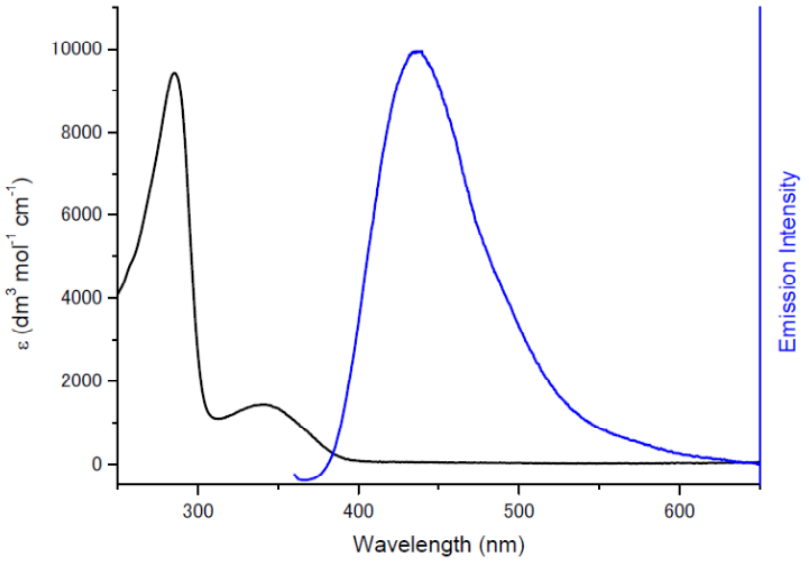
ε (dm3 mol-1 cm-1)
Emission Intensity
Wavelength (nm)

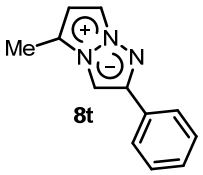
Me

8t

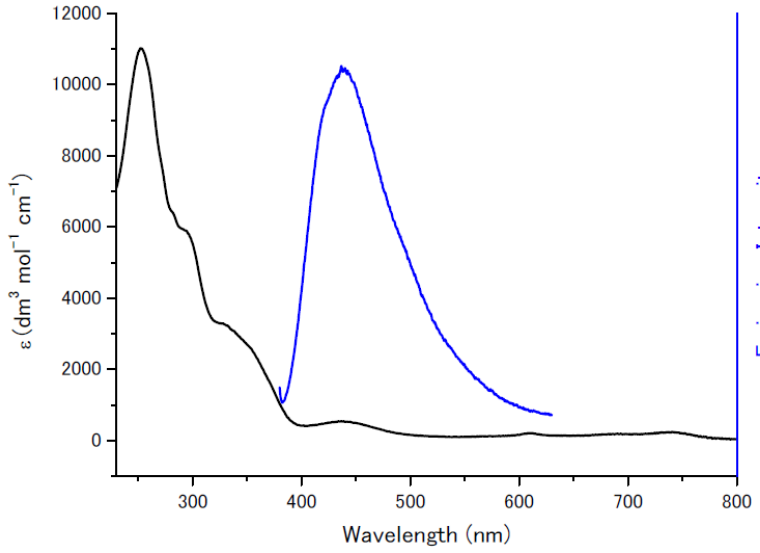
ε (dm3 mol-1 cm-1)
Emission Intensity
Wavelength (nm)

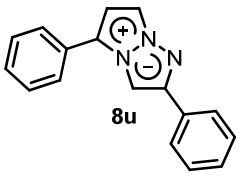
8u

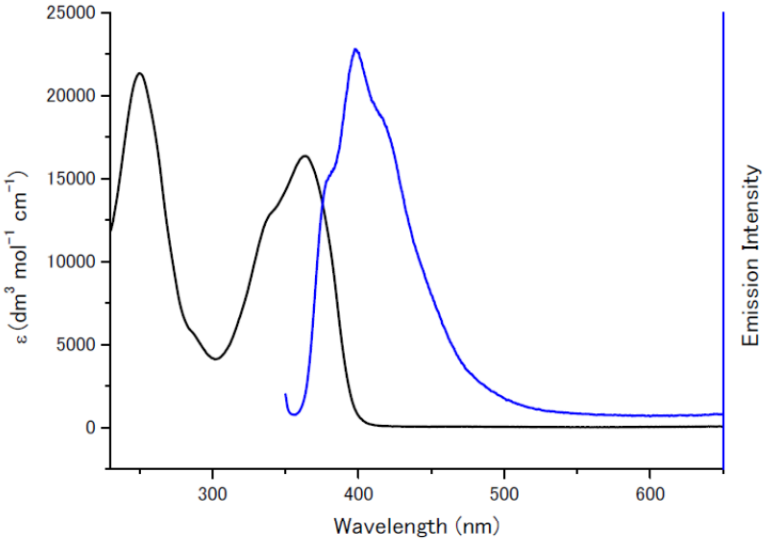
25000
20000
15000
10000
5000
0
ε (dm3 mol-1 cm-1)
Emission Intensity
300
400
500
600
Wavelength (nm)

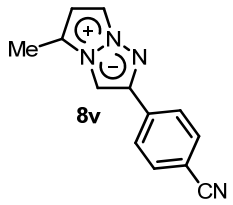
Me
8v
CN

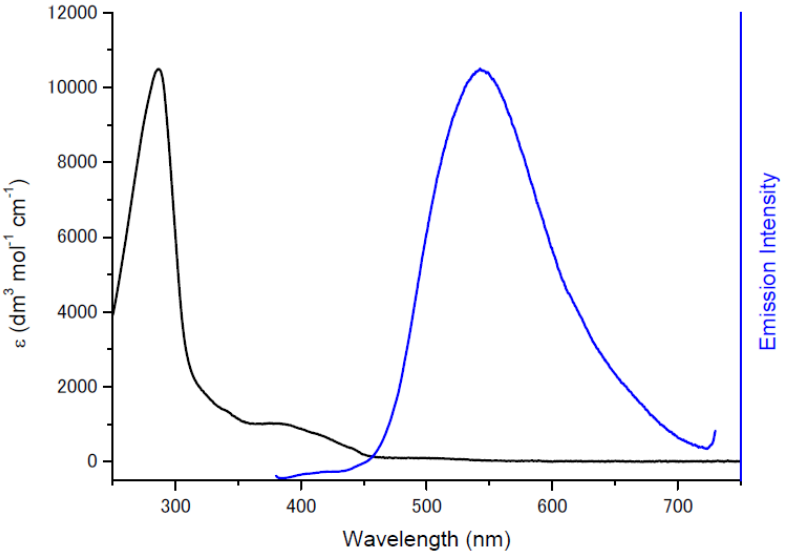
12000
10000
8000
6000
4000
2000
0
ε (dm3 mol-1 cm-1)
Emission Intensity
300
400
500
600
700
Wavelength (nm)

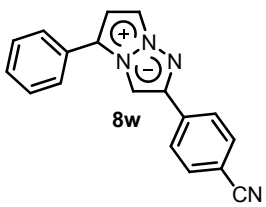
8w
CN

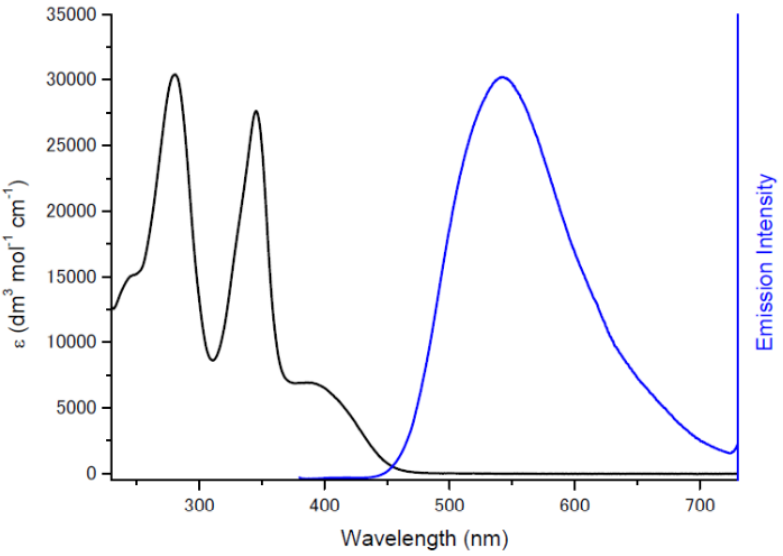
35000
30000
25000
20000
15000
10000
5000
0
ε (dm3 mol-1 cm-1)
Emission Intensity
300
400
500
600
700
Wavelength (nm)

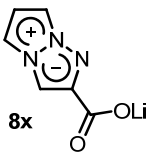
OLi
O

8x

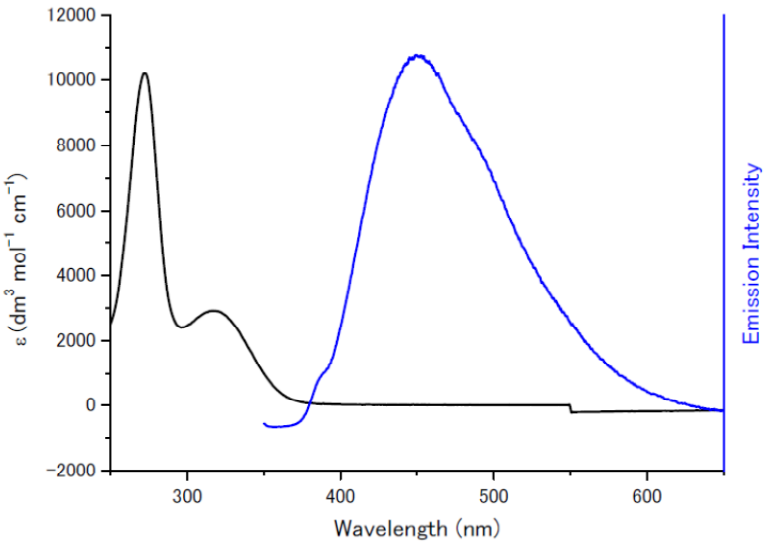
12000
10000
8000
6000
4000
2000
0
−2000
ε (dm³ mol⁻¹ cm⁻¹)
300
400
500
600
Wavelength (nm)
Emission Intensity

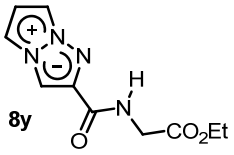
H
N
O
CO2Et

8y

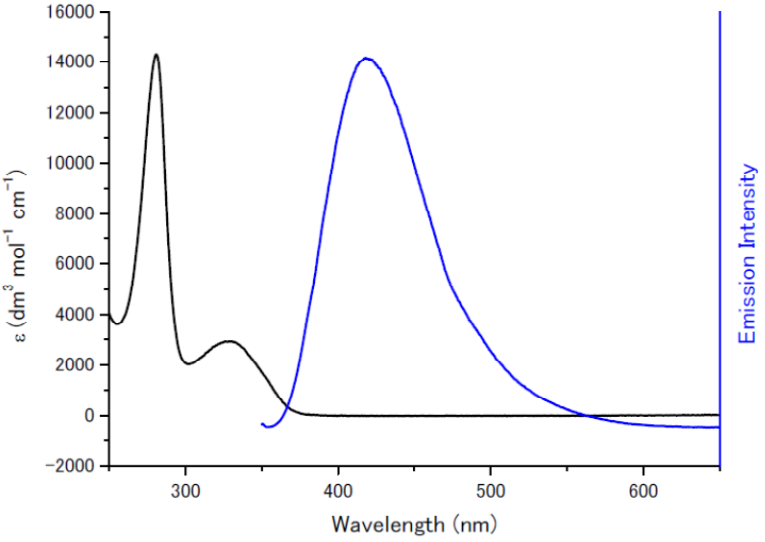
16000
14000
12000
10000
8000
6000
4000
2000
0
−2000
ε (dm³ mol⁻¹ cm⁻¹)
300
400
500
600
Wavelength (nm)
Emission Intensity

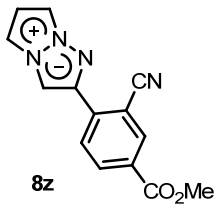
CN
CO2Me

8z

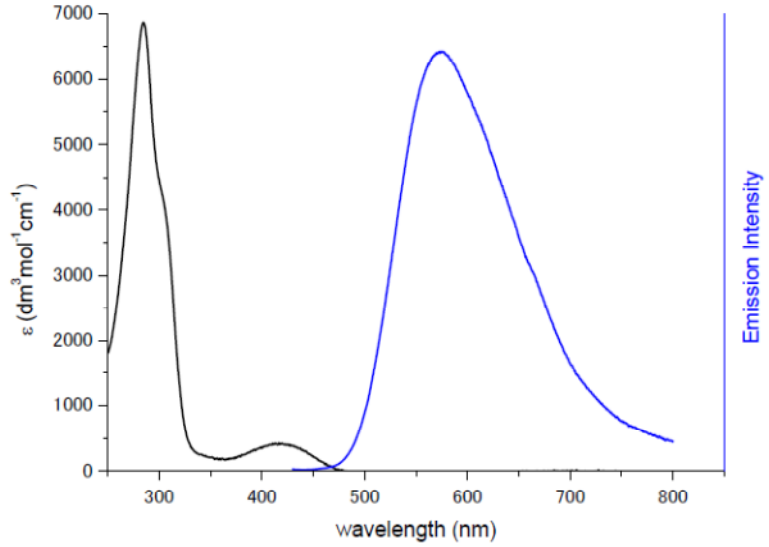
7000
6000
5000
4000
3000
2000
1000
0
ε (dm³mol⁻¹cm⁻¹)
300
400
500
600
700
800
wavelength (nm)
Emission Intensity

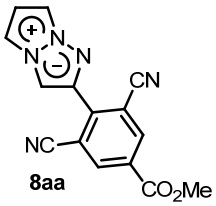
CN
NC
CO2Me

8aa

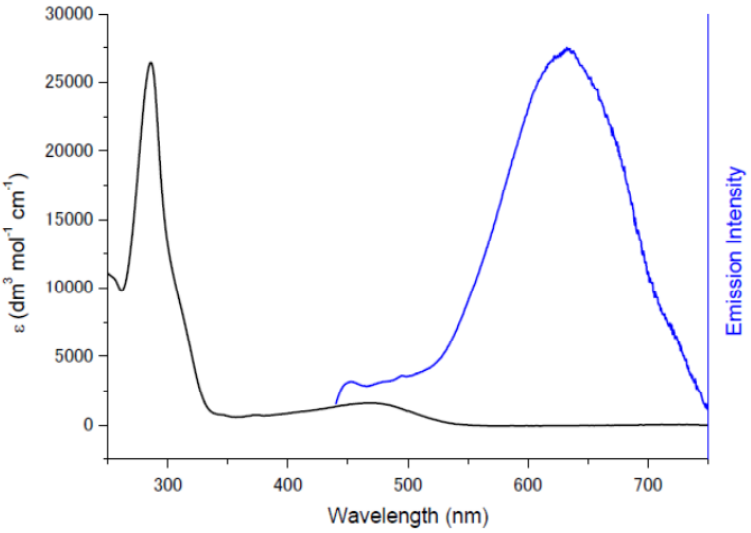
ε (dm3 mol-1 cm-1)
Emission Intensity
Wavelength (nm)

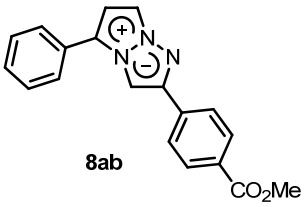
CO2Me

8ab

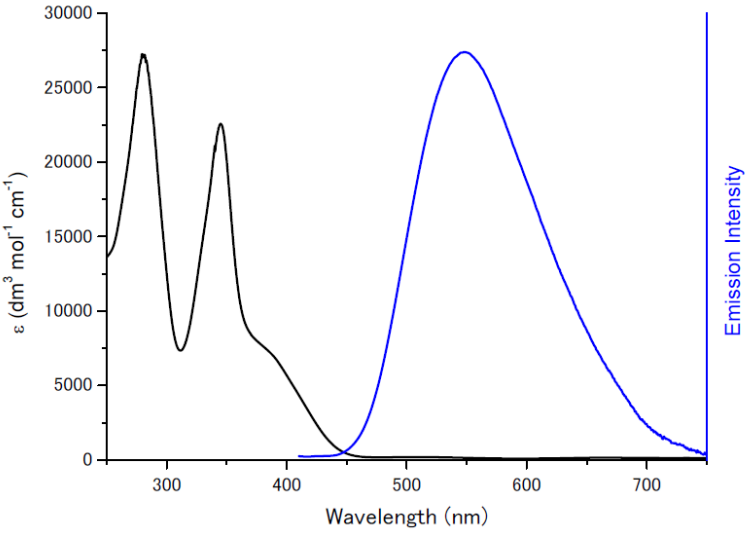
ε (dm3 mol-1 cm-1)
Emission Intensity
Wavelength (nm)

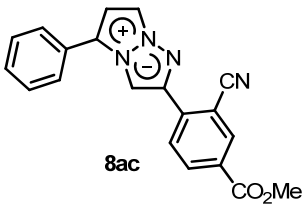
CN
CO2Me

8ac

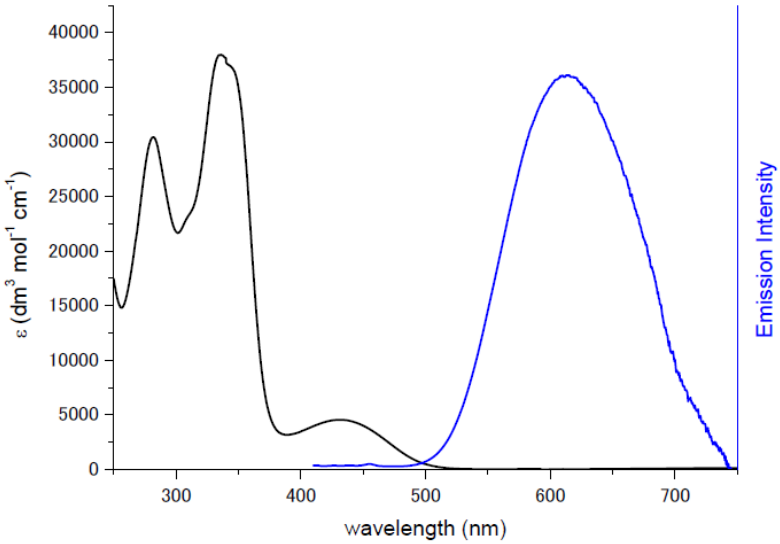
ε (dm3 mol-1 cm-1)
Emission Intensity
wavelength (nm)

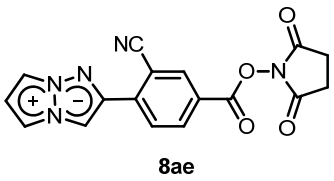
NC
O
O
N
O
O

8ae

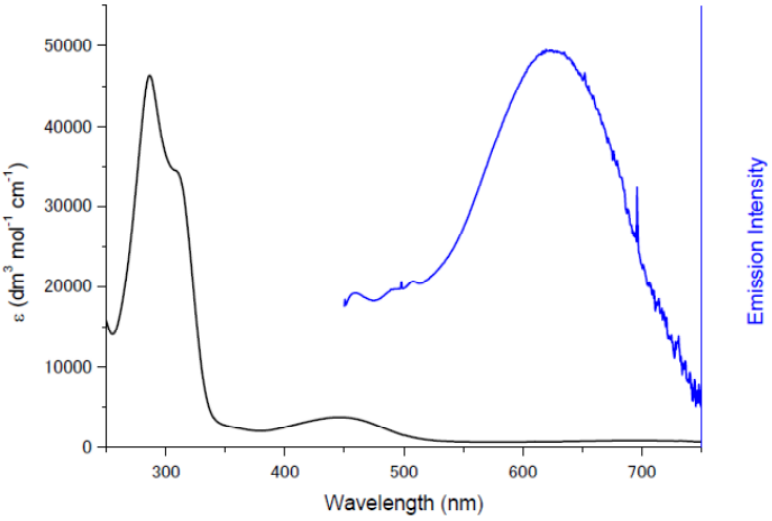
50000
40000
30000
20000
10000
0
ε (dm³ mol⁻¹ cm⁻¹)
300
400
500
600
700
Wavelength (nm)
Emission Intensity

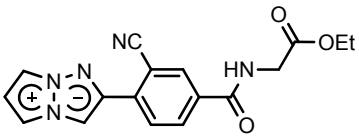
NC
O
OEt
HN
O

37a

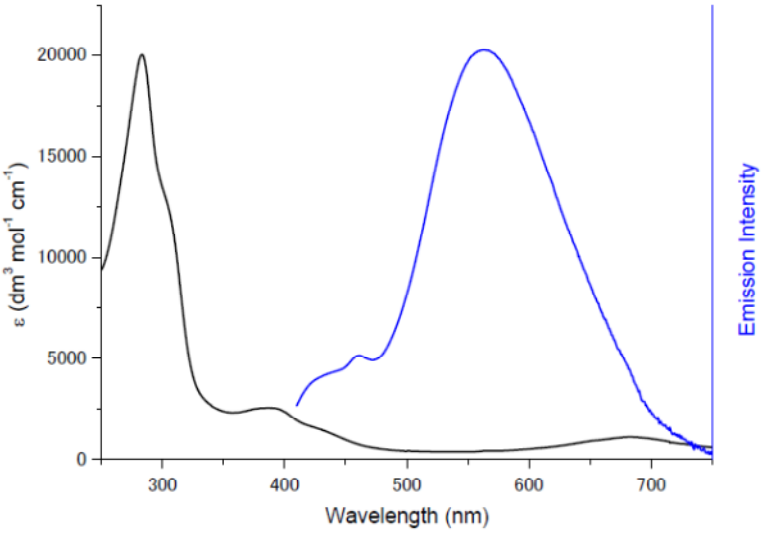
20000
15000
10000
5000
0
ε (dm³ mol⁻¹ cm⁻¹)
300
400
500
600
700
Wavelength (nm)
Emission Intensity

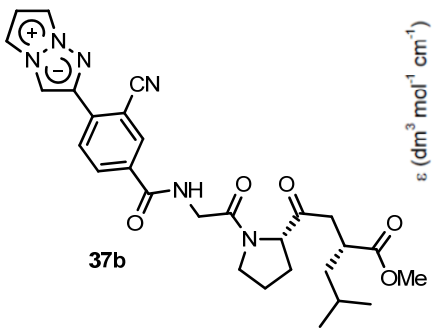
CN
NH
O
O
O
N
O
OMe

37b

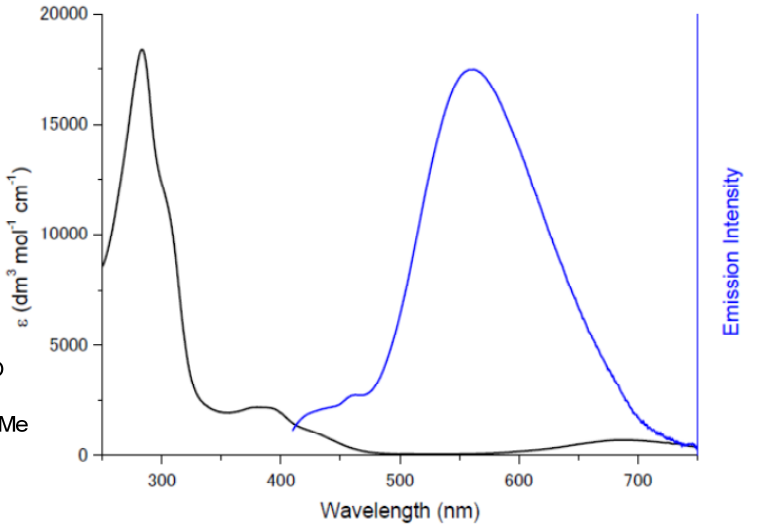
20000
15000
10000
5000
0
ε (dm³ mol⁻¹ cm⁻¹)
300
400
500
600
700
Wavelength (nm)
Emission Intensity

References

(1) For a recent review: Chudakov, D. M.; Matz, M. V.; Lukyanov, S.; Lukyanov, K. A. *Physiol. Rev.* **2010**, *90*, 1103–1163. References are therein.

(2) (a) Grynkiewicz, G.; Poenie, M.; Tsien, R. Y. *J. Biol. Chem.* **1985**, *260*, 3440–3450. (b) Tsien, R. Y.; Rink, T. J.; Poenie, M. *Cell Calcium* **1985**, *6*, 145–157. For a recent review of probes for various metal ions: (c) Terai, T.; Nagano, T. *Pflügers Arch. EJP*, **2013**, *465*, 347–359. References are therein.

(3) (a) Umezawa, N.; Tanaka, K.; Urano, Y.; Kikuchi, K.; Higuchi, T.; Nagano, T. *Angew. Chem. Int. Ed.* **1999**, *38*, 2899–2901. (b) Tanaka, K.; Miura, T.; Umezawa, N.; Urano, Y.; Kikuchi, K.; Higuchi, T.; Nagano, T. *J. Am Chem. Soc.* **2001**, *123*, 2530–2536. For a review of probes for inorganic active species inside cells: (c) Kobayashi, H.; Ogawa, M.; Alford, R.; Choyke, P. L.; Urano, Y. *Chem. Rev.* **2010**, *110*, 2620–2640.

(4) (a) Ikeda, S.; Okamoto, A. *Chem. Asian. J.* **2008**, *3*, 958–968. (b) Kubota, T.; Ikeda, S.; Okamoto, A. *Bull. Chem. Soc. Jpn.* **2009**, *82*, 110–117. (c) Ikeda, S.; Kubota, T.; Yuki, M.; Okamoto, A. *Angew. Chem. Int. Ed.* **2009**, *48*, 6480–6484. (d) Okamoto, A. *Chem. Soc. Rev.* **2011**, *40*, 5815–5828.

(5) Other type of nucleotide probes: (a) Boutorine, A. S.; Novopashina, D. S.; Krasheninina, O. A.; Nozeret, K.; Venyaminova, A. G. *Molecules* **2013**, *18*, 15357–15397. (b) Langer-Safer, P. R.; Levine, M.; Ward, D. C. *Proc. Natl. Acad. Sci. USA*, **1982**, *79*, 4381–4385. (c) Amann, R.; Fuchs, B. M. *Nature Rev. Microbiol.* **2008**, *6*, 339–348.

(6) (a) Delmotte, C.; Delmas, A.; *Bioorg. Med. Chem. Lett.* **1999**, *9*, 2989–2994. (b) Bettio, A.; Dinger, M. C.; Beck-Sickinger, A. G. *Protein Science* **2002**, *11*, 1834–1844. (c) Krueger, A. T.; Imperiali, B. *ChemBioChem* **2013**, *14*, 788–799.

(7) For examples of fluorescent probes of (a) Yoshida, A.; Hirooka, Y.; Sugata, Y.; Nitta, M.; Manabe, T.; Ido, S.; Murakami, K.; Saha, R. K.; Suzuki, T.; Ohshima, M.; Yoshida, A.; Itoh, K.; Shimizu, K.; Oku, N.; Furuta, T.; Asakawa, T.; Wakimoto, T.; Kan, T. *Chem. Commun.* **2011**, *47*, 1794–1796. (b) Sasaki, S.; Suzuki, H.; Ouchi, H.; Asakawa, T.; Inai, M.; Sakai, R.; Shimamoto, K.; Hamashima, Y.; Kan, T. *Org. Lett.* **2014**, *16*, 564–567. (c) Imagawa, H.; Saijo, H.; Yamaguchi, H.; Maekawa, K.; Kurisaki, T.; Yamamoto, H.; Nishizawa, M.; Oda, M.; Kabura, M.; Nagahama, M.; Sakurai, J.; Kubo, M.; Nakai, M.; Makino, K.; Ogata, M.; Takahashi, H.; Fukuyama, Y. *Bioorg. Med. Chem. Lett.* **2012**, *22*, 2089–2093. (d) Sugimoto, T.; Wada, Y.; Yamamura, S.; Ueda, M. *Tetrahedron* **2001**, *57*, 9817–9825. (e) Sato, H.; Inada, M.; Sugimoto, T.; Kato, N.; Ueda, M. *Tetrahedron Lett.* **2005**, *46*, 5537–5541. (f) Piggott, A. M.; Karuso, P. *ChemBioChem* **2008**, *9*, 524–530. (g) Guizzunti, G.; Brady, T. P.; MalhotraV.; Theodorakis, E. A. *J. Am. Chem. Soc.* **2006**, *128*, 4190–4191. (h) Sandler, J. S.; Fenical, W.;

Gulledge, B. M.; Chamberlin, A. R.; La Clair, J. J. *J. Am. Chem. Soc.* **2005**, *127*, 9320–9321. (i) Kita, M.; Hirayama, Y.; Yamagishi, K.; Yoneda, K.; Fujisawa, R.; Kigoshi, H. *J. Am. Chem. Soc.* **2012**, *134*, 20314–20317. (j) Kotake, Y.; Sagane, K.; Owa, T.; Mimori-Kiyosue, Y.; Shimizu, H.; Uesugi, M.; Ishihama, Y.; Iwata, M.; Mizui, Y. *Nat. Chem. Biol.* **2007**, *3*, 570–575. (k) DeGuire, S. M.; Earl, D. C.; Du, Y.; Crews, B. A.; Jacobs, A. T.; Ustione, A.; Daniel, C.; Chong, K. M.; Marnett, L. J.; Piston, D. W.; Bachmann, B. O.; Sulikowski, G. A. *Angew. Chem. Int. Ed.* **2014**, *Early View.*

(8) The Molecular Probes® Handbook 11th Ed. **2010** Online ver.: http://www. lifetechnologies. com/handbook

(9) Namba, K.; Kobayashi, K.; Murata, Y,; Hirakawa, T.; Yamagaki, T.; Iwashita, T.; Nishizawa, M.; Kusumoto, S.; Tanino, K. *Angew. Chem. Int. Ed.* **2010**, *49*, 9956–9959.

(10) Isolation and structural determination of mugineic acid: (a) Takagi, S. *Soil Sci. Plant Nutr.* **1976**, *22*, 423 – 433. (b) Marschner, H.; Römheld, H.; Kissel, M. *J. Plant Nutr.* **1986**, *9*, 695–713. (c) Takemoto, T.; Nomoto, K.; Fushiya, S.; Ouchi, R.; Kusano, H.; Hikino, H.; Takagi, S.; Matuura, Y.; Kakudo, M. *Proc. Jpn. Acad.* **1978**, *54*, 469 – 473.

(11) Ma, J. F.; Nomoto, K. *Physiol. Plant.* **1996**, *97*, 609 – 617.

(12) (a) Murata, Y.; Ma, J. F.; Yamaji, N.; Ueno, D.; Nomoto, K.; Iwashita, T. *Plant J.* **2006**, *46*, 563 – 572. (b) Namba, K.; Murata, Y. *The Chemical Record* **2010**, *10*, 140–150.

(13) (a) Tsuge, O.; Samura, H. *Chem. Lett.* **1973**, 175–180. (b) Kim, T.; Kim, K.; Park, Y. J. *Eur. J. Org. Chem.* **2002**, 493–502. (c) The computational structural study of **8a**. See: Carra, C.; Bally, T.; Jenny, T. A.; Albini, A. *Photochem. Photobiol. Sci.* **2002**, *1*, 38–44.

(14) (a) McRobbie, I. M.; Meth-Cohn, O.; Suschitzky, H. *Tetrahedron Lett.* **1976**, *12*, 925–928. (b) Albini, A.; Bettinetti, G. F.; Minoli, G. *Chem. Lett.* **1981**, 331–334. (c) Albini, A.; Bettinetti, G. F.; Minoli, G. *J. Org. Chem.* **1983**, *48*, 1080–1083. (d) Albini, A.; Bettinetti, G. F.; Minoli, G. *J. Am. Chem. Soc.* **1991**, *113*, 6928–6934. (e) Albini, A.; Bettinetti, G.; Minoli, G. *J. Am. Chem. Soc.* **1997**, *119*, 7308–7315. (f) Albini, A.; Bettinetti, G.; Minoli, G. *J. Am. Chem. Soc.* **1999**, *121*, 3104–3113. (g) Nyffenegger, C.; Pasquinet, E.; Suzenet, F.; Poullain, D.; Jarry, C.; Léger, J.-M.; Guillaumet, C. *Tetrahedron* **2008**, *64*, 9567–9573. (h) Nyffenegger, C.; Pasquinet, E.; Suzenet, F.; Poullain, D.; Guillaumet, G. *Synlett* **2009**, 1318–1320. (i) Kim, T.; Kim, K.; Park, Y. J. *Eur. J. Org. Chem.* **2002**, 493–502. (j) Choi, Y.-A.; Kim, K.; Park, Y. J. *Tetrahedron Lett.* **2003**, *44*, 7506–7511.

(15) (a) Koga, H.; Hirobe, M.; Okamoto, T. *Tetrahedron Lett.* **1978**, *19*, 1291–1294. (b) Chen, Y.; Wang, D.; Petersen, J. L.; Akhmedov, N. G.; Shi, X. *Chem. Commun.* **2010**, *46*, 6147–6149. For a very recent example: (c) Cai, R.; Wang, D.; Chen, Y.; Yan, W.; Geise, N. R.; Sharma, S.; Li, H.; Petersen, J. L.;Li, M. ; Shi, X. *Chem. Commun.* **2014**, *50*, 7303–7305.

(16) (a) Namba, K.; Osawa, A.; Ishizaka, S.; Kitamura, N.; Tanino, K. *J. Am. Chem. Soc.* **2011**, *133*, 11466–11469. (b) Namba, K.; Osawa, A.; Nakayama, A.; Mera, A.; Tano, F.; Chuman, Y.; Sakuda, E.; Taketsugu, T.; Sakaguchi, K.; Kitamura, N.; Tanino, K. *Chem. Sci.* **2014**, *in press*

(17) (a) Kolb, H. C.; Finn,M. G.; Sharpless, K. B. *Angew. Chem., Int. Ed.* **2001**, *40*, 2004–2021. (b) Rostovtsev, V. V.; Green, L. G.; Fokin, V. V.; Sharpless, K. B. *Angew. Chem. Int. Ed.* **2002**, *41*, 2596–2599. (c) Tornøe, C. W.; Christnesen, C.; Meldal, M. *J. Org. Chem.* **2002**, *67*, 3057–3064. (d) Wu, P.; Fokin, V. V. *Aldrichimica Acta* **2007**, *40*, 7–17.

(18) The starting material, 3-chloro-1,2-propanediol was purchased by Tokyo Chemical Industry (TCI). The price was in 2014.

(19) In the triflation reaction, although *i*-Pr_2EtN was also available as a base, use of 2,6-lutidine resulted in better yield. This reaction required low temperature because it was possible to generate hazardous azido-epoxide under higher temperature.

(20) We found that bis[2-(N,N-dimethylamino)ethyl] ether was an effective ligand to click reaction of benzyl azide with 1-hexyne as a result of screening of various ligands (unpublished result).

(21) Similar safety evaluation by TGA, see; Murakami, M.; Sakita, K.; Igawa, K.; Tomooka, K. *Org. Lett*. **2006**, *8*, 4023-4026.

(22) The spectral data of **8c** agreed with reported one in ref. 10 (a)

(23) (a) Hammett, L. P. *J. Am. Chem. Soc.* **1937**, *59*, 96–103. (b) Hansch, C.; Leo, A.; Taft, R. W. *Chem. Rev.* **1991**, *91*, 165–195.

(24) For emission tunable fluorophores, see (a) Demchenko, A. P. *Advanced Fluorescence Reporters in Chemistry and Biology I*, Springer, Berlin, **2010**. (b) Choi, E. J.; Kim, E.; Lee, Y.; Jo, A.; Park, S. B. *Angew. Chem. Int. Ed.* **2014**, *53*, 1346–1350. (c) Kim, E.; Koh, M.; Ryu, J.; Park, S. B. *J. Am. Chem. Soc.* **2008**, *130*, 12206–12207. (d) Lavis, L. D.; Raines, R. T. *ACS Chem. Biol.* **2008**, *3*, 142–155.

(25) For large Stokes Shift dyes, see (a) Lakowicz, J. R. Principles of Fluorescence Spectroscopy, Springer, New York, 3rd ed. **2006**. For selected recent examples; (b) Rihn, S.; Retailleau, P.; Nicola, A. D.; Ulrich, G.; Ziessel, R. *J. Org. Chem.* **2012**, *77*, 8851–8863. (c) Benniston, A. C.; Winstanley, T. P. L.; Lemmetyinen, H.; Tkachenko, N. V.; Harrington R. W.; Wills, C. *Org. Lett.* **2012**, *14*, 1374–1377. (d) Areneda, J. F.; Piers, W. E.; Heyne, B.; McDonald, R. *Angew. Chem. Int. Ed.* **2011**, *50*, 12214–12217, and references are therein.

(26) For selected recent examples: (a) Saito, Y.; Suzuki, A.; Imai, K.; Nemoto, N.; Saito, I. *Tetrahedron Lett.* **2010**, *51*, 2606–2609. (b) Chen, J.; Tang, R.; Luo, Z.; Yang, C. *J. Mol. Struct.* **2009**, *917*, 170–175. (c) Itami, K.; Yamazaki, D.; Yoshida, J. *J. Am. Chem. Soc.*

2004, *126*, 15396–15397. (d) Yamaguchi, S.; Shirasaka, T.; Tamao, K. *Org. Lett.* **2000**, *2*, 4129–4132.

(27) For examples of environment-sensitive fluorescent dyes: (a) Parasassi, T.; Stasio, G. D.; Ravagnan, G. Rusch, R. M.; Gratton, E. *Biophys. J.* **1991**, *60*, 179–189; (b) Parasassi, T.; Stefano, M. D.; Loiero, M.; Ravagnan, G.; Gratton, E. *Biophys. J.* **1994**, *66*, 763–768; (c) Diwu, Z.; Zhang, C.; Klaubert, D. H.; Haugland, R. P. *J. Photochem. Photobiol. A* **2000**, *131*, 95–100; (d) Turner, D. C.; Brand, L. *Biochemistry* **1968**, *7*, 3381–3390; (e) Slavik, J.; *Biochim. Biophys. Acta, Rev. Biomembr.* **1982**, *694*, 1–25; (f) Matulis, D.; Lovrien, R. *Biophys. J.* **1998**, *74*, 422–429; (g) Kung, C. E.; Reed, J. K. *Biochemistry* **1986**, *25*, 6114–6121; (h) Dreger, Z. A.; Lang, J. M.; Drickamer, H. G. *Chem. Phys.* **1993**, *169*, 351–359.

(28) For recent examples of commercially available probe for membrane: (a) Son, S-H.; Yamagishi, Y.; Tani, M.; Yuasa, M.; Yamada, K. *Chem. Lett.* **2011**, *40*, 989–991; (b) Omura, R.; Nagao, K.; Kobayashi, N.; Ueda, K.; Saito, H. *J. Lipid Res.* **2014**, *55*, 2423–2431; and commercial source (Goryo Chemical): http://goryochemical.com/

(29) We also investigated the properties of 2,5-di-substituted TAPs: Namba, K.; Mera, A.; Osawa, A.; Sakuda, E.; Kitamura, N.; Tanino, K. *Org. Lett.* **2012**, *14*, 5554–5557.

(30) Benedetti, F.; Berti, F.; Norbedo, S. *Tetrahedron Lett.* **1998**, *39*, 7971–7974.

(31) (a) Newman, M. S.; Boden, H. *J. Org. Chem.* **1961**, *26*, 2525–2528; (b) Sheehan, J. C.; Preston, J.; Cruikshank, P. A. *J. Am. Chem. Soc.* **1965**, *87*, 2492–2493.

(32) Sonogashira, K.; Tohda, Y.; Hagihara, N. *Tetrahedron Lett.* **1975**, *50*, 4467–4470.

(33) S. Ullrich, Z. Nazir, A. Büsing, U. Scheffer, D. Wirth, J. W. Bats, G. Dürner and M. W. Göbel, *ChemBioChem* **2011**, *12*, 1223–1229.

(34) Other palladium source and ligand such as $Pd(acac)_2$, $Pd(OAc)_2$, $Pd(OCOCF_3)_2$, $PdCl_2(CH_3CN)_2$, $PdCl_2(PhCN)_2$, $Pd(PPh_3)_4$, Pd_2 $(dba)_3$, P(*t*-Bu)$_3$, dppf, xantphos, P(O*i*-Pr)$_3$, and P(*o*-tol)$_3$ gave **35** in trace to poor yield.

(35) Yanai, T.; Tew, D. P.; Handy, N. C. *Chem. Phys. Lett.* **2004**, *393*, 51–57.

(36) Celani, P.; Werner, H.-J. *J. Chem. Phys.* **2000**, *112*, 5546–5557.

(37) Roos, B. O.; Andersson, K. *Chem. Phys. Lett.* **1995**, *245*, 215–223.

(38) Cossi, M.; Scalmani, G.; Rega, N.; Barone, V. *J. Chem. Phys.* **2002**, *117*, 43–54.

(39) Rappe, A. K.; Casewit, C. J.; Colwell.; K. S.; Goddard, W. A.; Skiff, W. M. *J. Am. Chem. Soc.* **1992**, *114*, 10024–10035.

(40) Frisch, M. J.; Trucks, G. W.; Schlegel, H. B.; Scuseria, G. E.; Robb, M. A.; Cheeseman, J. R.; Scalmani, G.; Barone, V.; Mennucci, B.; Petersson, G. A.; Nakatsuji, H.; Caricato, M.; Li, X.; Hratchian, H. P.; Izmaylov, A. F.; Bloino, J.; Zheng, G.; Sonnenberg, J. L.; Hada, M.; Ehara, M.; Toyota, K.; Fukuda, R.; Hasegawa, J.; Ishida, M.; Nakajima, T.; Honda, Y.;

Kitao, O.; Nakai, H.; Vreven, T.; Montgomery, J. A.; Peralta, J. E.; Ogliaro, F.; Bearpark, M.; Heyd, J. J.; Brothers, E.; Kudin, K. N.; Staroverov, V. N.; Kobayashi, R.; Normand, J.; Raghavachari, K.; Rendell, A.; Burant, J. C.; Iyengar, S. S.; Tomasi, J.; Cossi, M.; Rega, N.; Millam, J. M.; Klene, M.; Knox, J. E.; Cross, J. B.; Bakken, V.; Adamo, C.; Jaramillo, J.; Gomperts, R.; Stratmann, R. E.; Yazyev, O.; Austin, A. J.; Cammi, R.; Pomelli, C.; Ochterski, J. W.; Martin, R. L.; Morokuma, K.; Zakrzewski, V. G.; Voth, G. A.; Salvador, P.; Dannenberg, J. J.; Dapprich, S.; Daniels, A. D.; Ö Farkas; Foresman, J. B.; Ortiz, J. V.; Cioslowski, J.; Fox, D. J *Gaussian 09*, *Revision C.01*.

(41) Werner, H.-J.; Knowles, P. J.; Knizia, G.; Manby, F. R.; Schütz, M. *et al. MOLPRO, version 2010.1, a package of ab initio programs.*

Acknowledgement

All the studies described in this thesis were carried out under the supervision of Professor Dr. Keiji TANINO, Department of Chemistry, Faculty of Science, Hokkaido University. The author would like to express deeply sincere appreciation to Professor Tanino for his guidance and constant encouragement and helpful discussion in the preparation of this thesis.

Grateful acknowledgement is made to Professor Dr. Kosuke NAMBA for his considerable advice, valuable discussions, and constant encouragement throughout the course of this work. It was a great honor to get an opportunity for his guidance. The author also expresses his sincere thanks to Assistant Professor Dr. Fumihiko YOSHIMURA for practical advice and helpful discussion.

The author would like to show his greatest appreciation to Professor Dr. Takanori SUZUKI, Professor Dr. Hideaki OIKAWA, Professor Dr. Masaya SAWAMURA, and Professor Dr. Hajime ITO for serving the author's dissertation committee at Hokkaido University.

Professor Dr. Noboru KITAMURA, Associate Professor Dr. Shoji ISHIZAKA, and Assistant Professor Dr. Eri SAKUDA gave practical suggestion for optical measurement of TAPs to the author. Associate Professor Dr. Hidetoshi KAWAI made a contribution to X-ray crystallographic analysis of TAP **8n**. The thermogravimetry analysis of azide **22a** was performed by Professor Dr. Kazuki SADA, Assistant Professor Dr. Kenta KOKADO, and Mr. Takumi ISHIWATA. Tremendous contributions to fluorescence observation of TAPs inside cells were made by Professor Dr. Kazuyasu SAKAGUCHI, Associate Professor Dr. Yoshiro Chuman, and Ms. Fumi TANO. The quantum chemical calculation for the structure and the molecular orbital of TAPs was performed by Professor Dr. Tetsuya TAKETSUGU and Associate Professor Dr. Akira NAKAYAMA. The author would like to offer his special thanks to these contributors.

A part of this work was accomplished at Professor Namba's laboratory, Faculty of Pharmaceutical Sciences, Tokushima University. The author would like to thank Associate Professor Dr. Masahiro YOSHIDA and Assistant Professor Dr. Atsushi NAKAYAMA for useful discussion and comments, sincerely. The author is grateful to all colleagues at Tanino group, Hokkaido University and Namba group, Tokushima University. Special Thanks to Mr. Ryohei UEMATSU, Ms. Ayano KOWATA, Mr. Ryusuke SAKOH, Mr. Takashi TOYOTA, and Ms. Shoko OHNO for extensive discussion and considerable encouragement. The author also expresses his appreciation to the member of the TAP project, Ms. Akane MERA, Ms. Michika KANAKI, Mr. Akira OTANI, Ms. Tsukiho HAYASHI, Ms. Masami ITO, and Mr. Satoshi NISHIO and the member of second laboratory at Namba group, Mr. Ryota KOTAKA and Mr. Akira SAKAMOTO for invaluable contributions and encouragement.

This work was partially supported by Grant-in-Aid for JSPS fellow. The author sincerely

thanks to Research Fellowship for Young Scientists from JSPS and scholarship from The Mitsubishi UFJ Trust Scholarship Foundation.

Finally, the author would like to thank sincerely his family, Kazuhiro, Fumiko, Shusuke, and late Yuuki and Sumiko for their encouragement and understanding.